1984

Extensions of the full optimized reaction space model for molecular electronic wavefunctions

Miu-to Brenda Lam
Iowa State University

Lam, Miu-to Brenda

EXTENSIONS OF THE FULL OPTIMIZED REACTION SPACE MODEL FOR MOLECULAR ELECTRONIC WAVEFUNCTIONS

Iowa State University PH.D. 1984

Extensions of the full optimized reaction space model for molecular electronic wavefunctions

by

Miu-to Brenda Lam

A Dissertation Submitted to the
Graduate Faculty in Partial Fulfillment of the
Requirements for the Degree of
DOCTOR OF PHILOSOPHY
Department: Chemistry
Major : Physical Chemistry

Approved:

Signature was redacted for privacy.

In Charge of Major Work

Signature was redacted for privacy.

For the Major Department

Signature was redacted for privacy.

For the Graduate College

Iowa State University
Ames, Iowa

1984

TABLE OF CONTENTS

I. INTRODUCTION

Before the advent of the electronic computer, quantum chemistry depended to a large extent upon experimental knowledge of physical and chemical properties of molecules and upon chemical intuition. With the exception of H_2, only highly approximate non-empirical calculations were possible for small molecules, and only semi-empirical calculations for larger molecules. The computer brought with it the possibility of performing accurate non-empirical calculations, commonly referred as ab initio calculations, for polyatomic molecules of chemical interest. For a non-specialist the term "ab initio" may have too sweeping a meaning. It might give the impression that ab initio calculations provide "accurate" and "objective" solutions. However, the traditional definition of ab initio calculations as introduced by R. S. Mulliken is that stated by Allen and Karo[1] in 1960, namely: (i) all electrons are taken into account simultaneously; (ii) the exact non-relativistic Hamiltonian with fixed nuclei is used,

$$H = -\frac{1}{2}\sum_i \nabla_i^2 - \sum_{i,a}\frac{Z_a}{r_{ia}} + \sum_{i>j}\frac{1}{r_{ij}} + \sum_{a,b}\frac{Z_a Z_b}{r_{ab}} \quad , \qquad (1.1)$$

where the indices i,j refer to the electrons, the indices a,b refer to the nuclei with nuclear charges Z_a and Z_b and the atomic units one bohr and one hartree are used; (iii) all integrals are evaluated rigorously.

Until the early seventies, ab initio calculations were almost exclusively SCF calculations. Over the past fifteen years, however, a variety of effective algorithms have been developed to yield correlated wavefunctions. Implementation and improvement of such algorithms rely on sophisticated computer programs. The advances in computer technology and availability in the last two decades have enhanced the development in computational quantum chemistry.

The capability of performing accurate non-empirical calculations has bridged the gap between experimental and theoretical chemistry and experimentalists have begun to look to theoretical predictions for directions in their research. Before a theory can produce meaningful results for the experimentalists, it has to go through three stages: (i) development of the mathematical relationships, (ii) implementation of the algorithm, and the corresponding computer programs and (iii) application of the programs to specific cases. Many algorithms and systems of computer programs have been developed over the years. The Hartree-Fock (HF) approximation containing a single determinant, known as the self-consistent-field (SCF), wavefunction has become almost standardized. The essence, if not the detailed theory, of different systems can be found in many quantum chemistry books[2-3] and references therein.

The Hamiltonian (1.1) inherently neglects the

relativistic effects. The relativistic corrections calculated by Fraga et al.[4] using the Dirac-Breit-Pauli-Hartree-Fock method range from -70 microhartree for helium to -130 millihartree for neon to -1020 hartree for mercury. Computationally, the estimation of relativistic effects in molecules is difficult. Fortunately, the largest contributions to the relativistic energy are due to inner electronic shells. For the lighter atoms, there is sound reason to assume that the total atomic relativistic energy is almost independent of the atomic electronic state and the chemical environment in molecules, which implies cancellation of relativistic effects in chemical processes. Experience shows that neglecting the relativistic effects, especially for the first- and second-row elements, are indeed usually justifiable.

The more crucial sources for the shortcomings of theoretical calculations in chemical applications are inadequate basis sets and correlation effects, i.e. the neglect of the instantaneous repulsions between electrons. The difference between the Hartree-Fock energy and the exact non-relativistic energy of a particular system is usually considered as the correlation energy. As a rule, it is a small percentage of the total energy of an atom or molecule. For example, for fluorine atom, the correlation energy, 0.4 hartree, is only 0.4% of the total energy -99.8053 hartree[5].

The small percentage translates however into an actual value of more than 10 eV which is considerably larger than the experimental dissociation energy of F_2 of 1.7 eV[6].

Much effort has been spent over the past two decades to search for optimal basis sets. An overview of different basis set types is given by Carsky and Urban[3]. All calculations reported in this work use the contracted even-tempered Gaussian basis set developed by Raffenetti[7,8], Bardo and Ruedenberg[9], Feller and Ruedenberg[10], Schmidt and Ruedenberg[11]. Polarization functions were also included whenever appropriate.

Total recovery of the correlation effect seems impossible at this time. However, from the chemical point of view, it is the relative variation of the energy surface of a chemical system which is of interest rather than the absolute values of its energies. Upon molecule formation and in chemical reactions, only part of the correlation energy changes. Thus, the important goal of quantum chemical research is to identify this changing part and seek for mathematical formulations to recover it in a computationally feasible manner. A useful and quite successful model of this type which has recently been formulated to this end is the FORS model.

A Full Optimized Reaction Space (FORS) wavefunction is defined as the optimal configuration interaction wavefunction in a full space of N-electron configurations where all

orbitals are optimized, so that $\langle\Psi|H|\Psi\rangle$ is an extremum. The dimension of such a full configurational spaces may be quite large. The definition and generation of full configurational reaction spaces are outlined in Chapter II. A procedure is developed for generating all Symmetry-Adapted Antisymmetrized Products (SAAPs) which span such full configuration space and the algorithm described has been implemented into a computer program labelled SAAP. This code has been incorporated as part of the ALIS program package[12]. In Chapter III, multi-configuration self-consistent-field (MCSCF) calculations using FORS wavefunctions are reported for the low-lying electronic states of allene at planar geometries. This provides the ground work for study of torsion and bending in allene.

Although the FORS model provides an unambiguously general and unbiased approach to obtain reliable quantitative results on potential energy surfaces involving polyatomic molecules, it still fails to recover all correlation energies completely and, therefore, requires further refinement. Two possible augmentations are discussed in Chapters IV and V. In Chapter IV, the theory of a semi-empirical correction method termed IntraAtomic Correlation Correction (IACC) is developed and quantitative results of its application are discussed. In Chapter V, improvements of FORS wavefunction by the systematic inclusion of additional configurations involving orbitals

outside the valence space are investigated. Such calculations elucidate the origin of the unrecovered correlation effects.

II. GENERATION OF THE FULL REACTION SPACE

A. The Full Optimized Reaction Space Model

1. Objective

The model of Full Optimized Reaction Space (FORS) was first introduced by Ruedenberg, Sundberg and Cheung[13] and further developed by Ruedenberg, Schmidt, Gilbert and Elbert[14]. It has been applied to a number of reactions[15-20]. There are other MCSCF models with restricted configuration selections such as the Optimized Valence Configuration (OVC)[21], the Hartree-Fock plus Proper Dissociation (HF + PD)[22], the Separated Pair Independent Particle (SPIP)[23], the Generalized Valence Bond Configuration Interaction (GVB CI)[24] and a recent calculation by Kirby-Docken and Liu[25]. The FORS model is unique in its attempt to combine consistently the concept of a full valence space with the principle of orbital optimization and to explore systematically the implication of such a framework. The concept has been generalized by Roos and co-worker[26-29] to the "Complete Active Space Self-Consistent-Field (CASSCF)" procedure which has also proven to be successful.

The FORS model describes the electronic structure of a molecule in terms of the best wavefunction that can be obtained by a superposition of all those configurations which are generated by all possible occupancies and couplings from a "formal minimal basis" of valence orbitals on the constituent

atoms. These configurations span a "Full Reaction Space", and MCSCF optimization[30] of the orbitals in terms of an extended set of quantitative basis orbitals determines the "Full Optimized Reaction Space". A detailed description of the model and its application, and an analysis of the resulting molecular electronic wavefunction are given by Ruedenberg, Schmidt, Gilbert and Elbert[14].

For practical application of the FORS approach, an efficient general method of generating all configurations spanning the full configuration space for a specified set of orbitals is essential. The formulation of such a procedure and its implementation is discussed in the present chapter.

2. Configurational basis for the full reaction space

The N-electron function space of the FORS model is spanned by a basis of Spin Adapted Antisymmetrized Products (SAAPs) which are configurations of the form:

$$\Psi_{k\gamma}(1,\ldots,n) = A\{\Phi_k(1,\ldots,n)\Theta_\gamma^{SM}(1,\ldots,n)\} \qquad (2.1)$$

where Φ_k is a product of space orbitals

$$\Phi_k(1,\ldots,n) = f_{k1}(1)f_{k2}(2)\ldots f_{kn}(n) \quad , \qquad (2.2)$$

and Θ_γ^{SM} is an eigenfunction of the total spin (S^2) and its z

component (S_z). We choose in particular the Serber-type spin functions, making use of the construction process developed by Ruedenberg[31], Salmon and Ruedenberg[32], Salmon et al[33]. The antisymmetrizer **A** is defined as

$$\mathbf{A} = 2^{-d/2} \sum_{P} (-1)^{P} P$$

where d is the number of doubly occupied orbitals.

The MOs f_{ki} are called "configuration generating orbitals (CGOs)". In the FORS model, these CGOs are divided into two groups: (i) a set of "generalized core" or "closed-shell" orbitals, all of which are doubly occupied in <u>every</u> configuration, and (ii) a set of "open-shell" or "reactive" CGOs whose occupation numbers are <u>less than two in at least one</u> configuration. The space orbitals f_{kj} are chosen in various ways from <u>one</u> set of orthonormal spatial molecular orbitals $\phi_1, \phi_2, \phi_3, \ldots, \phi_M$ which may or may not be symmetry adapted. A basis for the full reaction space is obtained by making for $f_{k1}, f_{k2}, f_{k3}, \ldots, f_{kN}$ <u>all possible choices</u> out of the set $\phi_1, \phi_2, \phi_3, \ldots, \phi_M$ with occupation numbers 0, 1 or 2, compatible with the spatial symmetry of Ψ, and by associating with each orbital product so obtained all possible spin functions $\Theta_1^{SM}, \Theta_2^{SM}, \Theta_3^{SM}, \ldots$ yielding non-vanishing SAAPs.

The $\Psi_{k\gamma}$ of Equation (2.1) obtained in this manner merely

define a certain formal structure of the configuration space in terms of the orthonormal set of the CGOs. Determination of the CGOs by MCSCF optimization[30] completely determines the $\Psi_{K\gamma}$. An important feature of the full reaction space is that it is invariant against any non-singular, in particular, orthogonal transformation among the open-shell CGOs and against a similar transformation among the core CGOs.

3. Group theoretical considerations

Each SAAP is generated from a product of orbitals which, by virtue of the Pauli principle, can only have occupation numbers 1 or 2. Furthermore, in case the molecule has spatial symmetry, each SAAP can be required to belong to the irreducible representation (irrep) of the state to be calculated. If each orbital in turn belongs to a particular irrep, the total symmetry of a SAAP is obtained by taking the direct product of the occupied orbitals. Only the case of point groups with non-degenerate representations (i.e. the group D_{2h} and its subgroups) and that of the groups $C_{\infty v}$ and $D_{\infty h}$ are discussed here, since only for these have automated computer programs been constructed. A program, called SAAP, has been developed to generate a SAAP basis for the full reaction space of a given number of orbitals and electrons. It has been incorporated into the ALIS program package[12]. The program involves two major steps: (i) the possible

distributions of the valence electrons over the irreps are determined and (ii) all possible SAAPs are formed for each of these distributions. A description of the algorithm of the generation procedure is given in the following sections.

B. The Point Symmetry Group D_{2h} and its Subgroups

1. The spatial symmetry of orbital products

The irreps of D_{2h}, namely A_g, B_{3u}, B_{2u}, B_{1g}, B_{1u}, B_{2g}, B_{3g}, A_u can be associated with the binary numbers 000, 001, 010, 011, 100, 101, 110, 111 which correspond to the digits 0, 1, 2, 3, 4, 5, 6, 7. There are three reflection planes in the D_{2h} symmetry and each bit in the binary representation can be thought of describing the symmetry behavior with respect to one of the reflection operations. Combination of these operations uniquely defines the eight irreps in the group. The other non-degenerate point groups, namely D_2, C_{2h}, C_{2v}, C_2, C_i, C_s and C_1, are subgroups of D_{2h} and the binary representation also applies to them. Table 2.1 lists the decimal numbers associated with the irreps for all these groups.

For any one of these groups, the symmetry of an orbital product is simply obtained by combining the set of binary numbers corresponding to the irreps of the individual orbitals by means of the "Exclusive OR (XOR)" operation. For example, in D_{2h}:

$$\text{XOR}\{(001),(101),(111)\} = (011) \qquad (2.3)$$

corresponds to

$$B_{3u} \otimes B_{2g} \otimes A_u = B_{1g} \, . \qquad (2.4)$$

Table 2.1. The correspondence between the elements of the point group and binary numbers

Point group	Irreducible representation	Digits equivalent to binary numbers plus 1
D_{2h}	$A_g, B_{3u}, B_{2u}, B_{1g}, B_{1u}, B_{2g}, B_{3g}, A_u$	1,2,3,4,5,6,7,8
C_{2h}	A_g, B_g, B_u, A_u	1,2,3,4
C_{2v}	A_1, B_1, B_2, A_2	1,2,3,4
D_2	A, B_1, B_2, B_3	1,2,3,4
C_2	A,B	1,2
C_i	A_g, A_u	1,2
C_s	A',A"	1,2
C_1	A	1

Suppose one has an orbital product containing n(α) orbitals of representation α, for several one-dimensional irreps, then it is seen that any even occupancy yields

A_g = (000) symmetry, so that only the irreps occupied by an odd number of electrons have to be taken into account. For example, if one has a product of ten orbitals with n(001) = 3, n(101) = 2 and n(111) = 5, then the irrep of product is simply

$$XOR\{(001),(111)\} = (110) \quad .$$

It is furthermore apparent that the symmetry of any orbital products is determined by the number of singly occupied orbitals only.

2. Determination of distributions

Suppose now that there are A one-dimensional irreps α = 1, 2, ..., A and that among the set of configuration generating orbitals ϕ_1, ϕ_2, ..., ϕ_M from which the orbitals in Equation (2.2) can be chosen, there are m_α orbitals belonging to the irrep α. then $\nu_\alpha = 2m_\alpha$ is the maximal electron occupancy of the irrep α. The orbital products that can be formed from the set ϕ_1, ..., ϕ_M (and hence the SAAPs that are the basis of the Full Reaction Space) can now be grouped into subsets, such that all configurations in one subset have the same number n_α of orbitals in each irrep α. These subsets are called here "distributions of orbitals among irreps". Any particular distribution D is thus characterized by a set of irrep occupancies

$$D = D(n_1, n_2, \ldots, n_\alpha, \ldots, n_A) \quad .$$

If N is the total number of electrons one clearly must have

$$n_\alpha \leq \nu_\alpha \ , \qquad \sum_{\alpha=1}^{A} n_\alpha = N \ , \qquad \sum_{\alpha=1}^{A} \nu_\alpha \geq N \ . \qquad (2.5)$$

It is useful to determine first all possible distributions for the desired irrep of the state to be investigated.

Given the number of available orbitals in each irrep and the total number of electrons, the generation of all possible distributions of a particular symmetry is a combinatorial problem. It is solved here by a sequence of steps which is best illustrated by an example. Suppose that there are eleven electrons and two orbitals of symmetry 1, three orbitals of symmetry 2, one orbital of symmetry 3 and two orbitals of symmetry 4, so that $\nu_1 = 4$, $\nu_2 = 6$, $\nu_3 = 2$ and $\nu_4 = 4$, then the first distribution formed is

$$D_1 = D(n_1=\nu_1=4, n_2=\nu_2=6, n_3=1, n_4=0) \quad .$$

The other distributions are then generated from D_1 by moving one electron at a time in the sequence illustrated by Table 2.2. The flow diagram of Figure 2.1 displays the sequence of logical steps of this process. Only distributions which

Table 2.2. Sequence of distributions generated by SAAP with eleven electrons, $\nu_1=4$, $\nu_2=6$, $\nu_3=2$ and $\nu_4=4$

$n_1n_2n_3n_4$	$n_1n_2n_3n_4$	$n_1n_2n_3n_4$
4 6 1 0	3 6 0 2	2 4 2 3
4 6 0 1	3 5 2 1	2 4 1 4
4 5 2 0	3 5 1 2	2 3 2 4
4 5 1 1	3 5 0 3	1 6 2 2
4 5 0 2	3 4 2 2	1 6 1 3
4 4 2 1	3 4 1 3	1 6 0 4
4 4 1 2	3 4 0 4	1 5 2 3
4 4 0 3	3 3 2 3	1 5 1 4
4 3 2 2	3 3 1 4	1 4 2 4
4 3 1 3	3 2 2 4	0 6 2 3
4 3 0 4	2 6 2 1	0 6 1 4
4 2 2 3	2 6 1 2	0 5 2 4
4 2 1 4	2 6 0 3	
4 1 2 4	2 5 2 2	
3 6 2 0	2 5 1 3	
3 6 1 1	2 5 0 4	

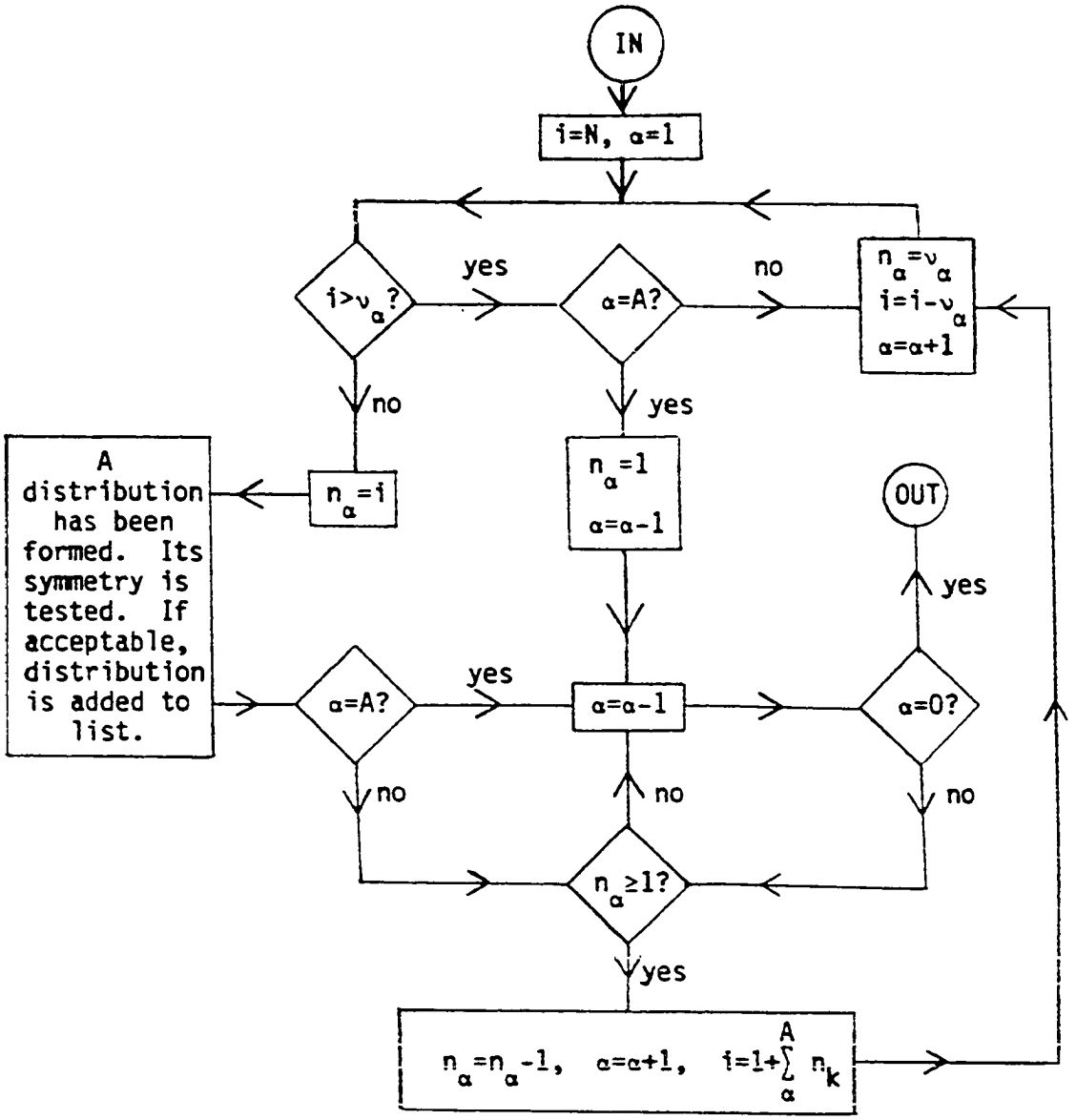

N = total number of electrons
α = label of irreducible representations
A = total number of irreducible representations
ν_α = maximum number of electrons in irrep α
n^α = number of electrons in irrep α for a given distribution
i^α = running counting index representing the number of electrons to be distributed

Figure 2.1. Flow chart for generation of distributions

satisfy the set of Equations (2.5) are kept. In Table 2.2, all distributions obtained in this manner are listed. If the molecule belongs to a symmetry other than C_1, then the symmetry of each distribution is tested after it has been formed by the XOR operation discussed above and, only if it has the desired symmetry, will it be added to the list.

3. Formation of SAAPs

The first step in generating the individual SAAPs is to find all possible orbital products for each of the distributions found by the procedure described in the preceding section. If the distribution is $D(n_1 n_2 n_3 \ldots n_A)$, then it can be shown that the total number of orbital products which can be formed is given by

$$P(n_1 n_2 \ldots n_A) = \prod_{\alpha=1}^{A} P_\alpha(n_\alpha) \tag{2.6}$$

where

$$P_\alpha(n_\alpha) = \sum_{k=K_\alpha}^{K'_\alpha} \binom{m_\alpha}{k} \binom{k}{n_\alpha - k} , \tag{2.7}$$

with

$P_\alpha(n_\alpha)$ = number of possible orbital products of n_α electrons in m_α orbitals

m_α ($= \nu_\alpha/2$) = number of available reaction orbitals belonging to irrep α

n_α = number of reaction electrons occupying irrep α in the distribution

k = number of <u>different</u> orbitals being occupied in irrep α in a given product

$n_\alpha - k$ = number of orbitals being doubly occupied in irrep α in a given product

K_α = $[(n_\alpha+1)/2]$ = the largest integer $\leq (n_\alpha+1)/2$

K'_α = minimum of (n_α, m_α)

To find the $P(n_1 n_2 \ldots)$ products explicitly for a given distribution, one first generates separately all $P_\alpha(n_\alpha)$ products for the n_α orbitals in each irrep α. To do this, one can use exactly the same algorithm as the one depicted by the flow chart in Figure 2.1, if one makes the following specifications: (i) n_α is substituted for N, the total number of electrons; (ii) j = orbital index is substituted for α, the irrep index; (iii) $j = 1, 2, \ldots, m_\alpha$ is substituted for $\alpha = 1, 2, \ldots, A$; (iv) the value 2 = maximum number of electrons in any one orbital is substituted for $\nu_1, \nu_2, \ldots, \nu_A$, the maximum number of electrons in each irrep; (v) the actual occupation of orbital j, namely 0, 1 or 2, is substituted for n_α, the irrep occupation. Furthermore, the symmetry check is omitted. After all products have been formed for each irrep,

the various combinations between the products from different irreps yield all possible total products for a given distribution.

When the orbital products, have been found, the individual SAAPs can be determined. In any given orbital product the doubly occupied orbitals are listed first and the singly occupied ones thereafter, both separately in order of increasing index number. The number of individual SAAPs which can be formed from one product is equal to the number of spin functions Θ_{γ}^{SM}, $\gamma = 1, 2, \ldots,$ that can be combined with it (see Equation 2.1). This number depends upon the total spin quantum number S, which is determined by the state to be calculated and by the number of <u>singly</u> occupied orbitals in the product, say T. It can be calculated using the branching diagram and is given by the formula[34]

$$\Gamma(S,T) = \begin{pmatrix} T \\ T/2 + S \end{pmatrix} - \begin{pmatrix} T \\ T/2 + S+1 \end{pmatrix}$$

$$= \frac{(2S+1)\ T!}{(T/2 + S+1)!\ (T/2 - S)!} \quad . \qquad (2.8)$$

This number is all that is needed for identifying the SAAPs. This is because each SAAP is completely characterized by the orbitals it contains, their occupancies and the <u>index</u> γ of its spin function. The explicit forms of the individual spin

functions associated with the possible indices γ = 1, 2, ..., $\Gamma(S,T)$, are generated in another part of the ALIS program system[12].

We were not able to find a formula predicting the number of orbital products having a certain number of singly occupied orbitals without explicitly generating them. For this reason, it was not possible to calculate the number of possible SAAPs without generating the individual space orbital products. The program has an option of going through the entire procedure without storing the information characterizing the individual SAAPs, but just counting the total number.

C. The Point Symmetry Groups $C_{\infty v}$ and $D_{\infty h}$

1. Irreducible representations

Consider a linear molecule lying on the z-axis. The symmetry transformations of such a molecule are of two types: (i) rotations $C(\omega)$ about the z-axis by any angle ω and (ii) mirror reflections σ_v in any plane containing the z-axis. These symmetry transformations form the group $C_{\infty v}$. Every rotation $C(\omega)$ and its inverse $C^{-1}(\omega) = C(-\omega)$ form a class. But all reflections σ_v belong to a single class.

The irreps of $C_{\infty v}$ can be obtained by considering the effect of typical class elements $C(\omega)$ and $\sigma_v(xz)$ on a spherical harmonic $Y_{lm}(\theta,\phi)$:

$$C(\omega)Y_{lm}(\theta,\phi) = e^{-im\omega}Y_{lm}(\theta,\phi) \quad , \tag{2.9}$$

and

$$\sigma_v(xz)Y_{lm}(\theta,\phi) = Y_{lm}(\theta,-\phi) = Y_{l-m}(\theta,\phi) \quad . \tag{2.10}$$

The eigenvalue m is the magnetic quantum number of the complex atomic orbital containing Y_{lm}. It is apparent that, for $m \neq 0$ the spherical harmonics (Y_{lm},Y_{l-m}) form the basis for a two-dimensional representation of $C_{\infty v}$. It can be shown to be irreducible. In matrix form, one has

$$C(\omega)(Y_{lm},Y_{l-m}) = (Y_{lm},Y_{l-m}) \begin{pmatrix} e^{-im\omega} & 0 \\ 0 & e^{im\omega} \end{pmatrix}$$

and

$$\sigma_v(xz)(Y_{lm},Y_{l-m}) = (Y_{lm},Y_{l-m}) \begin{pmatrix} 0 & 1 \\ 1 & 0 \end{pmatrix} \quad , \tag{2.11}$$

the characters are therefore

$$X^{(m)}(C(\omega)) = e^{-im\omega} + e^{im\omega} = 2 \cos m\omega$$

and

$$X^{(m)}(\sigma_v) = 0 \quad . \tag{2.12}$$

A list of characters for the first few elements for the point group $C_{\infty v}$ is given in Table 2.3. When $m = 0$, it is clear that Y_{10} form bases for the identity representation. There exists however another one-dimensional representation. If ψ

Table 2.3. Character table of $C_{\infty v}$

$C_{\infty v}$	E	2C(ω)	$\infty\sigma_v$
Σ^+	1	1	1
Σ^-	1	1	-1
Π	2	2cosω	0
Δ	2	2cos2ω	0
Φ	2	2cos3ω	0
...	...	...	...

is a basis for an one-dimensional representation, then one must have

$$\sigma_v \psi = a \psi \quad , \tag{2.13}$$

and since

$$\sigma_v^2 = \text{identity} \quad , \tag{2.14}$$

it follows that

$$\psi = \sigma_v^2 \psi = a^2 \psi \quad , \tag{2.15}$$

so that

$$a = \pm 1 \quad . \tag{2.16}$$

Thus, there exist two types of basis functions denoted as ψ_+ and ψ_- where

$$\sigma_v \psi_+ = \psi_+ \qquad \text{and} \qquad \sigma_v \psi_- = -\psi_- \quad . \tag{2.17}$$

Under a rotation $C(\omega)$, ψ_- behaves in the same manner as ψ_+

$$C(\omega)\ \psi_+ = \psi_+ \qquad \text{and} \qquad C(\omega)\ \psi_- = \psi_- \quad . \tag{2.18}$$

The function ψ_+ is a basis function for the identity representation denoted by Σ^+, while the function ψ_- is a basis function for another one-dimensional representation denoted by Σ^- which does not occur for one-electron functions. Its character is also included in Table 2.3.

If a linear molecule also possesses an inversion centre then the appropriate symmetry group is

$$D_{\infty h} = C_{\infty v} \otimes C_i \quad . \tag{2.19}$$

Its character table is readily obtained from that of $C_{\infty v}$ and given in Table 2.4.

2. Orbital symmetries

Complex symmetry adapted orbitals of linear molecules can be expressed as linear combinations of atomic orbitals located at various points on the molecular axis and have the same magnetic quantum number m. They have therefore one of the following forms:

Table 2.4. Character table of $D_{\infty h}$

$D_{\infty h}$	E	2C(ω)	$\infty\sigma_v$	i
Σ_g^+	1	1	1	1
Σ_g^-	1	1	-1	1
Π_g	2	2cosω	0	2
Δ_g	2	2cos2ω	0	2
...	...	...	...	...
Σ_u^+	1	1	1	-1
Σ_u^-	1	1	-1	-1
Π_u	2	2cosω	0	-2
Δ_u	2	2cos2ω	0	-2
...	...	...	...	...

$\psi_0 = f_0(r,z)$: σ orbitals

$\psi_1 = f_1(r,z)\ \exp(i\phi)$: π_+ orbitals

$\psi_{-1} = f_1(r,z)\ \exp(-i\phi)$: π_- orbitals

$\psi_2 = f_2(r,z)\ \exp(i2\phi)$: δ_+ orbitals

$\psi_{-2} = f_2(r,z)\ \exp(-i2\phi)$: δ_- orbitals

...

$\psi_m = f_m(r,z)\ \exp(im\phi)$

$\psi_{-m} = f_m(r,z)\ \exp(-im\phi)$

In general, there will be available several orbitals of each symmetry:

$|i\sigma\rangle$, $i = 1, 2, \ldots, m(\sigma)$

$|j\pi_+\rangle$, $|j\pi_-\rangle$, $j = 1, 2, \ldots, m(\pi)$

$|k\delta_+\rangle$, $|k\delta_-\rangle$, $k = 1, 2, \ldots, m(\delta)$

... etc.

The orbitals $|j\pi_+\rangle$ and $|j\pi_-\rangle$ have the same factor $f(r,z)$ and together, span the irrep π of $C_{\infty v}$. The orbitals $|j\pi_+\rangle$ and $|j'\pi_+\rangle$, on the other hand, have different radial factors and do not span any irrep together. The same holds for the indices i, k etc.

It was shown in the preceding section that the class σ_v introduces a differentiation of the symmetry classification (+,-) only for the one-dimensional representation Σ, but not

for any of the two-dimensional representations. This is related to the fact that the character of σ_v vanishes in the two-dimensional irreps for m > 0. Since on the other hand, orbitals cannot have Σ^- symmetry, as mentioned earlier, the class σ_v can be disregarded in discussing the symmetry behavior of individual orbitals, i.e. the group C_∞ is adequate to identify the orbital irreps. However, within the group C_∞, the orbitals ψ_m and ψ_{-m} belong to different one-dimensional irreducible representations when $m \neq 0$. Therefore, if one works with complex orbitals, the situation is similar to D_{2h} in that all orbitals can be considered as belonging to one-dimensional irreps. In C_∞, these are labelled by

0, +1, -1, +2, -2, +3, -3, etc.

In $D_{\infty h}$, they are labelled by

0g, 0u, +1g, +1u, -1g, -1u, +2g, +2u, -2g, -2u, etc.

3. Determination of complex orbital products

Since the complex orbitals can be treated as belonging to one-dimensional representations, one can use the procedure described for D_{2h} also in the present case. First, one determines the possible distributions of electrons over the one-dimensional orbital irreps, then one finds all possible

orbital products for each distribution. Finally, one could combine each orbital product with the various spin functions appropriate for the number of singly occupied orbitals in the product. The only part which is different for $C_{\infty v}$ is the symmetry testing.

From the form of the orbitals, it is apparent that any one orbital product can be written as

$$P = F(r_1 r_2 \ldots r_N, z_1 z_2 \ldots z_N) \exp[i(\sum_{k=1}^{N} m_k \phi_k)]$$

and also that

$$C(\omega)\, P = P \exp[i\omega(\sum_{k=1}^{N} m_k)] \qquad (2.20)$$

so that P belongs to the one-dimensional irrep with $M = (\sum_{k}^{N} m_k)$ of $C_{\infty v}$. Thus, in generating all possible distributions one follows exactly the combinatorial procedure outlined in the flow chart of Figure 2.1. The symmetry test is now an examination of the total magnetic quantum number $\sum_{k} m_k$. Only if this quantity is equal to the value M of the state which is to be calculated, will the distribution be kept. In case that M is non-zero, the state is doubly degenerate in $C_{\infty v}$, so that the wavefunction for +M and -M have the same energy. For this reason, the program tests only on values $M \geq 0$.

If the symmetry is $D_{\infty h}$, then there is an additional test

of the g/u character of the product. For g symmetry, there must be an even number of u orbitals and for u symmetry, there must be an odd number of u orbitals.

After the distributions have been found, all possible orbital products of complex orbitals are formed for each distribution by exactly the same procedure as was described in Section II.B.3 for the case of D_{2h} symmetry.

4. Determination of real orbital products

From the products of complex orbitals just found, one can form complex SAAPs by combination with the appropriate spin functions Θ_γ^{SM}. Such SAAPs belong to irreps of $C_{\infty v}$ and $D_{\infty h}$ and are eigenfunctions of S^2 and S_z. However, most molecular programs, including ALIS, use only real orbitals. It is therefore necessary to determine those real SAAPs which are required to express each complex SAAP having the appropriate irrep of $C_{\infty v}$ or $D_{\infty h}$.

Now any product of complex orbitals such as considered above can be expressed in terms of real orbitals by expanding the right hand side of the equation

$$P = \prod_k f_k(r_k, z_k) \exp(i m_k \phi_k)$$

$$= \prod_k f_k(r_k, z_k) (\cos \Sigma m_k \phi_k + i \sin \Sigma m_k \phi_k) \qquad (2.21)$$

in terms of a real and a complex part

$$P = P_x + i\, P_y \quad . \tag{2.22}$$

It is evident that P_x and P_y are linear combinations of products of real orbitals containing the factors $\cos(m\phi)$ and $\sin(m\phi)$ instead of the complex factors $\exp(im\phi)$ and $\exp(-im\phi)$. It should be noted that, P_x contains only products having an even number of factor $\sin(m\phi)$, and that P_y contains only products having an odd number of factor $\sin(m\phi)$. It is therefore straightforward to identify all those products of real orbitals which are needed to express P_x or P_y for any given product P of complex orbitals.

When $\sum_k m_k$ does not vanish, P_x and P_y span one two-dimensional representation of $C_{\infty v}$ which is identical to that spanned by P and its complex conjugate

$$P^* = \prod_k f_k(r_k, z_k) \exp(-im_k\phi_k) \quad . \tag{2.23}$$

Consequently, for $M \neq 0$, one can choose only to consider those real products which are required to expand P_x. However, if $\sum_k m_k$ vanishes, then P_x belongs to the one-dimensional irrep Σ^+, whereas P_y belongs to the one-dimensional irrep Σ^- and thus the real products needed for P_x or P_y must be considered, depending upon whether the required symmetry is Σ^+ or Σ^-.

Consider for example, the product

$$P = |1\pi_+\rangle^2 |2\pi_+\rangle |1\delta_-\rangle |2\delta_+\rangle \quad . \tag{2.24}$$

It has $M = \sum_i m_i = 1+1+1-2+2 = 3 \neq 0$ and only its real part P_x is considered. It contains the following twelve real products

$$\begin{aligned}
&|1\pi_x\rangle^2 |2\pi_x\rangle |1\delta_x\rangle |2\delta_x\rangle && |1\pi_y\rangle^2 |2\pi_x\rangle |1\delta_x\rangle |2\delta_x\rangle \\
&|1\pi_x\rangle^2 |2\pi_y\rangle |1\delta_y\rangle |2\delta_x\rangle && |1\pi_y\rangle^2 |2\pi_y\rangle |1\delta_y\rangle |2\delta_x\rangle \\
&|1\pi_x\rangle^2 |2\pi_y\rangle |1\delta_x\rangle |2\delta_y\rangle && |1\pi_y\rangle^2 |2\pi_y\rangle |1\delta_x\rangle |2\delta_y\rangle \\
&|1\pi_x\rangle^2 |2\pi_x\rangle |1\delta_y\rangle |2\delta_y\rangle && |1\pi_y\rangle^2 |2\pi_x\rangle |1\delta_y\rangle |2\delta_y\rangle \\
&|1\pi_x\rangle |1\pi_y\rangle |2\pi_y\rangle |1\delta_x\rangle |2\delta_x\rangle && |1\pi_x\rangle |1\pi_y\rangle |2\pi_x\rangle |1\delta_x\rangle |2\delta_y\rangle \\
&|1\pi_x\rangle |1\pi_y\rangle |2\pi_x\rangle |1\delta_y\rangle |2\delta_x\rangle && |1\pi_x\rangle |1\pi_y\rangle |2\pi_y\rangle |1\delta_y\rangle |2\delta_y\rangle
\end{aligned} \tag{2.25}$$

where the notations

$$\begin{aligned}
\pi_x &= f_1(r,z) \cos\phi \ , & \pi_y &= f_1(r,z) \sin\phi \ , \\
\delta_x &= f_2(r,z) \cos 2\phi \ , & \delta_y &= f_2(r,z) \sin 2\phi
\end{aligned}$$

have been used. On the other hand, the product

$$P = |\pi_+\rangle^2 |\delta_-\rangle \tag{2.26}$$

has $M = \sum_i m_i = 1+1-2 = 0$. If the desired symmetry is Σ^-, then

the complex part P_y is required, and the real orbital products

$$|\pi_x\rangle^2|\delta_y\rangle \quad , \quad |\pi_y\rangle^2|\delta_y\rangle \quad , \quad |\pi_x\rangle|\pi_y\rangle|\delta_x\rangle \tag{2.27}$$

are relevant.

5. Formation of real SAAPs

Each of the real products found by the procedure of the preceding section is combined with all spin functions appropriate for the number of singly occupied orbitals to form real SAAPs. Thus, a number of real SAAPs are derived from each one product of complex orbitals.

In this context, it is to be noted that the number of singly occupied orbitals which are relevant for the choice of spin functions is not the number of singly occupied orbitals found in the individual real orbital products, but the number of singly occupied orbitals occurring in the complex orbital product from which the real products are derived. Thus, e.g., there are three singly occupied orbitals in the complex product if Equation (2.24). Consequently, assuming a doublet state (S=1/2) say, all twelve real orbital products of Equation (2.25), even those containing five singly occupied orbitals, have to be combined only with the two doublet spin functions corresponding to three electrons. Thus, the orbital product of Equation (2.24) yield twenty-four real doublet

SAAPs which are required to express the real parts of the two complex SAAPs that result from combining the two three-electron doublet spin functions with the complex product of Equation (2.24).

In this manner, all necessary real SAAPs are deduced from every previously determined complex orbital distribution. This procedure generates all those SAAPs, made from real orbitals belonging to irreps of $C_{\infty v}$ or $D_{\infty h}$, which are required in the Full Reaction Space for the construction of N-electron spin eigenfunctions belonging to the desired irreducible representation of $C_{\infty v}$ or $D_{\infty h}$ and having the desired spin multiplicity. Those linear combinations of these SAAPs which form bases for irreducible representations of $C_{\infty v}$ or $D_{\infty h}$ obtain by diagonalization of the Hamiltonian matrix during the molecular calculation.

D. Additional Features of the Program SAAP

There is an option in the program SAAP which allows to generate all excitations of a certain type (i.e. single, double, triple, etc) out of the Full Reaction Space into a space of additional "external" orbitals. For example, in the case of double excitations, the program will generate all possible occupancies of external orbitals by two electrons. Each of these is then combined with all distributions of (N-2) electrons over the FORS orbitals. The symmetry test is of course applied to all N electrons.

The program also has the option that additional specified distributions of electrons over the available orbitals can be included in the configuration list by explicit input. This option allows for deletion or addition of configurations from or to the Full Reaction Space. It also makes possible the construction of SAAPs for symmetry groups with multi-dimensional irreducible representation by providing appropriate distribution as explicit input.

III. POLARIZED NONVERTICAL EXCITED STATES: A FORS STUDY OF D_{2h} AND C_{2v} PLANAR ALLENE

A. Introduction

The allene excited states investigated in this chapter is an application of the FORS model. The location and characteristics of minima on excited state potential energy surfaces often are controlling features in photochemical reactions[35-40]. It is essential for photochemists to have a detailed understanding of the electronic nature and dynamics of molecules at these minima if mechanisms and reactivity are to be understood. For many organic molecules containing π bonds, the location of minima has long been accepted to occur at 90° twisting, however, it was only recently recognized that strong excited state polarization, approaching zwitterionic character, will exist at this nonvertical geometry[41]. Salem termed this unusual phenomenon "sudden polarization"; however, it now seems, at least for ethylene, that the degree of suddenness depends critically on the reaction path[42]. This polarization has been the subject of numerous theoretical studies[17,41-43] and its existence seems no longer controversial. Polarized nonvertical excited states have been suggested as intermediates in a variety of organic photoreactions[41,44] which include isomerizations and addition of protic solvents to π bonds, although definitive experimental evidence is difficult to obtain and interpret.

Allenes, like most alkenes, have long been believed to twist to planar geometries in their lowest singlet and triplet excited states[45]. Obvious photochemical manifestations of this are the facile photoracemization and photoresolution of chiral allenes[46]. As one example, it has been observed that optically active 1,2-cyclononadiene undergoes rapid racemization on direct irradiation, in addition to isomerization to a bicyclic cyclopropene[47].

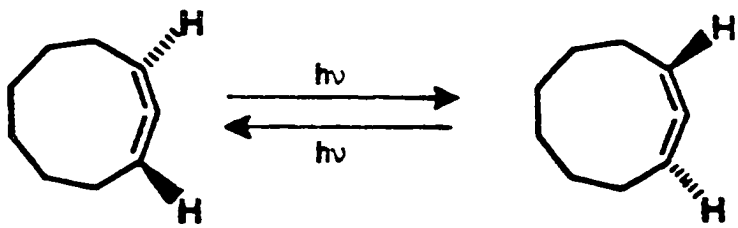

The first theoretical study in which the involvement of planar excited states in allene photochemistry was explicitly considered was an often overlooked but insightful paper by Borden[45]. Based on Pariser-Parr-Pople calculations, Borden concluded that excited state twisting in both S_1 and T_1 should be facile and that the lowest singlet D_{2h} state is open-shell (A_u), with two low-lying closed-shell excited states. This is precisely the situation required for "sudden polarization"[41].

For thermal isomerization, the intermediacy of planar geometries has been the subject of a number of ab initio[48,49a-h] and semi-empirical[49i] theoretical studies,

which have led to a wide range (48-82 kcal/mol) of predicted values for the barrier to rotation in allene. In many of these studies, energies of the low-lying D_{2h} states, ^1A_u, ^3A_u, 1^1A_g and 2^1A_g, were calculated, however, the major point of interest was the ground state rotational barrier. In the most definitive study, Seeger et al. have shown that this ground state barrier should occur at a bent (C_{2v}) geometry[49g], and an open-shell ^1A_u state. More recently, Krough-Jespersen has recalculated this barrier using extended basis set geometry optimization and with inclusion of correlation energy[49h]. A value of ca. 50 kcal/mol is predicted in both studies, which is in good agreement with estimates from experimental work of Roth and co-workers[50].

B. Electronic Structure of D_{2h} and C_{2v} Planar Allene

Figure 3.1 shows schematic π molecular orbitals for planar allene, and their correlation on passing from D_{2h} to C_{2v}. On inplane bending, the $2b_{2u}$ nonbonding orbital (correlating with $6a_1$) acquires significant hybrid character[48,50] and is lowered in energy, while the $1b_{2g}$ nonbonding orbital (correlating with $1a_2$) is raised somewhat. As it is shown below, the resultant orbital crossing on bending has potentially important photochemical consequences, since this defines the existence of two excited state minima.

Population of these orbitals gives rise to low-lying states which have either pronounced diradical (D) or

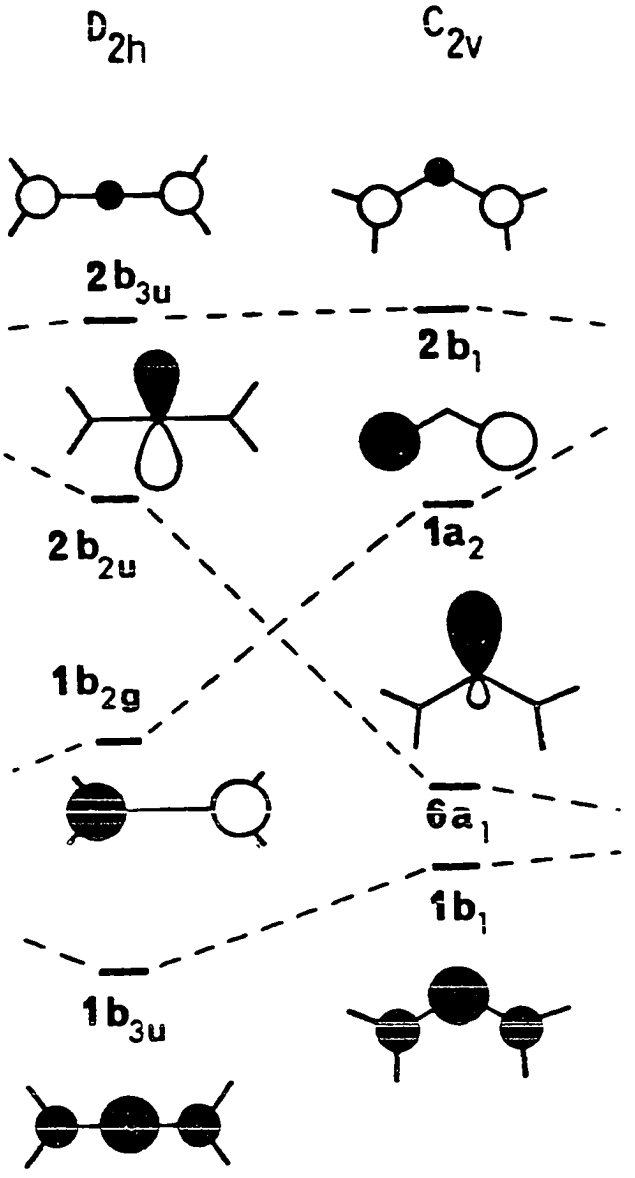

Figure 3.1. Molecular orbitals of planar allene

zwitterionic (Z) character. For D_{2h}, these are:

^1A_u, ^3A_u	$\ldots(1b_{3u})^2(1b_{2g})^1(1b_{2u})^1$	$^1D_1$, $^3D_1(D_{2h})$
1^1A_g	$\ldots(1b_{3u})^2(1b_{2g})^2$	$^1Z_1(D_{2h})$
2^1A_g	$\ldots(1b_{3u})^2(1b_{2u})^2$	$^1Z_2(D_{2h})$

Here, ... represents the four a_g, one b_{3g}, three b_{1u} and one b_{2u} closed-shells comprising the σ molecular framework. For C_{2v}:

$^1A_2$, $^3A_2$	$\ldots(1b_1)^2(6a_1)^1(1a_2)^1$	$^1D_1$, $^3D_1(C_{2v})$
1^1A_1	$\ldots(1b_1)^2(6a_1)^2$	$^1Z_1(C_{2v})$
2^1A_1	$\ldots(1b_1)^2(1a_2)^2$	$^1Z_2(C_{2v})$

In this case, ... represents five a_1 and four b_2 closed-shells of the σ skeleton.

It is readily predicted that the open-shell states (A_u or A_2 symmetry) will be nonpolar, while the four closed-shell states (A_g or A_1 symmetry) will be strongly polarized in specific planes, as represented by structures 1 - 4 below (inplane orbital occupation shown).

C. Geometries and Basis Sets

FORS calculations were performed at three points: the two relative minima (180° and 102.8°) and the intermediate point (135.4°); these are shown below as I, II and III.

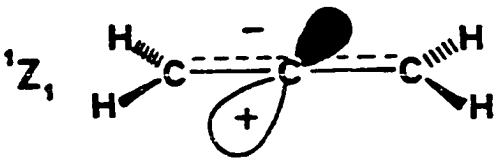
$^1Z_1$
H
C
C
C
H
H
H
−
+

1

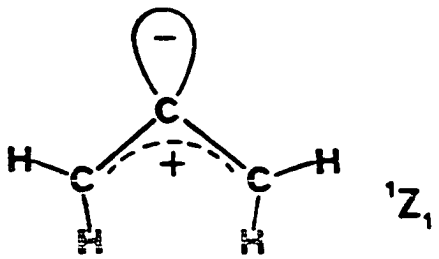
−
C
H
C
+
C
H
H
H
$^1Z_1$

3

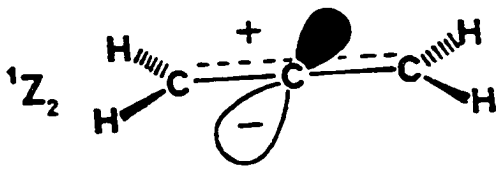
$^1Z_2$
H
C
C
C
H
H
H
+
−

2

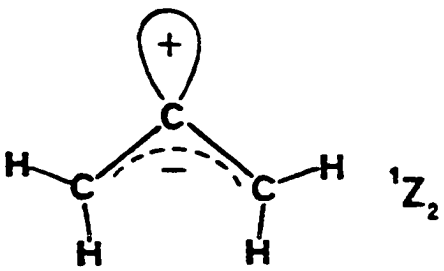
+
C
H
C
−
C
H
H
H
$^1Z_2$

4

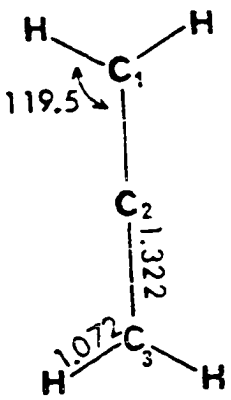
H
H
C_1
119.5
C_2
1.322
1.072
C_3
H
H

I

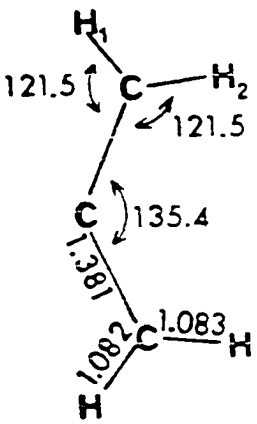
H_1
121.5
C
H_2
121.5
C
135.4
1.381
1.082
C
1.083
H
H

II

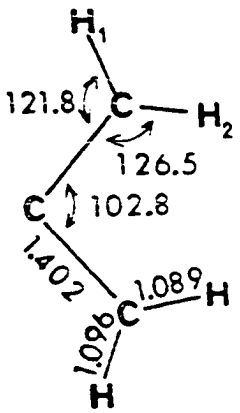
H_1
121.8
C
H_2
126.5
C
102.8
1.402
1.089
H
1.096
C
H

III

It is important to recognize that 180° and 102.8° correspond to excited state minima; remaining state energies will be vertical with respect to these.

The atomic basis used in the calculations was of double zeta quality. This consisted of a 10s/5p set of even-tempered Gaussian primitives[11] generally contracted to 3s/2p on carbon, and a 4s set of Gaussian primitives scaled by 1.2 and generally contracted to 2s on hydrogen.

In the FORS wavefunction for each planar allene state, inner shell and σ framework orbitals are held to double occupancy, while the remaining four electrons are distributed among the four π-type orbitals shown in Figure 3.1. This leads to eight SAAPS for the zwitterionic states, and four SAAPs of like symmetry for the diradical at each geometry. The small number of configurations permits optimization for each state separately in an MCSCF calculation. The σ skeleton can then readjust to the varying π electron distributions. These configurations also include the important near-degeneracy correlations associated with $\pi \rightarrow \pi^{*}$ double excitations (up-down correlation). Thus, the FORS-MCSCF calculations may be expected to yield reliable estimates for electronic distributions and excitation energies. For comparison, SCF calculations also were performed for each state.

D. Results of Calculations

SCF and FORS-MCSCF total energies and excitation energies for $^1D_1$, $^1Z_1$ and $^1Z_2$ states of planar allene at geometries I-III are listed in Table 3.1. Each energy listed is from an individual optimization for that particular state. Orbital occupation numbers for the two minima are given in Table 3.2, gross Mulliken populations in Table 3.3 and molecular dipole moments are listed in Table 3.4. For comparison, we note that absolute SCF energies for the 1^1A_g (D_{2h}) and 1^1A_1 (C_{2v}) states are within 0.04 hartree of the previously reported 6.31G* at the same geometries[50]. Energies given are the appropriate roots of SCF or MCSCF calculations. Figure 3.2 plots the relative energies.

Polarization in S_1 is well-described by the simple zwitterionic structures 1 and 3, since these configurations dominate the MCSCF wavefunctions. This is reflected in the occupation numbers, Mulliken populations and dipole moments. Inspection of Table 3.3 shows that the $^1D_1$ states have balanced σ and π electron distributions, while ^1Z states are strongly polarized. The localization of central carbon polarization in orthogonal σ and π molecular orbitals is fundamentally different from a twisted π bond (e.g. ethylene) in which positive or negative character is associated with different carbons. Additionally, this σ/π polarization permits significant minimization of effective charge

Table 3.1. Energies of electronic states of planar allenes

	Geometry	State	No. of SAAPs	Energies (in hartree)[a] MCSCF	SCF
I	D_{2h}	^1A_u ($^1D_1$)	4	-115.7973	-115.7510
				(0.657)	(0.465)
		1^1A_g ($^1Z_1$)	8	-115.7472	-115.7208
				(2.020)	(1.286)
		2^1A_g ($^1Z_2$)	8	-115.6568	-115.6152
				(4.480)	(4.159)
II	C_{2v} (135.4°)	$^1A_2$ ($^1D_1$)	4	-115.8214	-115.7680
				(0.0)	(0.0)
		1^1A_1 ($^1Z_1$)	8	-115.7166	-115.6680
				(2.852)	(2.724)
		2^1A_1 ($^1Z_2$)	8	-115.6785	-115.6575
				(3.889)	(3.007)
III	C_{2v} (102.8°)	$^1A_2$ ($^1D_1$)	4	-115.7741	-115.7175
				(1.287)	(1.377)
		1^1A_1 ($^1Z_1$)	8	-115.7405	-115.6951
				(2.202)	(1.985)
		2^1A_1 ($^1Z_2$)	8	-115.5396	-115.5045
				(7.669)	(7.170)

[a] Numbers in parentheses (in eV) are relative to the lowest state calculated $^1A_2$ (C_{2v}, 135.4°).

Table 3.2. Occupation numbers for π orbitals of D_{2h} and C_{2v} planar allenes

D_{2h}		Orbital occupation numbers $1b_{3u}$	$1b_{2g}$	$2b_{2u}$	$2b_{3u}$
^1A_u ($^1D_1$)	SCF	2.0	1.0	1.0	0.0
	MCSCF	1.906	1.0	1.0	0.094
1^1A_g ($^1Z_1$)	SCF	2.0	2.0	0.0	0.0
	MCSCF	1.983	1.937	0.007	0.072
2^1A_g ($^1Z_2$)	SCF	2.0	0.0	2.0	0.0
	MCSCF	1.805	0.229	1.956	0.010
C_{2v} (102.8°)		Orbital occupation numbers $1b_1$	$6a_1$	$1a_2$	$2b_1$
$^1A_2$ ($^1D_1$)	SCF	2.0	1.0	1.0	0.0
	MCSCF	1.866	1.0	1.0	0.134
1^1A_1 ($^1Z_1$)	SCF	2.0	2.0	0.0	0.0
	MCSCF	1.820	1.980	0.172	0.028
2^1A_1 ($^1Z_2$)	SCF	2.0	0.0	2.0	0.0
	MCSCF	1.975	0.036	1.854	0.135

Table 3.3. Charge distribution in planar allene states[a]

	State		Mulliken populations (MCSCF) C_1	C_2	H_1	H_2
D_{2h}	^1A_u ($^1D_1$)	σ	5.390	4.880	0.84	---
		π	1.010	0.980		
	1^1A_g ($^1Z_1$)	σ	5.285	4.336	0.77	---
		π	1.405	1.184		
	2^1A_g ($^1Z_2$)	σ	5.511	5.464	0.87	---
		π	0.689	0.666		
C_{2v}	$^1A_2$ ($^1D_1$)	σ	5.370	4.889	0.85	0.83
		π	1.020	0.961		
	1^1A_1 ($^1Z_1$)	σ	5.549	5.451	0.83	0.88
		π	0.761	0.499		
	2^1A_1 ($^1Z_2$)	σ	5.183	4.449	0.83	0.78
		π	1.337	1.291		

[a] At geometries I and III shown in the text.

Table 3.4. Dipole moments for C_{2v} (102.8°) geometry

State	Dipole moments (debye) SCF	MCSCF
$^1A_2$ ($^1D_1$)	0.75	0.72
1^1A_1 ($^1Z_1$)	4.01	3.39
2^1A_1 ($^1Z_2$)	-1.11	-0.71

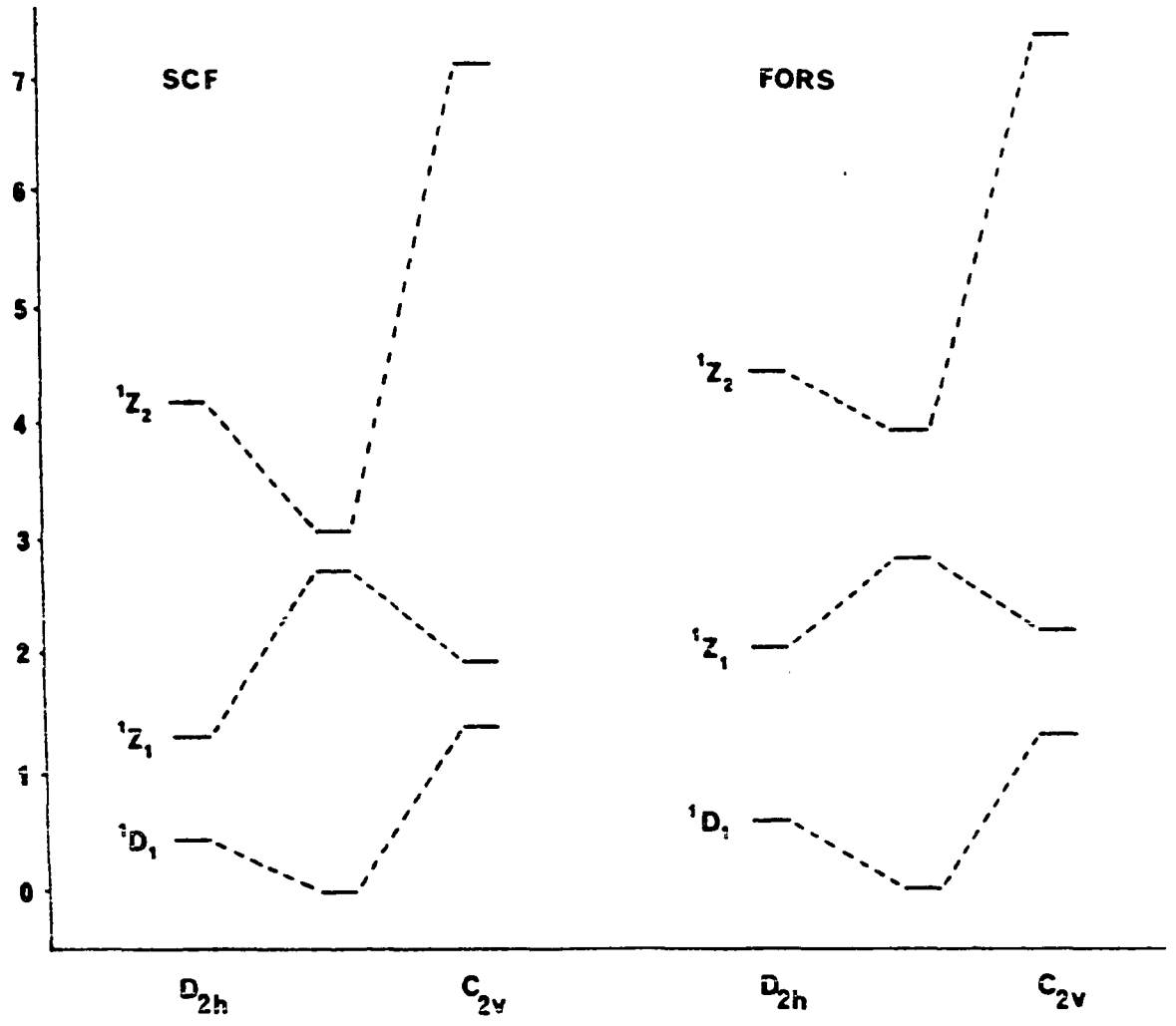

Figure 3.2. Relative energies for planar allene

separation through weightings of the $1b_{3u}$ (D_{2h}) and $1b_1$ (C_{2v}) orbital coefficients, which can partly compensate for central carbon charge deficiency or excess. The 3.39 debyes MCSCF dipole moment (Table 3.4) calculated for the lowest C_{2v} 1^1A_1 state is quite substantial for a C_3 hydrocarbon. Due to its substantial Rydberg character, $^1Z_2$ (C_{2v}) is not well represented by the simple valence representation 4. This can be corrected by having a Rydberg function in addition to the basis set used.

The order of the various states is in excellent agreement with qualitative predictions and the results of previous calculations[48-50]. SCF and MCSCF results are qualitatively similar, however, the energy difference between $^1Z_1$ (D_{2h}) and $^1Z_1$ (C_{2v}) decreases from 0.70 eV (SCF) to 0.18 eV (MCSCF). At the intermediate geometry (II) in the vicinity of the avoided crossing, SCF energies for $^1Z_1$ and $^1Z_2$ are quite close (0.28 eV); inclusion of correlation energy in MCSCF calculation predictably increases this to 1.04 eV. It is noteworthy that the gap between the $^1D_1$ and $^1Z_1$ is quite small: 1.36 eV in D_{2h} and 0.61 eV in C_{2v}. Nonadiabatic coupling might lead to relatively rapid internal conversion at these geometries[43], but it is still anticipated that a finite lifetime (10^{-9}-10^{-12} s) for these polarized species. It has also been suggested that in highly polar media, $^1Z_1$ might become the ground state[51] due to solvation.

E. Discussion

Previous theoretical investigations of the C_3H_4 potential energy surface have explored the barrier to inversion in allene[49], thermal and photochemical opening of cyclopropene to a vinyl carbene[52], and the cyclopropylidene to allene conversion[53]. There is also an immense interest in the excited state surfaces, specifically the location and electronic nature of "sudden polarized" minima or "funnels" and their potential involvement in allene photoreactions[17]. It was suggested Scheme 3.1 may be the two possible pathways toward planarity in allene through twisting and bending or simply twisting of the π bond. As in ethylene derivatives, this π bond rotation provides a simple mechanism for interconversion of stereoisomers which, in allene, are enantiomers. Racemization from both singlet and triplet states of allene has been observed experimentally[46].

Zwitterionic planar species have been proposed for the structure of small-ring allenes such as 1,2-cyclohexadiene[54], in which the allene is constrained to near-planarity. However, it has been shown theoretically[55], and supported by experiment[56] that this molecule has a chiral equilibrium structure. The zwitterions are excited states and should not be involved in ground state reactions.

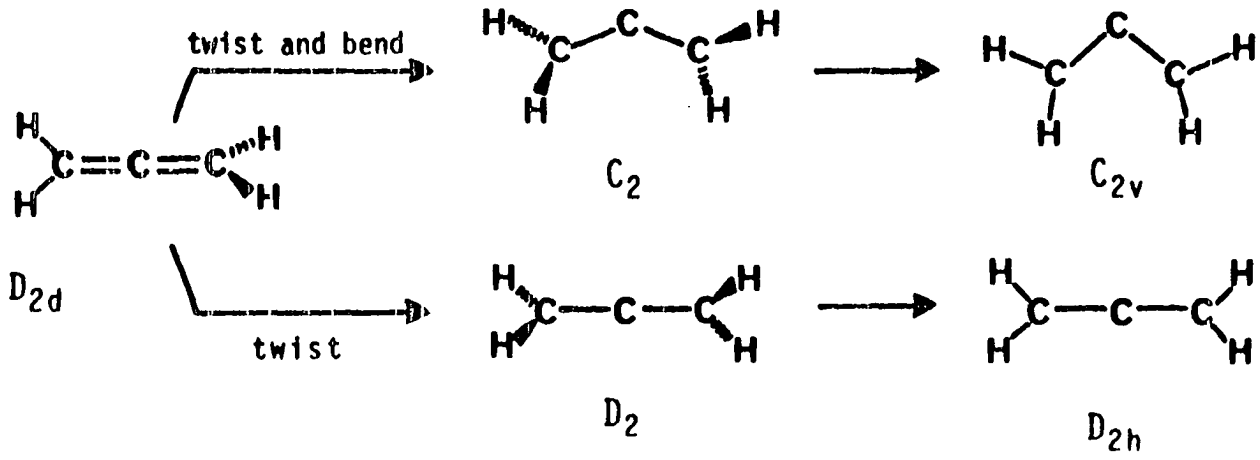

Scheme 3.1. Two possible pathways toward planarity in allene

IV. THE INTRAATOMIC CORRELATION CORRECTION TO THE FORS MODEL

A. Introduction

For more than a century, chemists have thought of molecules as collections of atoms held by chemical forces in close proximity to each other, and this view quite naturally prevailed during the early stages of quantum chemistry, when the valence bond (VB) approach as well as the molecular orbital (MO) approach were formulated in terms of minimal basis sets of atomic orbitals. However, as the originally used minimal basis of Slater AOs gave way to the modern practice of using extended AO bases, and as self-consistent-field wavefunctions augmented by configuration interaction supplanted the simple VB and MO models, the role played by atoms in molecules became obscured. In the context of accurate ab initio work, the traditional picture of a molecule formed by atoms appeared blurred and its validity limited to the realm of rough arguments.

Through the recent development of the FORS model[14] the concept of the atomic minimal basis set has however been rehabilitated within the framework of quantitative ab initio calculations with extended bases because, as discussed in references 14b and 14c, FORS wavefunctions can be cast in a form which reveals the manner in which atoms participate in molecular binding.

In the present chapter, it will be shown that this atomic

analysis has a further benefit: it permits the improvement of FORS wavefunctions through a semi-empirical correction for that part of the electron correlation which still remains unaccounted for in the FORS model. It is based on reasoning which is related to the "Atoms-in-Molecules" (AIM) approach advanced over three decades ago by Moffitt[57-59] and subsequently improved by Hurley[60-67]. Before discussing the extension of the FORS model in more detail, essential features of the Atoms-in-Molecules method will be outlined. An earlier review of this subject was given by Parr[68] and a later one by Balint-Kurti and Karplus[69].

B. Atoms-in-Molecules Model

1. Intraatomic and interatomic energy contributions

In the early fifties, Moffitt realized the fact that the errors in molecular ab initio calculations of his day, even though amounting to only about one percent of the total molecular energies, were still larger than most chemical energy differences, such as bond energies, excitation energies and activation energies, and he recognized that it was impossible to remove such errors with computational techniques available at the time. This error, Moffitt argued however, lay mainly in certain intraatomic energy contributions which occur in the molecule as well as in the free atoms, and he proposed therefore a correction scheme based on a partitioning

of quantum mechanical molecular energy expressions into intraatomic and interatomic terms. The former are much larger, but they are presumed to be obtainable from spectroscopic data of free atoms with much greater accuracy than they can be calculated. The latter on the other hand are substantially smaller than the former, and they are presumed to be obtainable with sufficient accuracy from molecular calculations. Moffitt[57] successfully applied improved potential curves for several valence states of molecular oxygen and he subsequently explored the concept of atomic valence states in molecules[59].

Moffitt's approach is based on the expansion of molecular electronic wavefunctions in terms of what he termed "Composite Functions" (CFs). Consider for example a diatomic molecule and let $|A_i\rangle$ and $|B_j\rangle$ be the exact wavefunction of the i-th state of the free atom A and the j-th state of the free atom B respectively. For simplicity of language and discussion, the states $|A_i\rangle$ and $|B_j\rangle$ will also include ground and excited states of all positive and negative ions of atoms A and B. A composite function for the diatomic molecules AB is then any function

$$|A_iB_j\rangle = N_{ij}\mathbf{A}^*\{|A_i\rangle|B_j\rangle\} \quad , \tag{4.1}$$

where $\mathbf{A}^*$ is the coset antisymmetrizer which produces a totally

antisymmetric molecular wavefunction from the product of the two antisymmetric atomic state functions, and N_{ij} is a distance-dependent factor that normalizes $|A_iB_j\rangle$. At finite molecular geometries different composite functions are usually non-orthogonal, just as atomic orbitals on A and B have non-vanishing overlap integrals. In order to determine molecular wavefunctions as expansions in terms of CFs, such as given by Equation (4.1), it is necessary to evaluate the matrices

$$S_{ij,kl} = \langle A_iB_j|A_kB_l\rangle \quad , \tag{4.2}$$

$$H_{ij,kl} = \langle A_iB_j|H|A_kB_l\rangle \quad , \tag{4.3}$$

where H is the Hamiltonian, and to solve the corresponding eigenvalue problem in which the eigenfunctions are a complete set of composite functions.

Moffitt then made the observation that the quantities

$$V_{ij,kl} = H_{ij,kl} - S_{ij,kl}\{E(A_i) + E(B_j) + E(A_k) + E(B_l)\}/2 \tag{4.4}$$

have the character of interatomic interaction energies. In this equation, the quantities E denote the energies of the respective free-atom states, e.g.

$$E(A_i) = \langle A_i|H_A|A_i\rangle \quad , \quad \text{etc.} \; , \tag{4.4a}$$

where H_A is the Hamiltonian of atom A. This contention Moffitt[58] justified for the case that $|A_i\rangle$ and $|B_j\rangle$ are exact atomic states, and he made it also plausible for analogous quantities

$$\begin{aligned}\tilde{V}_{ij,kl} &= \tilde{H}_{ij,kl} \\ &\quad - \tilde{S}_{ij,kl}\{\tilde{E}(A_i) + \tilde{E}(B_j) + \tilde{E}(A_k) + \tilde{E}(B_l)\}/2\end{aligned} \tag{4.5}$$

which are derived from approximations $|\tilde{A}_i\rangle$, $|\tilde{B}_j\rangle$ to the exact atomic states $|A_i\rangle$ and $|B_j\rangle$.

The conjecture made by Moffitt was that reasonably good approximate ab initio wavefunctions will yield usable approximate values for the interatomic quantities $S_{ij,kl}$ and $V_{ij,kl}$, but not for the total matrix elements $H_{ij,kl}$ which are mixtures of interatomic and intraatomic quantities. Specifically, Moffitt[58] proposed that the quantities $\tilde{S}_{ij,kl}$ and $\tilde{V}_{ij,kl}$ can be taken as adequate approximations for $S_{ij,kl}$ and $V_{ij,kl}$ in Equation (4.4). Introduction of these substitutions in Equation (4.4) and combination of Equations (4.4) and (4.5) yields then directly the following approximation for the matrix elements $H_{ij,kl}$:

$$H_{ij,kl} \approx \tilde{H}_{ij,kl} + \Delta E_{ij,kl}\,\tilde{S}_{ij,kl} = \tilde{\tilde{H}}_{ij,kl} \quad , \tag{4.6}$$

where

$$\Delta E_{ij,kl} = [\Delta E(A_i) + \Delta E(B_j) + \Delta E(A_k) + \Delta E(B_l)]/2 \ , \quad (4.6a)$$

with

$$\Delta E(A_i) = E(A_i) - \tilde{E}(A_i) \quad , \quad \text{etc.} \quad (4.6b)$$

Equation (4.6) defines the AIM Hamiltonian in Moffitt's final formulation. The second term on the right hand side of Equation (4.6) manifestly represents corrections which are expected to remedy the intraatomic deficiencies in the approximate Hamiltonian matrix $\tilde{H}_{ij,kl}$. From an operational point of view, the procedure is to work in terms of certain approximate CFs using the corrected Hamiltonian $\tilde{\tilde{H}}_{ij,kl}$ instead of the "direct" Hamiltonian $\tilde{H}_{ij,kl}$ in solving the eigenvalue problem. Any specific implementation of the AIM approach clearly depends upon the number and types of approximate CFs included in the wavefunction expansion and upon the manner in which the correction terms $\Delta E_{ij,kl}$ are determined.

2. The AIM approach and electron correlation

To date, the AIM method has only been applied to valence states of molecules and, for these cases, it has been assumed that the expansion bases are derived from atomic states $|A_i\rangle$ corresponding to those approximate atomic configurations

$|\tilde{A}_i\rangle$ which are obtained from the various possible occupancies and couplings of a minimal basis set of atomic valence orbitals through atomic open-shell SCF calculations. When the CFs formed from such approximate state functions $|\tilde{A}_i\rangle$ and $|\tilde{B}_j\rangle$ are used to calculate the matrices $\tilde{S}$, $\tilde{H}$ and $\tilde{E}$, it is apparent that the corrective energy differences $\Delta E(A_i)$ etc. of Equation (4.6b) are nothing else but the correlation energies for the respective states of the free atoms. Moreover, assuming that all possible valence AO configurations, adapted to spherical symmetry, are included in the calculation of the $E(A_i)$, it is known that the $|A_i\rangle$ actually include "degeneracy-type" correlations such as result, for example, from the mixing of configurations of the types s^2p^n and s^0p^{n+2} ($n \leq 4$) in some atomic states. More specifically then, the energy differences $\Delta E(A_i)$ represent the "dynamical" parts of the correlation energies of the various atomic states.

On the other hand, it is also apparent that expansions of approximate molecular wavefunctions in terms of the full set of CFs formed from these approximate atomic states $|\tilde{A}_i\rangle$ and $|\tilde{B}_j\rangle$ take into account all those types of correlations which result from different occupations and couplings of the valence orbitals of both atoms in a diatomic molecule. Such approximate molecular wavefunctions include therefore again all degeneracy-type correlations, some of them being of the

aforementioned intraatomic type, but most of them now having interatomic character.

In light of these considerations, it must be inferred that the corrective terms in Equation (4.6) can be expected to compensate mainly for dynamical correlations which are missing in the described approximate wavefunctions. The manner in which this correlation is accomplished moreover implies that this implementation of the AIM concept provides a way of estimating molecular dynamical correlations based on the assumption that, even in molecules, they are essentially atomic in nature. It is for this reason that Hurley called his further developments of the AIM approach the Intraatomic Correlation Correction (ICC) method.

3. Choices of atomic orbitals

The discussed AIM implementation is based on approximate CFs which are constructed from a minimal basis set of atomic orbitals (MBS AOs). Any quantitative implementation depends therefore on the manner in which these MBS AOs are chosen. The decision is non-trivial as is illustrated by the data in Tables 4.1 and 4.2 for fluorine atom. Table 4.1 offers a comparison of errors due to approximation of the Hartree-Fock AOs (lines 3 and 4 minus line 2) with the correlation error (line 2 minus line 1) and the relativistic correction (line 1) for the ground state $^2P(1s^2 2s^2 2p^5)$. Table 4.2 exhibits the

Table 4.1. Errors in calculating the fluorine ground state

Type of calculation	Error(hartree)[a]
1. Correlated, unrelativistic	0.0805
2. Uncorrelated, unrelativistic	0.4085
3. Uncorrelated, unrelativistic, optimized single exponential AOs instead of exact SCF AOs	0.9413
4. Similar to 3, but with Slater AOs instead of exact SCF AOs	0.9517

[a] Error = (Energy of quoted calculation) - (Exact energy), Exact energy = -99.8834 hartrees[70a].

Table 4.2. Errors in calculating various states of fluorine with the same minimal basis set[a]

	State	Error(hartree)[b]
F	$^2P(1s^2 2s^2 2p^5)$	0.0016
F^*	$^2S(1s^2 2s 2p^6)$	0.0190
F^-	$^1S(1s^2 2s^2 2p^6)$	0.1518
F^+	$^3P(1s^2 2s^2 2p^4)$	0.1075

[a] The minimal basis set is that of the near Hartree-Fock AOs obtained variationally for the $^2P(1s^2 2s^2 2p^5)$ ground state with an even-tempered 14s, 7p basis of gaussian primitives.

[b] Error = (Energy obtained for Hartree-Fock type energy with basis set quoted under a) - (Exact SCF energy for each state).

basis set errors incurred when the MBS which is optimal for the ground state SCF approximation is used to calculate Hartree-Fock-type energies of other states. Also noteworthy in this context is the error resulting from using a minimal basis set rather than an extended basis set in molecular calculations. Even if the minimal basis is of Hartree-Fock-type quality (the optimal case), the calculated energy of F_2 in a full set of CFs differs by about 40 millihartrees from that obtained with an extended basis and, in other diatomics, the error can be even more substantial.

Although it might seem reasonable that the atomic correction terms $\Delta E(A_i)$ of Equations (4.6a,b) should be calculated with approximate AOs which are identical to those that actually occur in the molecular calculations, such a procedure consistently yields substantial overestimates for the molecular binding energies. Hurley[60] attributed this to the large corrections obtained for the approximate CFs of excited and, in particular, ionic states when ground state AOs are used to calculate them. This insight led him to formulate the Intraatomic Correlation Correction (ICC) procedure[61,62], a substantive and essential advance over the AIM approach. The ICC calculations are based on a minimal basis set of Slater-type atomic orbital, and the approximate atomic energies $\tilde{E}(A_i)$, $\tilde{E}(B_j)$ needed for the determination of the corrected terms $\Delta E(A_i)$, $\Delta E(B_j)$ are calculated by optimizing

the orbital exponents for each atomic and ionic states separately, regardless of the value which these exponents have in the molecular calculation that yields $\tilde{S}_{ij,kl}$ and $\tilde{V}_{ij,kl}$. The orbital exponents in the molecular calculation, on the other hand, are most advantageously obtained by minimizing the uncorrected molecular energy for the molecular state under consideration.

A physical justification of this way of determining the intraatomic correction terms is provided by the observation that dynamical correlation energies are surprisingly independent of orbital size and shape. Consider for example the correlation error of two electrons in one s-type orbital. This error[70] is 1.08 eV for H^-, 1.14 eV for He, 1.18 eV for Li^+ and 1.24 eV for Ne^{8+}; and it varies from 1.12 eV to 1.00 eV for the inner shell correlations from Li^- to Ne^{6+} [71]. It even remains approximately constant when atoms are "compressed" by enclosing them in a finite box: Ludena and Gregori[72] found that the correlation energies of He, Li^+ and Be^{2+} changed by at most 0.02 eV when the radius of the enclosing box was reduced from R=∞ to R=1 bohr. The same is true even with an additional center as the correlation energy for the H_2 molecule is 1.1 eV[19]. Considering larger systems, the correlation error for F, Ne^+ and Na^{2+} are 8.82, 8.92 and 9.14 eV respectively[73]. It may also be noted that a similar constancy persists for optimal Slater-type minimal-basis-set

SCF approximations; for example, the correlation-plus-MBS truncation errors of H^-, He and Li^+ are 1.49, 1.51 and 1.54 eV respectively[61].

In later work, Hurley[66] took a further step in the MBS approach, namely he used optimal atomic Hartree-Fock SCF AOs (linear combinations of Slater-type AOs) for the determination of the correction terms $\Delta E(A_i)$, and scaled atomic HF-SCF AOs for the molecular calculations. The problem with this procedure is that atomic HF-SCF AOs are known to perform more poorly as minimal basis sets for molecular calculation than do Slater-type AOs, as discussed in Reference 14c.

Arai[74] also considered the need for distortions of atomic wavefunctions in molecules. However, the mathematical complexity of his "Deformed-Atoms-in-Molecules" method has precluded wider application.

4. The non-orthogonality problem

The implementation of the basic ICC idea, namely, to correct for intraatomic correlation errors, would be conceptually most straightforward if the CFs would remain orthogonal at all internuclear distances. If they were, then the fundamental Equation (4.6) would reduce to

$$H_{ij,kl} \approx \tilde{\tilde{H}}_{ij,kl} = \tilde{H}_{ij,kl} - \Delta E_{ij}\, \delta_{ij,kl} \quad , \qquad (4.7)$$

with

$$\Delta E_{ij} = \Delta E(A_i) + \Delta E(B_j) \quad , \tag{4.7a}$$

and the meaning of this equation would be physically clear, namely: the Hamiltonian diagonal element of each CF embodies a correlation error which is the sum of the correlation errors of the atomic states contained in that CF, and these errors are corrected separately for each CF by Equation (4.7). From this perspective, Moffitt's Equation (4.6) can be viewed as an intuitive attempt to generalize the physically transparent Equation (4.7) to the less transparent case of non-orthogonal CFs. Hurley[65] has rather elegantly justified this generalization by the following alternative derivation. From the molecular wavefunction

$$\Psi = \sum_{ij} C_{ij} |A_i B_j\rangle \quad , \tag{4.8}$$

he derives "occupation numbers" for CFs, in analogy to Mulliken's[75] "gross atomic populations" for non-orthogonal atomic orbitals, by the definition

$$n_{ij} = C_{ij} \sum_{kl} S_{ij,kl} C_{kl} \quad . \tag{4.9}$$

He then defines the correlation-corrected molecular energy reasonably as

$$\tilde{\tilde{E}} = \sum_{ij}\sum_{kl} \tilde{H}_{ij,kl}\, C_{ij}\, C_{kl} + \sum_{ij} n_{ij}\, \Delta E_{ij} \quad , \qquad (4.10)$$

where the ΔE_{ij} are the same as in Equation (4.7a). It is readily verified that Equations (4.9) and (4.10) together are equivalent to

$$\tilde{\tilde{E}} = \sum_{ij}\sum_{kl} \tilde{\tilde{H}}_{ij,kl}\, C_{ij}\, C_{kl} \quad , \qquad (4.11)$$

where the matrix $H_{ij,kl}$ is just the one given by Moffitt's Equation (4.6). The latter has thus been deduced from the occupation number assumption (4.9).

By contrast, Balint-Kurti and Karplus[69,76] have argued that, rather than introducing such an occupation number assumption, it would be preferable to introduce appropriate definitions of orthogonal composite functions. Specifically, they propose that the original non-orthogonal CFs $|A_i B_j\rangle$ be Schmidt-orthogonalized in the order of increasing AIM corrections. In many cases (H_2, HF, F_2), this Orthogonalized Moffitt (OM) procedure gives worse results for binding energies[69] than the ICC method. The OM procedure has been carried out using small numbers of Gaussians to expand the free atom MBS, and the resulting large basis superposition errors call into question the accuracy of the uncorrected wavefunctions. For instance, a (5s, 3p) Gaussian basis

contracted minimally gives an uncorrected bond strength of 1.39 eV for F_2[76], while a near Hartree-Fock quality (14s, 7p) MBS fails to predict binding, with a bond strength of -0.21 eV[14c]. Thus, the OM results seem spuriously good due to such basis superposition errors. We also note that the OM variant of the AIM theory has been applied to a number of triatomic surfaces[69].

In this context it should also be mentioned that Grevy and Verhaegen[77] and Lieven et al.[78] have developed a correction scheme which is similar in spirit to the AIM method, but whose formalism and operational equations are based on a somewhat different working hypothesis: the weights which multiply the intraatomic correction terms ΔE are derived from a Mulliken population analysis[75] (which involves orbital overlap!) of minimal-basis-set atomic orbitals. This procedure is simpler than the AIM method and can be applied to wavefunctions which are not even linear combinations of CFs. However, it determines only weights of atomic configurations and not of individual atomic states. This is most recently described by Lieven, Breulet and Verhaegen[78].

5. Correlation corrections for atomic and ionic states

Essential for the application of all AIM schemes is a knowledge of the atomic correction energies $\Delta E(A_i)$. They are deduced from the exact atomic energies $E(A_i)$ and the

calculated open-shell atomic Hartree-Fock limits $\tilde{E}(A_i)$. Fortunately, much more information is available on this subject at present than was the case in the early days of AIM theory.

For two-electron atomic systems (H^- to Ne^{8+}), very accurate calculations were performed by Pekeris[70a] to yield unrelativistic correlation energies as well as relativistic corrections. Near Hartree-Fock energies were given for H^-, He, Li^+ and Be^{2+} by Froese-Fischer[70b].

For atoms and many positive ions with three to ten electrons (Li to Ne), two thorough compilations have been prepared over a decade ago. Correlation energies have been determined by Verhaegen and Moser[73] for all states arising from ($1s^2 2s^2 2p^n$) configurations, in some cases corrected for the near-degeneracy-type configuration interaction between ($1s^2 2p^n$) and ($1s^2 2s 2p^{2n-2}$) states. Correlation energies for all ($1s^2 2p^n$) and ($1s^2 2s 2p^n$) states, as well as relativistic corrections for all three types of configurations were determined by Desclaux, Moser and Verhaegen[79].

For higher elements, less data are available. Clementi[80] has given correlation corrections for the ground states of the first 22 elements and some of their positive ions. Fraga et al.[4] have given relativistic corrections to Hartree-Fock energies for ground states of the first 102 elements and many of their positive ions.

Correlation and relativistic corrections for negative ions are considerably less available because of the difficulty in obtaining experimental data for these species. Generally, only the singly negative ion, at most, will be stable. Electron affinities are difficult to measure accurately, and are normally only available for the ground states of the ions. Hotop and Lineberger[81] have given experimental electron affinities for the first 85 elements of the the periodic table, including very few negative ion excited states. Schaefer et al.[82] have given less accurate theoretically derived electron affinities for atoms B to F, including a number of low-lying excited negative ion states. Correlation and relativistic corrections can be extracted from these electron affinities with the help of judicious extrapolation of the known corrections for the neutral and positive ions. Clementi and Roetti[70c] give SCF energies for singly negative ions from Li^- to I^-. For doubly negative ions, there are virtually no experimental data[80], and extrapolation to these or even more negative ions from the positive and neutral species is hazardous. The establishment of a more reliable data base for these negative ions will be a necessary prerequisite for general future applications of the AIM theory on a wider scale. Fortunately, CFs involving high negative ions usually have very small coefficients in the molecular wavefunctions.

From the compilation of Desclaux, Moser and Verhaegen[79], it is apparent that relativistic corrections can be substantial even for atoms in the first three rows of the periodic system where they arise from the inner shell only. If it can be assumed, however, that such relativistic corrections remained unchanged for the various atomic configurations as they enter the molecule, then the relativistic correction for the molecule can also be recovered by the AIM correction method, even though only the unrelativistic Hamiltonian is being used for the molecular calculation. For heavier atoms, however, where relativistic effects modify the valence shell, directly or indirectly, the inclusion of relativistic terms in the molecular Hamiltonian will most likely be necessary when calculating the matrix elements $\tilde{H}_{ij,kl}$.

C. The FORS-IACC Model

1. Theoretical formulation

The AIM approach can be combined with the FORS model because of two features characteristic for FORS wavefunction: (i) FORS MOs can be chosen as being so strongly localized that they are almost identical with the minimal basis of the Hartree-Fock SCF AOs of the free atoms; (ii) the full valence space of all possible configurations that are generated from the localized FORS MOs is identical with that spanned by the

set of all composite functions (CFs) which can be constructed from the localized FORS MOs.

In Reference 14b, the remarkable observation was made that projected localized FORS MOs (PLMOs) can be chosen in such a manner that each of them is almost identical (with an overlap usually exceeding 0.9) to one of the free-atom SCF AOs, and that they can therefore be considered as a "molecule-adapted minimal basis set of atomic orbitals". It is therefore a straightforward matter to substitute these PLMOs in place of the corresponding free-atom SCF AOs in the formulae for atomic configurations. The modified configuration state functions which result in this manner can thus be chosen to be the "approximate atomic state functions" $|\tilde{A}_i\rangle$, $|\tilde{B}_j\rangle$ from which "approximate composite functions" $|\tilde{A}_i\tilde{B}_j\rangle$ are constructed for the AIM procedure, as discussed in the preceding sections of this chapter. It is also evident that the number of independent CFs which can be constructed will be exactly the same as the number of linearly independent configuration state functions that can be constructed from the FORS MOs in the usual manner (e.g. in terms of SAAPs), namely equal to the dimension of the full reaction space. This choice of the approximate CFs for the AIM procedure has the following unique advantages.

FORS wavefunctions are entirely free of the constraints inherent in previous AIM models. The PLMOs are not simple MBS

AOs but are optimally expanded in an extended set of quantitative basis orbitals which can be as large as desired. The only restriction is the number of configuration generating orbitals used to generate the full reaction space. Within this limitation, the FORS wavefunction has complete flexibility and is the best possible function. Expressed in terms of CFs constructed from the PLMOs, FORS wavefunctions can be considered as the ultimate stage in the development begun by Arai and Hurley who realized that expansions in terms of a limited number of CFs made from exact atomic states would never do, but that deformed atoms in molecules were needed[74]. (Such deformations entail adjustments in the wavefunction which, in Moffitt's original model, could have been achieved only by admixtures of higher and even continuum exact states.) Since FORS wavefunctions result from MCSCF calculations, the CFs constructed from FORS PLMOs must be considered as representing those deformed atom states which are "intrinsic" to the particular molecule (assuming a sufficiently large extended set of quantitative basis orbitals has been used to exclude basis set errors).

Even though the PLMOs are so very similar to the SCF AOs of the the free atoms, they nevertheless form an orthonormal set, and so do the composite functions $|A_i B_j\rangle$ constructed from them. Thus, the non-orthogonality problem has been resolved in the most natural manner. It is as if the FORS PLMOs offer

the best of both worlds: they are optimal for the molecular calculation and they also generate orthogonal CFs. As a consequence the intraatomic correlation correction is achieved by the physically straightforward and conceptually transparent Equation (4.7), i.e., by simply modifying the diagonal elements $\tilde{H}_{ij,kl}$.

The price paid for these advantages is that the PLMOs differ from the free-atom SCF AOs by more than just a scale adjustment. They are somewhat distorted and even contain small admixtures from neighbouring atoms. Indeed, those PLMOs which correspond to a set of spherically degenerate free-atom AOs (such as $2p_x$, $2p_y$, $2p_z$) belong no more to a representation of the full rotation group around that atom, but they reflect the molecular symmetry. Thus, in a diatomic molecule, the PLMOs corresponding to the AOs $2p_x$ and $2p_y$ of an atom differ from each other by a rotation only, but the PLMO corresponding to $2p_z$ on the same atom has a slightly different shape.

For the calculation of the correlation corrections, the reasoning of Hurley[61], outlined in Section B.3 of this chapter, is however still pertinent, since it relies on the approximate independence of dynamic correlation errors upon changes in orbital size and shape. Therefore, for each state, the exact atomic correlation correction

$$\Delta E(A_i) = E(A_i) - \tilde{E}(A_i) \quad ,$$

where $\tilde{E}(A_i)$ is the Hartree-Fock limit for that state, is used in the approach proposed here. It is apparent that this procedure does not compensate for basis set truncation errors in the molecule. One might conjecture that such a compensation could be had cheaply by determining the $\tilde{E}(A_i)$ through Hartree-Fock SCF calculations in the free atom using exactly the same extended set of quantitative basis orbitals as is used in the molecular calculation. But such a scheme turns out to be unreliable. It is possible, for example, that the addition of certain basis functions will markedly lower an atomic energy $\tilde{E}(A_i)$ particularly for negative ions, while hardly affecting the molecular energy.

The approach outlined will be abbreviated as FORS-IACC (IntraAtomic Correlation Correction to the FORS model).

2. Mathematical formulation

The FORS-IACC method relies on choosing, as a basis for the full reaction space, that set of composite functions which are generated from the molecule-adapted minimal-basis atomic orbitals furnished by the PLMOs (the projected localized FORS MOs). These composite functions, $(CF)_V$ say, form an orthonormal set and there thus exists an orthogonal transformation between them and all possible spin-adapted antisymmetrized products, $(SAAP)_K$ say[14a], which can be constructed from the same PLMOs.

However, the subspace of those SAAPs which are needed to express a particular molecular state of a given spin multiplicity and spatial symmetry usually has a dimension that is smaller than the number of CFs required for expressing that state. This is because, in general, the CFs do not belong to irreducible representations of the appropriate space and/or spin symmetry. The number of CFs needed to express the SAAPs spanning the configuration space appropriate for a certain molecular state is therefore in general larger than the number of these SAAPs, which form the practical working basis for evaluating matrix elements and performing numerical computations. The transformation between the composite functions $(CF)_V$ and the spin-adapted antisymmetrized products $(SAAP)_K$ is therefore a rectangular matrix:

$$|SAAP_K\rangle = \sum_V |CF_V\rangle \, T_{VK} \quad . \tag{4.12}$$

$$K = 1, 2, \ldots M \qquad V = 1, 2, \ldots M' \qquad M' \geq M \quad . \tag{4.12a}$$

The matrix T is usually sparse and its elements are simply defined numbers. It is moreover independent of the molecular geometry. It satisfies the orthogonality condition

$$T^{\dagger}T = I, \tag{4.12b}$$

but $TT^{\dagger} \neq I$ since T^{-1}, in general, does not exist.

The Hamiltonian matrix between the CFs, H^{CF} say, is related to that between the SAAPs, H^{SAAP} say, by the similarity transformation

$$H^{SAAP} = T^{\dagger} H^{CF} T \quad . \tag{4.13}$$

The intraatomic correlation correction is accomplished by adding to H^{CF} the diagonal matrix

$$\Delta E^{CF} = \{\Delta E_V \delta_{VW}\} = \{\delta_{VW} \sum_A \Delta E_V(A)\} \quad , \tag{4.14}$$

where the sum goes over all atoms in the molecule and $\Delta E_V(A)$ is the atomic correlation correction for that state of the atom A which occurs in the composite function $(CF)_V$. Transforming back to the SAAP basis one obtains for the intraatomic correlation correction the matrix

$$\Delta E^{SAAP} = T^{\dagger} \Delta E^{CF} T = \{\sum_V T_{VI} T_{VK} \Delta E_V\} = \{\Delta E^{SAAP}_{IK}\} \quad , \tag{4.15}$$

which can be added to the FORS matrix H^{SAAP}_{IK}.

There are three possible options in using the corrected matrix $(H^{SAAP} + \Delta E^{SAAP})$ to determine energies and wavefunctions. The simplest is to find the energy correction approximately from the first order perturbation expression

$$\Delta E = \sum_{IK} \Delta E_{IK}^{SAAP} C_I C_K \quad , \qquad (4.16)$$

where C_K are the expansion coefficients of the FORS wavefunction in terms of $(SAAP)_K$. In many cases, this estimate is surprisingly accurate. Nonetheless, a better way is to solve the eigenvalue problem for the corrected matrix. This procedure yields not only improved energies, but also an improved wavefunction. These two procedures have been implemented into a computer program named IACC and a detailed description of which is given in next sections. Finally, it is possible to incorporate the corrected Hamiltonian matrix $(H^{SAAP} + \Delta E^{SAAP})$ into the MCSCF iteration procedure which yields the FORS wavefunction. This is possible since the correction matrix ΔE^{SAAP} depends neither on the MO expansion coefficients nor on the MC-CI expansion coefficients. In implementing such a procedure, it will be necessary, however, to see to it that the MOs remain projectively localized after each orbital improvement step.

3. The transformation from molecular SAAPs to composite functions

The mathematical manipulations required to determine the transformation matrix T of Equation (4.12) represent the only non-trivial aspect of the FORS-IACC implementation. This task is naturally divided into two stages. The first stage

consists of expressing molecular SAAPs in terms of atomic antisymmetrized products. The second stage is to find expressions relating these atomic antisymmetrized products to atomic states that are generated from real atomic orbitals, such as are used in molecular calculations.

(a)

The first stage, namely the expression of molecular SAAPs in terms of atomic antisymmetrized products is accomplished in two steps. First, one must regroup the spatial atom-localized orbitals (PLMOs) in a given molecular SAAP in such a manner that all those orbitals which belong to one atom are occupied by electrons in sequential order. This is achieved by an appropriate permutation of electrons. Next, the spin function Θ in the SAAP, as changed by this permutation, must be expanded in terms of products of spin functions from the various atoms. After this has been done, the total antisymmetrizer is decomposed into a product of atomic antisymmetrizers and a coset antisymmetrizer. Thereby, the molecular SAAP appears as an antisymmetrized product of atomic SAAPs.

As a simple example consider a covalent VB-type SAAP that can occur in Li_2,

$$\Psi = (1/2)A\{k_A^2 k_B^2 z_A s_B \Theta_0 \Theta_0 \Theta_0\} \quad , \tag{4.17}$$

where k_A and k_B are 1s orbitals on atoms A and B respectively; z_A is a $2p_z$ orbital on A and s_B is a 2s orbital on B;

$$\Theta_o = (\alpha\beta-\beta\alpha)/\sqrt{2} \quad ;$$

$$\mathbf{A} = (6!)^{-1/2} \sum_P (-1)^P P \quad ; \qquad (4.18)$$

and the factor 1/2 normalizes Ψ due to two doubly occupied orbitals.

Let (345) be the cyclic permutation which changes electron 3 into 4, 4 into 5 and 5 into 3. Since it is an even permutation, one has $\mathbf{A}(345) = \mathbf{A}$ and consequently

$$\begin{aligned}
\Psi &= (1/2)\mathbf{A}(345)\{k_A k_A k_B k_B z_A s_B \Theta_o \Theta_o \Theta_o\} \\
&= (1/2)\mathbf{A}\{k_A(1)k_A(2)k_B(4)k_B(5)z_A(3)s_B(6)\Theta_o(12)\Theta_o(45)\Theta_o(36)\} \\
&= (1/2)\mathbf{A}\{k_A k_A z_A k_B k_B s_B(\Theta_o\alpha\Theta_o\beta-\Theta_o\beta\Theta_o\alpha)/\sqrt{2}\} \\
&= (1/2)\mathbf{A}\{(k_A^2 z_A\Theta_o\alpha)(k_B^2 s_B\Theta_o\beta) - (k_A^2 z_A\Theta_o\beta)(k_B^2 s_B\Theta_o\alpha)\}/\sqrt{2} \\
&= (1/2)\mathbf{A}^*\{(\mathbf{A}_A k_A^2 z_A\Theta_o\alpha)(\mathbf{A}_B k_B^2 s_B\Theta_o\beta) \\
&\qquad - (\mathbf{A}_A k_A^2 z_A\Theta_o\beta)(\mathbf{A}_B k_B^2 s_B\Theta_o\alpha) \quad . \qquad (4.19)
\end{aligned}$$

Here,

$$\mathbf{A}_A = (3!)^{-1/2} \sum_P (-1)^P P$$

is the antisymmetrizer for electrons 1, 2 and 3; A_B is the corresponding antisymmetrizer for electrons 4, 5 and 6 and A^* is the coset antisymmetrizer defined by

$$A^* = (3!3!/6!)^{1/2} \sum_P^* (-1)^P P \quad ,$$

where the sum Σ^* goes over a set of 20 coset generating permutations which are defined as follows. If S_A is the symmetric group of all permutations between electrons 1, 2 and 3 and S_B is the group of all permutations between electrons 4, 5 and 6, then the group of permutations between all six electrons has the left coset decomposition

$$S = S^* \otimes S_A \otimes S_B \tag{4.20}$$

where S^* is a collection of $(6!/3!3!) = 20$ (non-unique) permutations called coset generators.

In the second stage, the four atomic antisymmetrized products of molecule-adapted atomic orbitals occurring in Equation (4.19), must be expressed in terms of atomic state functions. To this end, the molecule-adapted AOs are temporarily replaced by free-atom AOs. The case at hand is a simple one in that each atomic antisymmetrized product is already an atomic state, namely:

$$\mathbf{A}_A(k_A^2 z_A \alpha\beta\alpha) = |Az\ {}^2P(0,1/2)\rangle \quad , \qquad (4.21a)$$

$$\mathbf{A}_A(k_A^2 z_A \alpha\beta\beta) = |Az\ {}^2P(0,-1/2)\rangle \quad , \qquad (4.21b)$$

$$\mathbf{A}_B(k_B^2 s_B \alpha\beta\alpha) = |Bs\ {}^2S(0,1/2)\rangle \quad , \qquad (4.21c)$$

$$\mathbf{A}_B(k_B^2 s_B \alpha\beta\beta) = |Bs\ {}^2S(0,-1/2)\rangle \quad , \qquad (4.21d)$$

where the atomic state symbols are $|\text{atom}\ s^n p^m\ {}^{2S+1}L(M_l,M_s)\rangle$. The molecule-adapted AOs, i.e. the PLMOs, are now resubstituted for k_A, k_B, z_A, s_B, so that Equations (4.21) represent molecule-adapted atomic states. From these, the composite functions (CFs) are then directly defined as:

$$|{}^2P(0,1/2)/{}^2S(0,-1/2)\rangle = \mathbf{A}^* |Az\ {}^2P(0,1/2)\rangle |Bs\ {}^2S(0,-1/2)\rangle \quad ; \qquad (4.22a)$$

$$|{}^2P(0,-1/2)/{}^2S(0,1/2)\rangle = \mathbf{A}^* |Az\ {}^2P(0,-1/2)\rangle |Bs\ {}^2S(0,1/2)\rangle \quad . \qquad (4.22b)$$

By virtue of Equations (4.19) and (4.22a,b), the molecular SAAP of Equation (4.17) can then be expressed in terms of CFs as follows:

$$\Psi = \{|^2P(0,1/2)/^2S(0,-1/2)\rangle - |^2P(0,-1/2)/^2S(0,1/2)\rangle\}/\sqrt{2} \quad , \tag{4.23}$$

(b)

In general, the procedure is more complex. The most practical approach is to decompose the part of the spin factor which corresponds to the singly occupied orbitals into a sum of simple products of the form $(\eta_1\eta_2\eta_3\ldots)$ where each η is either α or β. After appropriate permutations, a molecular SAAP Ψ can then be expressed as

$$\Psi = \sum_{\nu\mu} C_{\nu\mu}\, A^{\star}\{\Phi^A_\nu \Phi^B_\mu\} \quad , \tag{4.24}$$

where $A^{\star}$ is an appropriate coset antisymmetrizer and Φ^A_ν, Φ^b_μ are antisymmetrized products on A and B respectively. These atomic antisymmetrized products can then be expressed in terms of state wavefunctions $|A_j\rangle$ and $|B_k\rangle$ of the atoms and their ions, i.e.

$$\Phi^A_\nu = \sum_j |A_j\rangle\, D_{j\nu} \quad ,$$

$$\Phi^B_\mu = \sum_k |B_k\rangle\, D_{k\mu} \quad . \tag{4.25}$$

Combining the Expansions (4.24) and (4.25) one obtains then

$$\Phi = \sum_{jk} |A_j B_k\rangle \, T_{jk} \quad , \quad \text{with } T = DCD^{\dagger} \quad , \tag{4.26}$$

where the functions

$$|A_j B_k\rangle = A^{*} \{A_j B_k\} \tag{4.27}$$

are just the composite functions (CFs).

For the case that the spatial orbitals are limited to a set of four valence orbitals of the type s, p_x, p_y, p_z (in addition to a closed core of doubly occupied inner orbitals), the atomic states arise from the configurations $s^n p^m$ with n = 0,1,2 and m = 1-6. It was found most convenient to prepare tables for all possible cases and they are listed as Table 4.3. This table consists of 54 subtables for the various configurations whose ordering is obtained as follows: reverse the order of the set of occupation numbers for (xyzs) listed at the head of each subtable, and interpret the resulting set of digits as a ternary or decimal number. The subtables are then arranged in the order of increasing values of these numbers.

As an example for the use of these tables, consider the column βαβ in the subtable corresponding to the occupation (xyzs) = (1211). The data given in this column imply that

$$A\{(y\alpha)(y\beta)(x\beta)(z\alpha)(s\beta)\} = -|^2D(1',-1/2)\rangle/\sqrt{2} + |^2P(1'',-1/2)\rangle/\sqrt{6} + |^4P(1'',-1/2)\rangle/\sqrt{3} \quad .$$

Similarly, the column αβ in the subtable for the occupation (xyzs) = (2121) implies that

$$A\{(x\alpha)(x\beta)(z\alpha)(z\beta)(y\alpha)(s\beta)\} = \{|^1P(1'',0)\rangle + |^3P(1'',0)\rangle\}/\sqrt{2} \quad .$$

The following conventions for the construction of SAAPs are apparent from these examples:

(i) Under the antisymmetrizer the doubly occupied orbitals precede the singly occupied orbitals;

(ii) The column list only the spin functions for the singly occupied orbitals - and the order of the individual spin factors corresponds to that of the singly occupied orbitals;

(iii) The singly occupied orbitals and their spin factors must be written in the order in which they occur in the occupation list at the head of the table, i.e. x,y,z,s.

Furthermore, the atomic state functions $|L,M_1'\rangle$ and $|L,M_1''\rangle$ occurring in these tables are defined as

$$|L,M_l'\rangle=\{|L,M_l\rangle+|L,-M_l\rangle*(-1)^{M_l}\}/\sqrt{2}$$
$$|L,M_l''\rangle=\{|L,M_l\rangle-|L,-M_l\rangle*(-1)^{M_l}\}/i\sqrt{2} \qquad (4.28)$$

where M_l is assumed to be positive and $|^{2S+1}L,M_l\rangle$, $|^{2S+1}L,-M_l\rangle$ are the conventional complex atomic states in the Condon-Shortley phase convention. The functions $|L,M_l'\rangle$ and $|L,M_l''\rangle$ are eigenfunctions of S^2, but not of S_z. However they are real functions and, for this reason, the listed transformation matrices are all real. In some cases, the functions $|L,M_l'\rangle$ and $|L,M_l''\rangle$ have been multiplied by an additional factor of (-1).

The transformations given in Table 4.3 are readily obtained by inverting the explicit expressions of the atomic states in terms of the real atomic valence orbitals s, p_x, p_y, p_z. These expressions have been derived for the free spherically symmetric atoms[83].

It ought to be noted that, in the present context, the free-atom expansions of Table 4.3 are of course applied to PLMOs which are not spherically symmetric.

Table 4.3. Expansions of antisymmetrized products of real atomic spin orbitals in terms of atomic states of the appropriate configurations for the minimal basis set of the 2s, $2p_x$, $2p_y$ and $2p_z$ shell

---

Occupation : (x y z s) = (0 0 0 0) ; Configuration : s^0p^0

Atomic States $^{2S+1}L(M_l, M_s)$	Spin Factors
$^1S(0, 0)$	1.000000

Occupation : (x y z s) = (1 0 0 0) ; Configuration : s^0p^1

Atomic States $^{2S+1}L(M_l, M_s)$	Spin Factors α	Spin Factors β
$^2P(1', 1/2)$	1.000000	0.000000
$^2P(1',-1/2)$	0.000000	1.000000

Occupation : (x y z s) = (2 0 0 0) ; Configuration : s^0p^2

Atomic States $^{2S+1}L(M_l, M_s)$	Spin Factors
$^1D(2', 0)$	-0.707107
$^1D(0, 0)$	0.408248
$^1S(0, 0)$	0.577350

Table 4.3 continued

Occupation : (x y z s) = (0 1 0 0) ; Configuration : s^0p^1

Atomic States $^{2S+1}L(M_l, M_s)$	Spin Factors α	β
$^2P(1", 1/2)$	1.000000	0.000000
$^2P(1",-1/2)$	0.000000	1.000000

Occupation : (x y z s) = (1 1 0 0) ; Configuration : s^0p^2

Atomic States $^{2S+1}L(M_l, M_s)$	Spin Factors αβ	αα	ββ	βα
$^1D(2", 0)$	0.707107	0.000000	0.000000	-0.707107
$^3P(0, 1)$	0.000000	1.000000	0.000000	0.000000
$^3P(0,-1)$	0.000000	0.000000	1.000000	0.000000
$^3P(0, 0)$	0.707107	0.000000	0.000000	0.707107

Occupation : (x y z s) = (2 1 0 0) ; Configuration : s^0p^3

Atomic States $^{2S+1}L(M_l, M_s)$	Spin Factors α	β
$^2D(1', 1/2)$	0.707107	0.000000
$^2P(1", 1/2)$	0.707107	0.000000
$^2D(1',-1/2)$	0.000000	0.707107
$^2P(1",-1/2)$	0.000000	0.707107

Table 4.3 continued

Occupation : (x y z s) = (0 2 0 0) ; Configuration : s^0p^2

Atomic States $^{2S+1}L(M_l, M_s)$	Spin Factors
$^1D(2', 0)$	0.707107
$^1D(0, 0)$	0.408248
$^1S(0, 0)$	0.577350

Occupation : (x y z s) = (1 2 0 0) ; Configuration : s^0p^3

Atomic States $^{2S+1}L(M_l, M_s)$	Spin Factors α	Spin Factors β
$^2D(1'', 1/2)$	0.707107	0.000000
$^2P(1', 1/2)$	0.707107	0.000000
$^2D(1'', -1/2)$	0.000000	0.707107
$^2P(1', -1/2)$	0.000000	0.707107

Table 4.3 continued

Occupation : (x y z s) = (2 2 0 0) ; Configuration : s^0p^4

Atomic States $^{2S+1}L(M_l, M_s)$	Spin Factors
$^1D(0, 0)$	-0.816497
$^1S(0, 0)$	0.577350

Occupation : (x y z s) = (0 0 1 0) ; Configuration : s^0p^1

Atomic States $^{2S+1}L(M_l, M_s)$	Spin Factors α	β
$^2P(0, 1/2)$	1.000000	0.000000
$^2P(0,-1/2)$	0.000000	1.000000

Occupation : (x y z s) = (1 0 1 0) ; Configuration : s^0p^2

Atomic States $^{2S+1}L(M_l, M_s)$	Spin Factors αβ	αα	ββ	βα
$^1D(1', 0)$	0.707107	0.000000	0.000000	-0.707107
$^3P(1", 1)$	0.000000	1.000000	0.000000	0.000000
$^3P(1",-1)$	0.000000	0.000000	1.000000	0.000000
$^3P(1", 0)$	0.707107	0.000000	0.000000	0.707107

Table 4.3 continued

Occupation : (x y z s) = (2 0 1 0) ; Configuration : s^0p^3

Atomic States $^{2S+1}L(M_l, M_s)$	Spin Factors α	β
$^2D(2", 1/2)$	0.707107	0.000000
$^2P(0, 1/2)$	0.707107	0.000000
$^2D(2",-1/2)$	0.000000	0.707107
$^2P(0,-1/2)$	0.000000	0.707107

Occupation : (x y z s) = (0 1 1 0) ; Configuration : s^0p^2

Atomic States $^{2S+1}L(M_l, M_s)$	Spin Factors αβ	αα	ββ	βα
$^1D(1", 0)$	0.707107	0.000000	0.000000	-0.707107
$^3P(1', 1)$	0.000000	1.000000	0.000000	0.000000
$^3P(1',-1)$	0.000000	0.000000	1.000000	0.000000
$^3P(1', 0)$	0.707107	0.000000	0.000000	0.707107

Table 4.3 continued

Occupation : (x y z s) = (1 1 1 0) ; Configuration : s^0p^3

Atomic States $^{2S+1}L(M_l, M_s)$	Spin Factors αβα	βαα	αββ	βαβ
$^2D(2', 1/2)$	0.707107	-0.707107	0.000000	0.000000
$^2D(2',-1/2)$	0.000000	0.000000	0.707107	-0.707107
$^2D(0, 1/2)$	-0.408248	-0.408248	0.000000	0.000000
$^2D(0,-1/2)$	0.000000	0.000000	0.408248	0.408248
$^4S(0, 1/2)$	0.577350	0.577350	0.000000	0.000000
$^4S(0,-1/2)$	0.000000	0.000000	0.577350	0.577350
$^4S(0, 3/2)$	0.000000	0.000000	0.000000	0.000000
$^4S(0,-3/2)$	0.000000	0.000000	0.000000	0.000000

Atomic States $^{2S+1}L(M_l, M_s)$	Spin Factors ααβ	ββα	ααα	βββ
$^2D(2', 1/2)$	0.000000	0.000000	0.000000	0.000000
$^2D(2',-1/2)$	0.000000	0.000000	0.000000	0.000000
$^2D(0, 1/2)$	0.816497	0.000000	0.000000	0.000000
$^2D(0,-1/2)$	0.000000	-0.816497	0.000000	0.000000
$^4S(0, 1/2)$	0.577350	0.000000	0.000000	0.000000
$^4S(0,-1/2)$	0.000000	0.577350	0.000000	0.000000
$^4S(0, 3/2)$	0.000000	0.000000	1.000000	0.000000
$^4S(0,-3/2)$	0.000000	0.000000	0.000000	1.000000

Table 4.3 continued

Occupation : (x y z s) = (2 1 1 0) ; Configuration : s^0p^4

Atomic States $^{2S+1}L(M_l, M_s)$	Spin Factors αβ	αα	ββ	βα
$^1D(1", 0)$	0.707107	0.000000	0.000000	-0.707107
$^3P(1', 1)$	0.000000	1.000000	0.000000	0.000000
$^3P(1',-1)$	0.000000	0.000000	1.000000	0.000000
$^3P(1', 0)$	0.707107	0.000000	0.000000	0.707107

Occupation : (x y z s) = (0 2 1 0) ; Configuration : s^0p^3

Atomic States $^{2S+1}L(M_l, M_s)$	Spin Factors α	β
$^2D(2", 1/2)$	-0.707107	0.000000
$^2P(0, 1/2)$	0.707107	0.000000
$^2D(2",-1/2)$	0.000000	-0.707107
$^2P(0,-1/2)$	0.000000	0.707107

Occupation : (x y z s) = (1 2 1 0) ; Configuration : s^0p^4

Atomic States $^{2S+1}L(M_l, M_s)$	Spin Factors αβ	αα	ββ	βα
$^1D(1', 0)$	0.707107	0.000000	0.000000	-0.707107
$^3P(1", 1)$	0.000000	1.000000	0.000000	0.000000
$^3P(1",-1)$	0.000000	0.000000	1.000000	0.000000
$^3P(1", 0)$	0.707107	0.000000	0.000000	0.707107

Table 4.3 continued

Occupation : (x y z s) = (2 2 1 0) ; Configuration : s^0p^5

Atomic States $^{2S+1}L(M_l, M_s)$	Spin Factors α	β
$^2P(0, 1/2)$	1.000000	0.000000
$^2P(0,-1/2)$	0.000000	1.000000

Occupation : (x y z s) = (0 0 2 0) ; Configuration : s^0p^2

Atomic States $^{2S+1}L(M_l, M_s)$	Spin Factors
$^1D(0, 0)$	-0.816497
$^1S(0, 0)$	0.577350

Occupation : (x y z s) = (1 0 2 0) ; Configuration : s^0p^3

Atomic States $^{2S+1}L(M_l, M_s)$	Spin Factors α	β
$^2D(1", 1/2)$	-0.707107	0.000000
$^2P(1', 1/2)$	0.707107	0.000000
$^2D(1",-1/2)$	0.000000	-0.707107
$^2P(1',-1/2)$	0.000000	0.707107

Table 4.3 continued

Occupation : (x y z s) = (2 0 2 0) ; Configuration : s^0p^4

Atomic States $^{2S+1}L(M_l, M_s)$	Spin Factors
$^1D(2', 0)$	0.707107
$^1D(0, 0)$	0.408248
$^1S(0, 0)$	0.577350

Occupation : (x y z s) = (0 1 2 0) ; Configuration : s^0p^3

Atomic States $^{2S+1}L(M_l, M_s)$	Spin Factors α	β
$^2D(1', 1/2)$	-0.707107	0.000000
$^2P(1", 1/2)$	0.707107	0.000000
$^2D(1',-1/2)$	0.000000	-0.707107
$^2P(1",-1/2)$	0.000000	0.707107

Occupation : (x y z s) = (1 1 2 0) ; Configuration : s^0p^4

Atomic States $^{2S+1}L(M_l, M_s)$	Spin Factors αβ	αα	ββ	βα
$^1D(2", 0)$	0.707107	0.000000	0.000000	-0.707107
$^3P(0, 1)$	0.000000	1.000000	0.000000	0.000000
$^3P(0,-1)$	0.000000	0.000000	1.000000	0.000000
$^3P(0, 0)$	0.707107	0.000000	0.000000	0.707107

Table 4.3 continued

Occupation : (x y z s) = (2 1 2 0) ; Configuration : s^0p^5

Atomic States $^{2S+1}L(M_l, M_s)$	Spin Factors α	Spin Factors β
$^2P(1", 1/2)$	1.000000	0.000000
$^2P(1",-1/2)$	0.000000	1.000000

Occupation : (x y z s) = (0 2 2 0) ; Configuration : s^0p^4

Atomic States $^{2S+1}L(M_l, M_s)$	Spin Factors
$^1D(2', 0)$	-0.707107
$^1D(0, 0)$	0.408248
$^1S(0, 0)$	0.577350

Occupation : (x y z s) = (1 2 2 0) ; Configuration : s^0p^5

Atomic States $^{2S+1}L(M_l, M_s)$	Spin Factors α	Spin Factors β
$^2P(1', 1/2)$	1.000000	0.000000
$^2P(1',-1/2)$	0.000000	1.000000

Table 4.3 continued

Occupation : (x y z s) = (2 2 2 0) ; Configuration : s^0p^6

Atomic States $^{2S+1}L(M_l, M_s)$	Spin Factors
$^1S(0, 0)$	1.000000

Occupation : (x y z s) = (0 0 0 1) ; Configuration : s^1p^0

Atomic States $^{2S+1}L(M_l, M_s)$	Spin Factors α	β
$^2S(0, 1/2)$	1.000000	0.000000
$^2S(0,-1/2)$	0.000000	1.000000

Occupation : (x y z s) = (1 0 0 1) ; Configuration : s^1p^1

Atomic States $^{2S+1}L(M_l, M_s)$	Spin Factors αβ	αα	ββ	βα
$^1P(1', 0)$	0.707107	0.000000	0.000000	-0.707107
$^3P(1', 1)$	0.000000	1.000000	0.000000	0.000000
$^3P(1',-1/2)$	0.000000	0.000000	1.000000	0.000000
$^3P(1', 0)$	0.707107	0.000000	0.000000	0.707107

Table 4.3 continued

Occupation : (x y z s) = (2 0 0 1) ; Configuration : s^1p^2

Atomic States $^{2S+1}L(M_l, M_s)$	Spin Factors α	β
$^2D(2', 1/2)$	0.707107	0.000000
$^2D(0, 1/2)$	-0.408248	0.000000
$^2S(0, 1/2)$	0.577350	0.000000
$^2D(2',-1/2)$	0.000000	0.707107
$^2D(0,-1/2)$	0.000000	-0.408248
$^2S(0,-1/2)$	0.000000	0.577350

Occupation : (x y z s) = (0 1 0 1) ; Configuration : s^1p^1

Atomic States $^{2S+1}L(M_l, M_s)$	Spin Factors αβ	αα	ββ	βα
$^1P(1", 0)$	0.707107	0.000000	0.000000	-0.707107
$^3P(1", 1)$	0.000000	1.000000	0.000000	0.000000
$^3P(1",-1)$	0.000000	0.000000	1.000000	0.000000
$^3P(1", 0)$	0.707107	0.000000	0.000000	0.707107

Table 4.3 continued

Occupation : (x y z s) = (1 1 0 1) ; Configuration : s^1p^2

Atomic States $^{2S+1}L(M_l, M_s)$	Spin Factors αβα	βαα	αββ	βαβ
$^2D(2", 1/2)$	0.707107	-0.707107	0.000000	0.000000
$^2D(2",-1/2)$	0.000000	0.000000	0.707107	-0.707107
$^2P(0, 1/2)$	-0.408248	-0.408248	0.000000	0.000000
$^2P(0,-1/2)$	0.000000	0.000000	0.408248	0.408248
$^4P(1", 1/2)$	0.577350	0.577350	0.000000	0.000000
$^4P(1",-1/2)$	0.000000	0.000000	0.577350	0.577350
$^4P(1", 3/2)$	0.000000	0.000000	0.000000	0.000000
$^4P(1",-3/2)$	0.000000	0.000000	0.000000	0.000000

Atomic States $^{2S+1}L(M_l, M_s)$	Spin Factors ααβ	ββα	ααα	βββ
$^2D(2", 1/2)$	0.000000	0.000000	0.000000	0.000000
$^2D(2",-1/2)$	0.000000	0.000000	0.000000	0.000000
$^2P(0, 1/2)$	0.816497	0.000000	0.000000	0.000000
$^2P(0,-1/2)$	0.000000	-0.816497	0.000000	0.000000
$^4P(1", 1/2)$	0.577350	0.000000	0.000000	0.000000
$^4P(1",-1/2)$	0.000000	0.577350	0.000000	0.000000
$^4P(1", 3/2)$	0.000000	0.000000	1.000000	0.000000
$^4P(1",-3/2)$	0.000000	0.000000	0.000000	1.000000

Table 4.3 continued

Occupation : (x y z s) = (2 1 0 1) ; Configuration : s^1p^3

Atomic States $^{2S+1}L(M_l, M_s)$	Spin Factors αβ	βα	αα	ββ
$^1D(1', 0)$	0.500000	-0.500000	0.000000	0.000000
$^1P(1", 0)$	0.500000	-0.500000	0.000000	0.000000
$^3D(1', 1)$	0.000000	0.000000	0.707107	0.000000
$^3P(1", 1)$	0.000000	0.000000	0.707107	0.000000
$^3D(1',-1)$	0.000000	0.000000	0.000000	0.707107
$^3P(1",-1)$	0.000000	0.000000	0.000000	0.707107
$^3D(1', 0)$	0.500000	0.500000	0.000000	0.000000
$^3P(1", 0)$	0.500000	0.500000	0.000000	0.000000

Occupation : (x y z s) = (0 2 0 1) ; Configuration : s^1p^2

Atomic States $^{2S+1}L(M_l, M_s)$	Spin Factors α	β
$^2D(2', 1/2)$	-0.707107	0.000000
$^2D(0, 1/2)$	-0.408248	0.000000
$^2S(0, 1/2)$	0.577350	0.000000
$^2D(2',-1/2)$	0.000000	-0.707107
$^2D(0,-1/2)$	0.000000	-0.408248
$^2S(0,-1/2)$	0.000000	0.577350

Table 4.3 continued

Occupation : (x y z s) = (1 2 0 1) ; Configuration : s^1p^3

Atomic States $^{2S+1}L(M_l, M_s)$	Spin Factors αβ	βα	αα	ββ
$^1D(1", 0)$	0.500000	-0.500000	0.000000	0.000000
$^1P(1', 0)$	0.500000	-0.500000	0.000000	0.000000
$^3D(1", 1)$	0.000000	0.000000	0.707107	0.000000
$^3P(1', 1)$	0.000000	0.000000	0.707107	0.000000
$^3D(1",-1)$	0.000000	0.000000	0.000000	0.707107
$^3P(1',-1)$	0.000000	0.000000	0.000000	0.707107
$^3D(1", 0)$	0.500000	0.500000	0.000000	0.000000
$^3P(1', 0)$	0.500000	0.500000	0.000000	0.000000

Table 4.3 continued

Occupation : (x y z s) = (2 2 0 1) ; Configuration : s^1p^4

Atomic States $^{2S+1}L(M_l, M_s)$	Spin Factors α	β
$^2D(0, 1/2)$	-0.816497	0.000000
$^2S(0, 1/2)$	0.577350	0.000000
$^2D(0,-1/2)$	0.000000	-0.816497
$^2S(0,-1/2)$	0.000000	0.577350

Occupation : (x y z s) = (0 0 1 1) ; Configuration : s^1p^1

Atomic States $^{2S+1}L(M_l, M_s)$	Spin Factors αβ	αα	ββ	βα
$^1P(0, 0)$	0.707107	0.000000	0.000000	-0.707107
$^2P(0, 1/2)$	0.000000	1.000000	0.000000	0.000000
$^2P(0,-1/2)$	0.000000	0.000000	1.000000	0.000000
$^2P(0, 0)$	0.707107	0.000000	0.000000	0.707107

Table 4.3 continued

Occupation : (x y z s) = (1 0 1 1) ; Configuration : s^1p^2

Atomic States $^{2S+1}L(M_l, M_s)$	Spin Factors αβα	βαα	αββ	βαβ
$^2D(1', 1/2)$	0.707107	-0.707107	0.000000	0.000000
$^2D(1',-1/2)$	0.000000	0.000000	0.707107	-0.707107
$^2P(1", 1/2)$	-0.408248	-0.408248	0.000000	0.000000
$^2P(1",-1/2)$	0.000000	0.000000	0.408248	0.408248
$^4P(1", 1/2)$	0.577350	0.577350	0.000000	0.000000
$^4P(1",-1/2)$	0.000000	0.000000	0.577350	0.577350
$^4P(1", 3/2)$	0.000000	0.000000	0.000000	0.000000
$^4P(1",-3/2)$	0.000000	0.000000	0.000000	0.000000

Atomic States $^{2S+1}L(M_l, M_s)$	Spin Factors ααβ	ββα	ααα	βββ
$^2D(1', 1/2)$	0.000000	0.000000	0.000000	0.000000
$^2D(1',-1/2)$	0.000000	0.000000	0.000000	0.000000
$^2P(1", 1/2)$	0.816497	0.000000	0.000000	0.000000
$^2P(1",-1/2)$	0.000000	-0.816497	0.000000	0.000000
$^4P(1", 1/2)$	0.577350	0.000000	0.000000	0.000000
$^4P(1",-1/2)$	0.000000	0.577350	0.000000	0.000000
$^4P(1", 3/2)$	0.000000	0.000000	1.000000	0.000000
$^4P(1",-3/2)$	0.000000	0.000000	0.000000	1.000000

Table 4.3 continued

Occupation : (x y z s) = (2 0 1 1) ; Configuration : s^1p^3

Atomic States $^{2S+1}L(M_l, M_s)$	Spin Factors αβ	βα	αα	ββ
$^1D(2", 0)$	0.500000	-0.500000	0.000000	0.000000
$^1P(0, 0)$	0.500000	-0.500000	0.000000	0.000000
$^3D(2", 1)$	0.000000	0.000000	0.707107	0.000000
$^3P(0, 1)$	0.000000	0.000000	0.707107	0.000000
$^3D(2",-1)$	0.000000	0.000000	0.000000	0.707107
$^3P(0,-1)$	0.000000	0.000000	0.000000	0.707107
$^3D(2", 0)$	0.500000	0.500000	0.000000	0.000000
$^3P(0, 0)$	0.500000	0.500000	0.000000	0.000000

Table 4.3 continued

Occupation : (x y z s) = (0 1 1 1) ; Configuration : s^1p^2

Atomic States $^{2S+1}L(M_l, M_s)$	Spin Factors αβα	βαα	αββ	βαβ
$^2D(1", 1/2)$	0.707107	-0.707107	0.000000	0.000000
$^2D(1",-1/2)$	0.000000	0.000000	0.707107	-0.707107
$^2P(1', 1/2)$	-0.408248	-0.408248	0.000000	0.000000
$^2P(1',-1/2)$	0.000000	0.000000	0.408248	0.408248
$^4P(1', 1/2)$	0.577350	0.577350	0.000000	0.000000
$^4P(1',-1/2)$	0.000000	0.000000	0.577350	0.577350
$^4P(1', 3/2)$	0.000000	0.000000	0.000000	0.000000
$^4P(1',-3/2)$	0.000000	0.000000	0.000000	0.000000

Atomic States $^{2S+1}L(M_l, M_s)$	Spin Factors ααβ	ββα	ααα	βββ
$^2D(1", 1/2)$	0.000000	0.000000	0.000000	0.000000
$^2D(1",-1/2)$	0.000000	0.000000	0.000000	0.000000
$^2P(1', 1/2)$	0.816497	0.000000	0.000000	0.000000
$^2P(1',-1/2)$	0.000000	-0.816497	0.000000	0.000000
$^4P(1', 1/2)$	0.577350	0.000000	0.000000	0.000000
$^4P(1',-1/2)$	0.000000	0.577350	0.000000	0.000000
$^4P(1', 3/2)$	0.000000	0.000000	1.000000	0.000000
$^4P(1',-3/2)$	0.000000	0.000000	0.000000	1.000000

Table 4.3 continued

Occupation : (x y z s) = (1 1 1 1) ; Configuration : s^1p^3

Atomic States $^{2S+1}L(M_l, M_s)$	Spin Factors αβαβ	αββα	βααβ	βαβα
$^1D(2', 0)$	0.500000	-0.500000	-0.500000	0.500000
$^1D(0, 0)$	-0.288675	-0.288675	-0.288675	-0.288675
$^3D(2', 1)$	0.000000	0.000000	0.000000	0.000000
$^3D(2',-1)$	0.000000	0.000000	0.000000	0.000000
$^3D(2', 0)$	0.500000	0.500000	-0.500000	-0.500000
$^3D(0, 1)$	0.000000	0.000000	0.000000	0.000000
$^3S(0, 1)$	0.000000	0.000000	0.000000	0.000000
$^3D(0,-1)$	0.000000	0.000000	0.000000	0.000000
$^3S(0,-1)$	0.000000	0.000000	0.000000	0.000000
$^3D(0, 0)$	-0.288675	0.288675	-0.288675	0.288675
$^3S(0, 0)$	0.408248	-0.408248	0.408248	-0.408248
$^5S(0, 2)$	0.000000	0.000000	0.000000	0.000000
$^5S(0,-2)$	0.000000	0.000000	0.000000	0.000000
$^5S(0, 1)$	0.000000	0.000000	0.000000	0.000000
$^5S(0,-1)$	0.000000	0.000000	0.000000	0.000000
$^5S(0, 0)$	0.408248	0.408248	0.408248	0.408248

Table 4.3 continued

Atomic States $^{2S+1}L(M_l, M_s)$	Spin Factors $\alpha\alpha\beta\beta$	$\beta\beta\alpha\alpha$	$\alpha\beta\alpha\alpha$	$\beta\alpha\alpha\alpha$
$^1D(2', 0)$	0.000000	0.000000	0.000000	0.000000
$^1D(0, 0)$	0.577350	0.577350	0.000000	0.000000
$^3D(2', 1)$	0.000000	0.000000	0.707107	-0.707107
$^3D(2',-1)$	0.000000	0.000000	0.000000	0.000000
$^3D(2', 0)$	0.000000	0.000000	0.000000	0.000000
$^3D(0, 1)$	0.000000	0.000000	-0.408248	-0.408248
$^3S(0, 1)$	0.000000	0.000000	-0.288675	-0.288675
$^3D(0,-1)$	0.000000	0.000000	0.000000	0.000000
$^3S(0,-1)$	0.000000	0.000000	0.000000	0.000000
$^3D(0, 0)$	0.577350	-0.577350	0.000000	0.000000
$^3S(0, 0)$	0.408248	-0.408248	0.000000	0.000000
$^5S(0, 2)$	0.000000	0.000000	0.000000	0.000000
$^5S(0,-2)$	0.000000	0.000000	0.000000	0.000000
$^5S(0, 1)$	0.000000	0.000000	0.500000	0.500000
$^5S(0,-1)$	0.000000	0.000000	0.000000	0.000000
$^5S(0, 0)$	0.408248	0.408248	0.000000	0.000000

Table 4.3 continued

Atomic States $^{2S+1}L(M_l, M_s)$	Spin Factors $\alpha\beta\beta\beta$	$\beta\alpha\beta\beta$	$\alpha\alpha\alpha\beta$	$\alpha\alpha\beta\alpha$
$^1D(2', 0)$	0.000000	0.000000	0.000000	0.000000
$^1D(0, 0)$	0.000000	0.000000	0.000000	0.000000
$^3D(2', 1)$	0.000000	0.000000	0.000000	0.000000
$^3D(2',-1)$	0.707107	-0.707107	0.000000	0.000000
$^3D(2', 0)$	0.000000	0.000000	0.000000	0.000000
$^3D(0, 1)$	0.000000	0.000000	0.000000	0.816497
$^3S(0, 1)$	0.000000	0.000000	0.866025	-0.288675
$^3D(0,-1)$	0.408248	0.408248	0.000000	0.000000
$^3S(0,-1)$	0.288675	0.288675	0.000000	0.000000
$^3D(0, 0)$	0.000000	0.000000	0.000000	0.000000
$^3S(0, 0)$	0.000000	0.000000	0.000000	0.000000
$^5S(0, 2)$	0.000000	0.000000	0.000000	0.000000
$^5S(0,-2)$	0.000000	0.000000	0.000000	0.000000
$^5S(0, 1)$	0.000000	0.000000	0.500000	0.500000
$^5S(0,-1)$	0.500000	0.500000	0.000000	0.000000
$^5S(0, 0)$	0.000000	0.000000	0.000000	0.000000

Table 4.3 continued

Atomic States $^{2S+1}L(M_l,\ M_s)$	Spin Factors $\beta\beta\alpha\beta$	$\beta\beta\beta\alpha$	$\alpha\alpha\alpha\alpha$	$\beta\beta\beta\beta$
$^{1}D(2', 0)$	0.000000	0.000000	0.000000	0.000000
$^{1}D(0, 0)$	0.000000	0.000000	0.000000	0.000000
$^{3}D(2', 1)$	0.000000	0.000000	0.000000	0.000000
$^{3}D(2',-1)$	0.000000	0.000000	0.000000	0.000000
$^{3}D(2', 0)$	0.000000	0.000000	0.000000	0.000000
$^{3}D(0, 1)$	0.000000	0.000000	0.000000	0.000000
$^{3}S(0, 1)$	0.000000	0.000000	0.000000	0.000000
$^{3}D(0,-1)$	-0.816497	0.000000	0.000000	0.000000
$^{3}S(0,-1)$	0.288675	-0.866025	0.000000	0.000000
$^{3}D(0, 0)$	0.000000	0.000000	0.000000	0.000000
$^{3}S(0, 0)$	0.000000	0.000000	0.000000	0.000000
$^{5}S(0, 2)$	0.000000	0.000000	1.000000	0.000000
$^{5}S(0,-2)$	0.000000	0.000000	0.000000	1.000000
$^{5}S(0, 1)$	0.000000	0.000000	0.000000	0.000000
$^{5}S(0,-1)$	0.500000	0.500000	0.000000	0.000000
$^{5}S(0, 0)$	0.000000	0.000000	0.000000	0.000000

Table 4.3 continued

Occupation : (x y z s) = (2 1 1 1) ; Configuration : s^1p^4

Atomic States $^{2S+1}L(M_l, M_s)$	Spin Factors αβα	βαα	αββ	βαβ
$^2D(1", 1/2)$	0.707107	-0.707107	0.000000	0.000000
$^2D(1",-1/2)$	0.000000	0.000000	0.707107	-0.707107
$^2P(1', 1/2)$	-0.408248	-0.408248	0.000000	0.000000
$^2P(1',-1/2)$	0.000000	0.000000	0.408248	0.408248
$^4P(1', 1/2)$	0.577350	0.577350	0.000000	0.000000
$^4P(1',-1/2)$	0.000000	0.000000	0.577350	0.577350
$^4P(1', 3/2)$	0.000000	0.000000	0.000000	0.000000
$^4P(1',-3/2)$	0.000000	0.000000	0.000000	0.000000

Atomic States $^{2S+1}L(M_l, M_s)$	Spin Factors ααβ	ββα	ααα	βββ
$^2D(1", 1/2)$	0.000000	0.000000	0.000000	0.000000
$^2D(1",-1/2)$	0.000000	0.000000	0.000000	0.000000
$^2P(1', 1/2)$	0.816497	0.000000	0.000000	0.000000
$^2P(1',-1/2)$	0.000000	-0.816497	0.000000	0.000000
$^4P(1', 1/2)$	0.577350	0.000000	0.000000	0.000000
$^4P(1',-1/2)$	0.000000	0.577350	0.000000	0.000000
$^4P(1', 3/2)$	0.000000	0.000000	1.000000	0.000000
$^4P(1',-3/2)$	0.000000	0.000000	0.000000	1.000000

Table 4.3 continued

Occupation : (x y z s) = (0 2 1 1) ; Configuration : s^1p^3

Atomic States $^{2S+1}L(M_l, M_s)$	Spin Factors αβ	βα	αα	ββ
$^1D(2", 0)$	-0.500000	0.500000	0.000000	0.000000
$^1P(0, 0)$	0.500000	-0.500000	0.000000	0.000000
$^3D(2", 1)$	0.000000	0.000000	-0.707107	0.000000
$^3P(0, 1)$	0.000000	0.000000	0.707107	0.000000
$^3D(2",-1)$	0.000000	0.000000	0.000000	-0.707107
$^3P(0,-1)$	0.000000	0.000000	0.000000	0.707107
$^3D(2", 0)$	-0.500000	-0.500000	0.000000	0.000000
$^3P(0, 0)$	0.500000	0.500000	0.000000	0.000000

Table 4.3 continued

Occupation : (x y z s) = (1 2 1 1) ; Configuration : s^1p^4

Atomic States $^{2S+1}L(M_l, M_s)$	Spin Factors αβα	βαα	αββ	βαβ
$^2D(1', 1/2)$	0.707107	-0.707107	0.000000	0.000000
$^2D(1',-1/2)$	0.000000	0.000000	0.707107	-0.707107
$^2P(1", 1/2)$	-0.408248	-0.408248	0.000000	0.000000
$^2P(1",-1/2)$	0.000000	0.000000	0.408248	0.408248
$^4P(1", 1/2)$	0.577350	0.577350	0.000000	0.000000
$^4P(1",-1/2)$	0.000000	0.000000	0.577350	0.577350
$^4P(1", 3/2)$	0.000000	0.000000	0.000000	0.000000
$^4P(1",-3/2)$	0.000000	0.000000	0.000000	0.000000

Atomic States $^{2S+1}L(M_l, M_s)$	Spin Factors ααβ	ββα	ααα	βββ
$^2D(1', 1/2)$	0.000000	0.000000	0.000000	0.000000
$^2D(1',-1/2)$	0.000000	0.000000	0.000000	0.000000
$^2P(1", 1/2)$	0.816497	0.000000	0.000000	0.000000
$^2P(1",-1/2)$	0.000000	-0.816497	0.000000	0.000000
$^4P(1", 1/2)$	0.577350	0.000000	0.000000	0.000000
$^4P(1",-1/2)$	0.000000	0.577350	0.000000	0.000000
$^4P(1", 3/2)$	0.000000	0.000000	1.000000	0.000000
$^4P(1",-3/2)$	0.000000	0.000000	0.000000	1.000000

Table 4.3 continued

Occupation : (x y z s) = (2 2 1 1) ; Configuration : s^1p^5

Atomic States $^{2S+1}L(M_l, M_s)$	Spin Factors αβ	αα	ββ	βα
$^1P(0, 0)$	0.707107	0.000000	0.000000	-0.707107
$^3P(0, 1)$	0.000000	1.000000	0.000000	0.000000
$^3P(0,-1)$	0.000000	0.000000	1.000000	0.000000
$^3P(0, 0)$	0.707107	0.000000	0.000000	0.707107

Occupation : (x y z s) = (0 0 2 1) ; Configuration : s^1p^2

Atomic States $^{2S+1}L(M_l, M_s)$	Spin Factors α	β
$^2D(0, 1/2)$	0.816497	0.000000
$^2S(0, 1/2)$	0.577350	0.000000
$^2D(0,-1/2)$	0.000000	0.816497
$^2S(0,-1/2)$	0.000000	0.577350

Table 4.3 continued

Occupation : (x y z s) = (1 0 2 1) ; Configuration : s^1p^3

Atomic States $^{2S+1}L(M_l, M_s)$	Spin Factors αβ	βα	αα	ββ
$^1D(1", 0)$	-0.500000	0.500000	0.000000	0.000000
$^1P(1', 0)$	0.500000	-0.500000	0.000000	0.000000
$^3D(1", 1)$	0.000000	0.000000	-0.707107	0.000000
$^3P(1', 1)$	0.000000	0.000000	0.707107	0.000000
$^3D(1",-1)$	0.000000	0.000000	0.000000	-0.707107
$^3P(1',-1)$	0.000000	0.000000	0.000000	0.707107
$^3D(1", 0)$	-0.500000	-0.500000	0.000000	0.000000
$^3P(1', 0)$	0.500000	0.500000	0.000000	0.000000

Occupation : (x y z s) = (2 0 2 1) ; Configuration : s^1p^4

Atomic States $^{2S+1}L(M_l, M_s)$	Spin Factors α	β
$^2D(2', 1/2)$	0.707107	0.000000
$^2D(0, 1/2)$	0.408248	0.000000
$^2S(0, 1/2)$	0.577350	0.000000
$^2D(2',-1/2)$	0.000000	0.707107
$^2D(0,-1/2)$	0.000000	0.408248
$^2S(0,-1/2)$	0.000000	0.577350

Table 4.3 continued

Occupation : (x y z s) = (0 1 2 1) ; Configuration : s^1p^3

Atomic States $^{2S+1}L(M_l, M_s)$	Spin Factors αβ	βα	αα	ββ
$^1D(1', 0)$	-0.500000	0.500000	0.000000	0.000000
$^1P(1'', 0)$	0.500000	-0.500000	0.000000	0.000000
$^3D(1', 1)$	0.000000	0.000000	-0.707107	0.000000
$^3P(1'', 1)$	0.000000	0.000000	0.707107	0.000000
$^3D(1',-1)$	0.000000	0.000000	0.000000	-0.707107
$^3P(1'',-1)$	0.000000	0.000000	0.000000	0.707107
$^3D(1', 0)$	-0.500000	-0.500000	0.000000	0.000000
$^3P(1'', 0)$	0.500000	0.500000	0.000000	0.000000

Table 4.3 continued

Occupation : (x y z s) = (1 1 2 1) ; Configuration : s^1p^4

Atomic States $^{2S+1}L(M_l, M_s)$	Spin Factors αβα	βαα	αββ	βαβ
$^2D(2", 1/2)$	0.707107	-0.707107	0.000000	0.000000
$^2D(2",-1/2)$	0.000000	0.000000	0.707107	-0.707107
$^2P(0, 1/2)$	-0.408248	-0.408248	0.000000	0.000000
$^2P(0,-1/2)$	0.000000	0.000000	0.408248	0.408248
$^4P(0, 1/2)$	0.577350	0.577350	0.000000	0.000000
$^4P(0,-1/2)$	0.000000	0.000000	0.577350	0.577350
$^4P(0, 3/2)$	0.000000	0.000000	0.000000	0.000000
$^4P(0,-3/2)$	0.000000	0.000000	0.000000	0.000000

Atomic States $^{2S+1}L(M_l, M_s)$	Spin Factors ααβ	ββα	ααα	βββ
$^2D(2", 1/2)$	0.000000	0.000000	0.000000	0.000000
$^2D(2",-1/2)$	0.000000	0.000000	0.000000	0.000000
$^2P(0, 1/2)$	0.816497	0.000000	0.000000	0.000000
$^2P(0,-1/2)$	0.000000	-0.816497	0.000000	0.000000
$^4P(0, 1/2)$	0.577350	0.000000	0.000000	0.000000
$^4P(0,-1/2)$	0.000000	0.577350	0.000000	0.000000
$^4P(0, 3/2)$	0.000000	0.000000	1.000000	0.000000
$^4P(0,-3/2)$	0.000000	0.000000	0.000000	1.000000

Table 4.3 continued

Occupation : (x y z s) = (2 1 2 1) ; Configuration : s^1p^5

Atomic States $^{2S+1}L(M_l, M_s)$	Spin Factors αβ	αα	ββ	βα
$^1P(1", 0)$	0.707107	0.000000	0.000000	-0.707107
$^3P(1", 1)$	0.000000	1.000000	0.000000	0.000000
$^3P(1",-1)$	0.000000	0.000000	1.000000	0.000000
$^3P(1", 0)$	0.707107	0.000000	0.000000	0.707107

Occupation : (x y z s) = (0 2 2 1) ; Configuration : s^1p^4

Atomic States $^{2S+1}L(M_l, M_s)$	Spin Factors α	β
$^2D(2', 1/2)$	-0.707107	0.000000
$^2D(0, 1/2)$	0.408248	0.000000
$^2S(0, 1/2)$	0.577350	0.000000
$^2D(2',-1/2)$	0.000000	-0.707107
$^2D(0,-1/2)$	0.000000	0.408248
$^2S(0,-1/2)$	0.000000	0.577350

Table 4.3 continued

Occupation : (x y z s) = (1 2 2 1) ; Configuration : s^1p^5

Atomic States $^{2S+1}L(M_l, M_s)$	Spin Factors αβ	αα	ββ	βα
$^1P(1', 0)$	0.707107	0.000000	0.000000	-0.707107
$^3P(1', 1)$	0.000000	1.000000	0.000000	0.000000
$^3P(1',-1)$	0.000000	0.000000	1.000000	0.000000
$^3P(1', 0)$	0.707107	0.000000	0.000000	0.707107

Occupation : (x y z s) = (2 2 2 1) ; Configuration : s^1p^6

Atomic States $^{2S+1}L(M_l, M_s)$	Spin Factors α	β
$^2S(0, 1/2)$	1.000000	0.000000
$^2S(0,-1/2)$	0.000000	1.000000

(c)

A complication exists for the near-degenerate atomic configurations s^2p^n and s^0p^{n+2}, since they give rise to some states with identical overall symmetry. That is

s^2 and p^2 both generate a ^1S state,
s^2p and p^3 both generate a ^2P state,
s^2p^2 and p^4 both generate ^1S, ^1D and ^3P states,
s^2p^3 and p^5 both generate a ^2P state,
s^2p^4 and p^6 both generate a ^1S state.

In such cases, the actual atomic state functions are linear combinations $^{2S+1}L_1$ and $^{2S+1}L_2$ of the one-configuration functions. These linear combinations are given by orthogonal transformation

	$\|^{2S+1}L_1(M_l,M_s)\rangle$	$\|^{2S+1}L_2(M_l,M_s)\rangle$
$\|s^2p^n\ ^{2S+1}L(M_l,M_s)$	a	b
$\|p^{n+2}\ ^{2S+1}L(M_l,M_s)$	-b	a

($a^2 + b^2 = 1$), where the numerical values of a and b result from atomic MCSCF calculations for the particular states of the particular atoms. It is readily verified that the same orthogonal transformations which hold between the functions

$|s^2p^n,L\rangle$, $|p^{n+2},L\rangle$ and the functions $|L_1\rangle$, $|L_2\rangle$ are also valid if, in all four functions, one replaces M_l by M_l' or M_l'' as introduced by Equation (4.28).

Since L_1 and L_2 are the correct theoretical state functions, the atomic correlation correction must be calculated with reference to these wavefunctions and, consequently, the composite functions, too, must be constructed from them. In cases where this applies, the orthogonal expansion of atomic antisymmetrized products in terms of the one-configuration atomic states aquired from Table 4.3 must therefore be followed by the expansion of the one-configuration states in terms of L_1 and L_2 in order to obtain the expansions of Equation (4.25). Consider for example the occupations (xyzs) = (2120) and (xyzs) = (0122) of the configurations p^5 and s^2p^3 respectively. From column α of subtable (2120) of Table 4.3, one finds

$$A\{(x\alpha)(x\beta)(z\alpha)(z\beta)(y\alpha)\} = |p^5\ {}^2P(1'',1/2)\rangle$$

From column α of subtable (0120) one finds, by adding s^2,

$$A\{(s\alpha)(s\beta)(z\alpha)(z\beta)(y\alpha)\}$$
$$= |s^2p^3\ {}^2P(1'',1/2)\rangle - |s^2p^3\ {}^2D(1',1/2)\rangle\}/\sqrt{2} \quad .$$

Since s^2p^3 and p^5 both yield a ^2P state, one must therefore transform to $^2P_1$ and $^2P_2$, which yield the expansions

$$A\{(x\alpha)(x\beta)(z\alpha)(z\beta)(y\alpha)\} = -b|^2P_1(1'',1/2)\rangle + a|^2P_2(1'',1/2)\rangle \quad ,$$

$$A\{(s\alpha)(s\beta)(z\alpha)(z\beta)(y\alpha)\} = \{a|^2P_1(1'',1/2)\rangle + b|^2P_2(1'',1/2)\rangle - |s^2p^3\ ^2D(1',1/2)\rangle\}/\sqrt{2} \ .$$

where the coefficients a and b must be known from an independent calculation of the two ^2P states on the atom in question.

4. Program TMAT

The purpose of the program TMAT is to expand all molecular SAAPs in terms of composite functions (CFs) as given in Equation (4.12) and the atomic states composite functions are also identified. An input description to the program can be found in the SKUNK[84] reference manual.

Before this program is called upon, SAAPs in terms of localized orbitals (PLMOs) have to be formed using the program SAAP described in Chapter II. The program reads in the SAAPs and generates the Serber-type spin functions corresponding to the SAAPs. In anticipation of permutation among orbitals, the singly occupied portion of each SAAP is then decomposed into a linear combination of products of spin-orbitals. For example, for the SAAP

$$\Psi = A\{\phi_1\phi_1\phi_2\phi_3\Theta_0\Theta_0\}$$

where $\Theta_0 = (\alpha\beta-\beta\alpha)/\sqrt{2}$, it becomes

$$\Psi = A\{\phi_1\phi_1\Theta_0\phi_2\alpha\phi_3\beta - \phi_1\phi_1\Theta_0\phi_2\beta\phi_3\alpha\}/\sqrt{2} \quad .$$

Ψ is now, in the program, effectively two products of spin-orbitals as defined, with coefficients $1/\sqrt{2}$ and $-1/\sqrt{2}$ respectively. The space orbitals are then permuted such that they are grouped by atom and, within an atom, all doubly occupied orbitals are put before the singles. Among the singly occupied orbitals, x comes before y, y before z and z before s, if they exist. This order coincides with the one used in the expansions of the atomic states in Table 4.3. The spin part of the products is then changed by the same permutation in the manner described in connection with Equation (4.19). With the space product and spin factor for each atom at hand, the program then looks up the pre-stored data given by Table 4.3 to obtain the atomic states and coefficients. The antisymmetrized products of atomic states from all atoms form the composite functions (CFs). Some of the CFs deduced from different SAAPs may be the same. Only the unique ones are kept and coefficients retained by summation.

This program also identifies the near-degenerate configurations s^2p^n and p^{n+2} and transform them into

$$a\ s^2p^n + b\ p^{n+2}$$

and $$-b\ s^2p^n + a\ p^{n+2} \qquad (4.29)$$

where a and b are real numbers supplied as input to the program. The energy corrections for the composite functions from data compiled from information available in the references mentioned in Section B.5. A collection of currently available correlation plus relativistic corrections for all atomic states arising from the s^np^m valence configurations has been compiled by the author et al.[85]

The program TMAT as it stands right now can only handle diatomic molecules, but the basic algorithm is the same for any number of atoms and generalization to polyatomic molecules should be straightforword.

5. Program IACC

The program IACC computes the intraatomic correlation correction to the FORS wavefunction in two ways: (i) by using the first order perturbation expression in Equation (4.16) and (ii) by diagonalizing the corrected Hamiltonian. So far, the incorporation of the correlation-corrected Hamiltonian matrix $\{H^{SAAP}+\Delta E^{SAAP}\}$ in the MCSCF procedure has not yet been implemented. An input description to the program can be found in the SKUNK[84] reference manual.

In order to obtain the corrected Hamiltonian, it needs to

have the correction matrix ΔE^{CF} in Equation (4.14), the transformation matrix T in Equation (4.15) and also the configuration mixing matrix U, if applicable. The matrix U is the mixing between configurations of types s^2p^n and p^{n+2} as described in Equation (4.29). All this information is produced by the program TMAT, although it may also be supplied or supplemented from the input stream to the program.

6. Illustrative application to the ground state of imidogen

The procedure is best illustrated with an example. Let us consider the ground state of the imidogen (NH) molecule.

For the $^3\Sigma^-$ symmetry, there are nine SAAPs in terms of PLMOs. All of them can be denoted by the symbols

$$|u^2v^2 1\rangle, \quad |u^2vw1\rangle \text{ or } \quad |u^2vw2\rangle,$$

which are defined as follows

$$|u^2v^2 1\rangle = 2^{-3/2}\, A\{k^2u^2v^2xy\Theta_1\} \tag{4.30}$$

$$|u^2vw1\rangle = 2^{-1}\, A\{k^2u^2vwxy\Theta_1\} \tag{4.31}$$

$$|u^2vw2\rangle = 2^{-1}\, A\{k^2u^2vwxy\Theta_2\} \tag{4.32}$$

where k, x, y denote the PLMOs corresponding to the atomic orbitals 1s, $2p_x$ and $2p_y$ on nitrogen respectively and u, v, w can be any one of the PLMOs s, z, h which correspond to the

atomic orbitals 2s, $2p_z$ on nitrogen and 1s on hydrogen respectively. The spin eigenfunctions are defined as

$$\Theta_1 = (\alpha\beta-\beta\alpha)(\alpha\beta-\beta\alpha)(\alpha\beta-\beta\alpha)\alpha\alpha/2^{3/2} \quad (4.33)$$

$$\Theta_2 = (\alpha\beta-\beta\alpha)(\alpha\beta-\beta\alpha)\{(\alpha\beta+\beta\alpha)\alpha\alpha-\alpha\alpha(\alpha\beta+\beta\alpha)\}/4 \quad (4.34)$$

The nine possible SAAPs are listed as column headings for the matrix given in Table 4.4.

On the other hand, there exist eleven different single configuration composite functions. They are denoted as follows

$$|nmSLM_lM_s/n'S'M_s'\rangle = A^*\{|N\ s^n p^m\ ^{2S+1}L(M_l,M_s)\rangle|H\ s^{n'}\ ^{2S'+1}L'(0,M_s')\rangle\} \quad (4.35)$$

where it has always $L' = 0$, an S-state. The eleven composite functions are listed as headings for the rows of the matrix in Table 4.4.

Table 4.4 expresses the nine SAAPs of $^3\Sigma^-$ symmetry in terms of the eleven composite functions. The matrix elements in the table are obtained by the procedure outlined in Section C.3.

A mixing of one-configuration atomic states occurs for the configurations $|N\ s^2p^2\ ^3P(0,1)\rangle$ and $|N\ p^5\ ^3P(0,1)\rangle$ of the nitrogen atom. The appropriate linear combinations are denoted by

Table 4.4. Expansions $^3\Sigma^-$ SAAPs of NH in terms of CFs

|nm S L M_l M_s / n S M_s⟩	$\|s^2zh1\rangle$	$\|s^2zh2\rangle$	$\|z^2sh1\rangle$
|23 1/2 D 0 1/2 / 1 1/2 1/2⟩	$-\sqrt{1/3}$	$-\sqrt{2/3}$	
|23 3/2 S 0 1/2 / 1 1/2 1/2⟩	$-\sqrt{1/6}$	$\sqrt{1/12}$	
|23 3/2 S 0 3/2 / 1 1/2 -1/2⟩	$\sqrt{1/2}$	-1/2	
|14 1/2 P 0 1/2 / 1 1/2 1/2⟩			$-\sqrt{1/3}$
|14 3/2 P 0 1/2 / 1 1/2 1/2⟩			$-\sqrt{1/6}$
|14 3/2 P 0 3/2 / 1 1/2 -1/2⟩			$\sqrt{1/2}$
|24 1 P 0 1 / 1 0 0⟩			
|22 1 P 0 1 / 2 0 0⟩			
|04 1 P 0 1 / 2 0 0⟩			
|13 1 D 0 1 / 2 0 0⟩			
|13 1 S 0 1 / 2 0 0⟩			

$\|z^2sh2\rangle$	$\|s^2z^21\rangle$	$\|s^2h^21\rangle$	$\|z^2h^21\rangle$	$\|h^2sz1\rangle$	$\|h^2sz2\rangle$
$-\sqrt{2/3}$					
$\sqrt{1/12}$					
$-1/2$					
	1				
		1			
			1		
				$-\sqrt{1/3}$	$\sqrt{2/3}$
				$\sqrt{2/3}$	$\sqrt{1/3}$

$$|N22(04)1P01\rangle = |N\ s^2p^2(p^4)\ {}^3P(0,1)\rangle \quad , \qquad (4.36)$$

$$|N04(22)1P01\rangle = |N\ p^4(s^2p^2)\ {}^3P(0,1)\rangle \quad . \qquad (4.37)$$

An MCSCF calculation of the free nitrogen atom yields the orthogonal transformation

Nitrogen	$\|s^2p^2\ {}^3P(0,1)\rangle$	$\|p^4\ {}^3P(0,1)\rangle$
$\|s^2p^2(p^4)\ {}^3P(0,1)\rangle$	0.9900	-0.1414
$\|p^4(s^2p^2)\ {}^3P(0,1)\rangle$	0.1414	0.9900

In order to obtain the expansions of the molecular SAAPs in terms of the actual atomic state composite functions, one must premultiply the matrix given in Table 4.4 by the matrix transformation given in Table 4.5. The resulting matrix is matrix T occurring in Equation (4.12).

Table 4.6 contains the results of FORS and the FORS-IACC calculations with a nitrogen (14s,7p,2d/5s,3p,2d) basis and a hydrogen (6s,2p/3s,2p) basis of even-tempered gaussian primitives, for which the superposition error is negligible. Given are the results corresponding to the equilibrium distance R_e = 2 bohr and the separated atom distance R_∞ = 1000 bohr. The first row lists the energies obtained for the ground state. The next nine rows list the expansion coefficients of the wavefunction in terms of the SAAPs. The

Table 4.5. Composite functions for NH in terms of atomic states including s^2p^n-p^{n+2} configuration interaction

No.	Composite function		
1	|23 1/2 D 0 1/2 / 1 1/2 1/2⟩		
2	|23 3/2 S 0 1/2 / 1 1/2 1/2⟩		
3	|23 3/2 S 0 3/2 / 1 1/2 -1/2⟩		
4	|14 1/2 P 0 1/2 / 1 1/2 1/2⟩		
5	|14 3/2 P 0 1/2 / 1 1/2 1/2⟩		
6	|14 3/2 P 0 3/2 / 1 1/2 -1/2⟩		
7	|24 1 P 0 1 / 1 0 0⟩		
		|22 1 P 0 1/2 0 0⟩	|04 1 P 0 1/2 0 0⟩
8	|22 1 P 0 1 / 2 0 0⟩	0.9900	-0.1414
9	|04 1 P 0 1 / 2 0 0⟩	0.1414	0.9900
10	|13 1 D 0 1 / 2 0 0⟩		
11	|13 1 S 0 1 / 2 0 0⟩		

Table 4.6. Energies and wavefunctions of FORS and FORS-IACC calculations for the $x^3\Sigma^-$ ground state of NH

Internuclear distance	FORS R_e	FORS R_∞	FORS+IACC R_e	FORS+IACC R_∞
Total energy(hartree)	-55.0025	-54.9002	-55.2501	-55.1150
$\|s^2zh1\rangle$	.6621	.8165	.6457	.8165
$\|s^2zh2\rangle$	-.0466	-.5773	-.0350	-.5773
$\|z^2sh1\rangle$	.3961	.0	.3760	.0
$\|z^2sh2\rangle$	-.0610	.0	-.0510	.0
$\|s^2z^21\rangle$	.5474	.0	.5694	.0
$\|s^2h^21\rangle$	.2253	.0	.2140	.0
$\|z^2h^21\rangle$	.0885	.0	.0927	.0
$\|h^2sz1\rangle$	-.2469	.0	-.2426	.0
$\|h^2sz2\rangle$	.0193	.0	.0220	.0
|23 1/2 D 0 1/2 /1 1/2 1/2⟩	-.3442	.0	.3442	.0
|23 3/2 S 0 1/2 /1 1/2 1/2⟩	-.2837	-.5	-.2737	-.5
|23 3/2 S 0 3/2 /1 1/2 -1/2⟩	.4914	.8660	.4741	.8660
|14 1/2 P 0 1/2 /1 1/2 1/2⟩	-.1633	.0	-.1755	.0
|14 3/2 P 0 1/2 /1 1/2 1/2⟩	-.1683	.0	-.1682	.0
|14 3/2 P 0 3/2 /1 1/2 -1/2⟩	.2915	.0	.2913	.0
|24 1 P 0 1 /1 0 0⟩	.5474	.0	.5694	.0
|22 1 P 0 1 /2 0 0⟩	.2105	.0	.1987	.0
|04 1 P 0 1 /2 0 0⟩	.1195	.0	.1220	.0
|13 1 D 0 1 /2 0 0⟩	.1583	.0	.1580	.0
|13 1 S 0 1 /2 0 0⟩	-.1905	.0	-.1853	.0

final eleven rows list its expansion coefficients in terms of the atomic state composite functions which were given in Table 4.5.

From the first line in Table 4.6, one obtains the binding energies

$$\Delta E(\text{FORS}) = 0.1023 \text{ hartree} = 2.78 \text{ eV}$$

and $$\Delta E(\text{FORS-IACC}) = 0.1350 \text{ hartree} = 3.68 \text{ eV}.$$

An SCF calculation yields $\Delta E(\text{SCF}) = 2.06$ eV. The experimental value is 3.85 eV.

Further applications and numerical results of the FORS-IACC approach is given in the next section.

D. Quantitative Results for Diatomic Molecules

The basic principles and the mathematical formulations of the FORS model and the FORS IACC model for molecular calculations were outlined in Reference 14 and the preceding sections respectively. While the FORS wavefunctions are expected to recover non-dynamical, degeneracy-type correlation energy changes, FORS IACC wavefunctions are expected to recover also dynamical correlation energy changes that occur along paths of chemical reactions.

During the formation of diatomic molecules, there occur extensive rearrangements of the electronic structure of the

combining atoms, and it is for this reason that the theoretical reproduction of diatomic dissociation curves presents one of the most severe tests of the ability of any electronic structure theory to predict quantitatively energy changes that occur during chemical reactions. Furthermore, extensive and accurate experimental information is available for these molecules[6], so that the performance of any theory can be readily assessed without any ambiguity.

In the present investigation, there are reported the results of applying the aforementioned two models to the calculations of binding energies of a series of diatomic molecules. Considering the conceptual and operational simplicity of the models, their quantitative performance is gratifying.

1. Basis sets

In order to test the effectiveness of the proposed models in a credible fashion, it is essential that any errors associated with the limitation of the basis set be smaller than those errors for which the model is to be held responsible. For this reason, very large atomic basis sets were employed in the present calculations, typically a (14s,7p,2d) even-tempered gaussian primitive set[7] contracted in Raffenetti-fashion[8] to a (5s,3p,2d) basis which corresponds to a basis of "triple zeta plus polarization" or better quality. In Table 4.7, there are listed the basis sets for

Table 4.7. Basis sets and basis set errors in SCF calculations of atoms and diatomic molecules

Molecule	Atomic basis set[a]	Atomic error[b](mh)	Polarization function[c]	Molecular error[d](mh)
		Homonuclear molecules		
H_2	10s3p1d/5s3p1d	0.005	ζ_p=0.3,1.3,5.4 ζ_d=1.96	0.015
H_2	6s2p/3s2p	0.16	ζ_p=0.4,1.6	0.54
Li_2	12s3p1d/6s3p1d	0.16	ζ_p=0.0678,0.264, 1.03, ζ_d=0.275	0.3
B_2	14s7p2d/4s3p2d	0.16	ζ_d=0.145,0.913	3.5
C_2	14s7p2d/4s3p2d	0.32	ζ_d=0.2,1.0	4.7
N_2	14s7p2d/5s3p2d	0.57	ζ_d=0.2,1.0	7.5
O_2	14s7p2d/4s3p2d	0.98	ζ_d=0.5,1.6	7.9
F_2	14s7p2d/4s3p2d	1.57	ζ_d=0.5,1.6	6.0

Molecular error in heteronuclear molecules (mh)

NO[e,f]	5.9	CN[e]	4.0	NH[g]	2.27
CO[e]	6.3	BH[g]	0.48	OH[g]	2.06
BO[e]	-1.1	CH[g]	0.78	FH[g]	3.66

---

[a] Even-tempered gaussian basis of Reference 11.

[b] Error of SCF calculation with respect to the exact Hartree-Fock limit for the ground states. See Reference 11.

[c] See Reference 10.

[d] Error of SCF calculation from with respect to SCF calculation with extensive exponential basis set for molecular ground states.

[e] Basis set as above.

[f] Basis set for NO is 14s7p2d/5s7p2d for both atoms.

[g] Basis set on hydrogen for all hydrides cited is the 6s2p/3s2p set.

the various atoms and their performance in the atomic and molecular SCF calculations. The intraatomic error increases from 0.1 millihartree in Li to 1.6 millihartree in F. It is safe to assume that, with this accuracy, basis set superposition errors leading to fortuitously good binding energies will be negligible. The molecular errors increase from 0.3 millihartree in Li_2 to about 8 millihartree in O_2. They are due to omission of f polarization orbitals, and, perhaps, to insufficient optimization of d-orbitals.

2. FORS calculations

The calculations reported here pertain to the ground states of diatomic molecules at their experimental equilibrium distances. The theoretical minima of SCF calculations often occur at smaller distances, whereas FORS calculations tend to yield slightly elongated bonds. In either cases, the calculated dissociation energies would increase only insignificantly by geometry optimization.

All atoms, except hydrogen, contribute a doubly filled core orbital, namely the 1s AO, and four reactive CGOs (configuration generating orbitals), namely 2s, $2p_x$, $2p_y$ and $2p_z$. The number of configurations obtained by allowing for all possible couplings between the CGOs in a molecule, i.e., the dimension of the full valence space, depends upon the number of electrons. It is largest when there are about as many electrons as there are orbitals.

In Table 4.8, there are listed various data for the molecules considered which are pertinent to the reported calculations, namely the symmetry of the molecular ground state, the symmetries of the ground states of the separated atoms, the internuclear equilibrium distance and the dimension of the full reaction space. The number listed for this dimension is actually the number of spin-adapted antisymmetrized products (SAAPs) which constitute the practical basis of our calculational procedure. It is possible to form certain linear combinations with fixed coefficients of the SAAPs with incompletely filled π-shells, yielding "configuration state functions (CSFs)" which belong to the appropriate irreducible representations of $C_{\infty v}$ or $D_{\infty h}$. The number of such CSFs with independently variable coefficients is often smaller than the number of SAAPs listed.

The calculations were performed with the ALIS system for molecular calculations[12]. The generation of the Full Reaction Space is accomplished by a program called SAAP which is described in detail in Chapter II. The resulting quantitative data are listed in Table 4.9, namely the SCF and FORS energies for the molecules and the separated atoms. The atomic FORS energies differ from the SCF energies for boron and carbon because the ground states of the two atoms involve configuration interactions: s^2p and p^3 in B, s^2p^2 and p^4 in C. (See Section IV.C.3(c)).

Table 4.8. Characterization of Full Reaction Space of ground state of some diatomic molecules

Molecule	Symmetry	Equilibrium distance(bohr)	No. of SAAPs[a]	States of Separated Atoms
		Homonuclear molecules		
H_2	$^1\Sigma_g^+$	1.4	2	$^2S + {}^2S$
Li_2	$^2\Sigma_g^+$	5.07	8	$^2S + {}^2S$
B_2	$^3\Sigma_g^-$	3.0905	136	$^2P + {}^2P$
C_2	$^1\Sigma_g^+$	2.3897	264	$^3P + {}^3P$
N_2	$^1\Sigma_g^+$	2.068	176	$^4S + {}^4S$
O_2	$^3\Sigma_g^-$	2.2817	44	$^3P + {}^3P$
F_2	$^1\Sigma_g^+$	2.68	8	$^2P + {}^2P$
		Heteronuclear molecules		
CN	$^2\Sigma^+$	2.2144	616	$^3P + {}^4S$
BO	$^2\Sigma^+$	2.2977	616	$^2P + {}^3P$
CO	$^1\Sigma^+$	2.132	316	$^3P + {}^3P$
NO	$^2\Pi$	2.1747	252	$^4S + {}^3P$
		Hydrides		
BH	$^1\Sigma^+$	2.3289	19	$^2P + {}^2S$
CH	$^2\Pi$	2.1163	18	$^3P + {}^2S$
NH	$^3\Sigma^-$	2.0	9	$^4S + {}^2S$
OH	$^2\Pi$	1.8324	10	$^3P + {}^2S$
FH	$^1\Sigma^+$	1.7325	8	$^2P + {}^2S$

[a] In terms of symmetry adapted molecular orbitals.

Table 4.9. Total energies from SCF and FORS calculations

Molecule	Energies (in hartrees) — Molecule — SCF	FORS	— Atom — SCF	FORS
		Homonuclear molecules		
H_2[a]	-1.1336	-1.1521	-0.5	-0.5
H_2[b]	-1.1331	-1.1514	-0.4998	-0.4998
Li_2	-14.8712	-14.9006	-7.4326	-7.4326
B_2	-49.0874	-49.2180	-24.5289	-24.5601
C_2	-75.4015	-75.6373	-37.6883	-37.7056
N_2	-108.9853	-109.1345	-54.4004	-54.4004
O_2	-149.6575	-149.7627	-74.8084	-74.8084
F_2	-198.7641	-198.8444	-99.4078	-99.4078
		Heteronuclear molecules		
CN	-92.2192	-92.3708	see above	
BO	-99.5566	-99.6782	see above	
CO	-112.7829	-112.9144	see above	
NO	-129.2894	-129.4055	see above	
		Hydrides		
BH	-25.1309	-25.1858	see above	
CH	-38.2786	-38.3135	see above	
NH	-54.9756	-55.0026	see above	
OH	-75.4188	-75.4432	see above	
FH	-100.0666	-100.0909	see above	

[a] Basis set is 10s3p1d/5s3p1d.

[b] Basis set is 6s2p/3s2p.

From the data in Table 4.9, one deduces the binding energies listed in Table 4.10. An appropriate measure of the effectiveness of the FORS model is the fraction of the correlation contribution to the binding energy which is recovered by the model, as defined by

$$\{\Delta E(FORS) - \Delta E(SCF)\} / \{\Delta E(exp) - \Delta E(SCF)\}$$

where

$$\Delta E = E(molecule) - E(separated\ atoms)$$

is the binding energy. It is seen that in most cases the FORS model recovers between 70% and 90% of the correlation error. By and large, the model is more effective when the number of valence electrons is smaller than the number of valence orbitals. In absolute values, the remaining errors lie between 5 and 30 Kcal/mole. This is larger than the 2-5 Kcal/mole error attributable to basis set deficiencies and it is still larger than the accuracy desired for many chemical predictions. It should be noted, however, that dissociation of diatomic molecules involves extreme changes in electron correlations. In many reactions between larger molecules, the changes in electron correlations are much less severe and the FORS model can then be expected to yield energies accurate to a few Kcal/mole.

Table 4.10. Dissociation energies of diatomic molecules

Molecule	SCF (eV)	FORS (eV)	exp[a] (eV)	Correlation recovered (%)	Error of FORS approximation (Kcal/mole)
		Homonuclear molecules			
H_2[b]	3.635	4.14	4.748	45	14.1
H_2[c]	3.629	4.13	4.748	45	14.3
Li_2	0.16	0.96	1.068	88	2.5
B_2	0.81	2.64	3.08	81	10.1
C_2	0.68	6.14	6.32	97	4.1
N_2	5.02	9.06	9.905	83	19.5
O_2	1.12	3.98	5.213	70	28.4
F_2	-1.40	0.78	1.658	71	20.2
		Heteronuclear molecules			
CN	3.55	7.21	7.89	84	15.7
BO	5.97	8.42	8.40	101	-0.5
CO	7.79	10.89	11.226	90	7.7
NO	2.19	5.35	6.615	71	29.2
		Hydrides			
BH	2.78	3.42	3.57	81	3.5
CH	2.46	2.95	3.63	41	15.7
NH	2.06	2.79	3.85	41	24.4
OH	3.01	3.67	4.62	41	21.9
FH	4.33	4.99	6.12	37	26.1

[a] Molecular data were obtained from Huber and Herzberg[86] except for D_o^o(NH) from Piper[87] and atomic data from Moore[6].

[b] Basis set is 10s3pad/5s3pld.

[c] Basis set is 6s2p/3s2p.

The present calculations allow us to make a prediction regarding the BO molecule which has received little experimental or theoretical attention. So far, its bond energy has not been well determined experimentally; published values range from 7.4 eV to 9.2 eV. Since in all cases, except for BO, the FORS model recovers 70-90% of the binding energy correlation error, and since it recovers 84% in the isoelectronic CN molecule, it seems most likely that a similar result is also valid for BO. Assuming that (85±10)% is in fact recovered for this molecule, the bond energy of BO would be predicted to be (8.85±0.3) eV, which is considerably larger than the recent thermochemical value of 8.44±0.12 eV[6].

In Table 4.11, there are listed dipole moments obtained from the FORS wavefunctions. In all cases the FORS values are improvements over the SCF values. The largest remaining error may be the failure to average over the vibrations of the atoms. The dipole moment of BO has not been measured so far. Its prediction in Table 4.11 is probably accurate to 0.3 Debye.

3. FORS IACC calculations

The FORS IACC method requires the FORS wavefunction to be expressed in terms of SAAPs which are constructed from projected localized FORS orbitals (PLMOs). For homonuclear diatomic molecules, the number of PLMO-generated SAAPs needed

Table 4.11. Dipole moments

Molecule	SCF	FORS (in Debye)	exp[a]
CN (C^+N^-)	2.30	1.62	1.45
BO (B^+O^-)	3.00	2.34	-
CO (C^-O^+)	-0.26	0.30	0.122
NO (N^-O^+)	-0.31	0.24	0.159

[a] Experimental values from Reference 6.

to span the Full Reaction Space is greater than the number of SAAPs generated from natural orbitals, because the g/u symmetry is not used. The number of composite functions (CFs) required to span the Full Reaction Space is in general still larger, as was discussed in Section IV.C.2. For the molecules investigated here, the specifics are given in Table 4.12. Listed are the symmetries and equilibrium distances of various states, the symmetries of the separated species, the number of PLMO-generated SAAPs and the number of CFs required to span the Full Reaction Space.

FORS IACC calculations on diatomic molecules were performed using the ALIS system[12] augmented by the program TMAT[84] to generate the transformation matrix in Equation (4.12) and the program IACC[84] to determine the corrected hamiltonian matrix. Both programs are described in detail in the preceding section.

The energies results of the FORS IACC calculations are presented in Table 4.13. For the sake of comparison, the results from SCF and FORS calculations are also included. As discussed in the preceding sections, it is possible to obtain approximations to the FORS IACC energies from FORS wavefunctions by first order perturbation theory. These approximate energies lie in all cases above those obtained by diagonalizing the corrected hamiltonian matrix. The deviations of the first order energies from the exact ones are also listed.

The dissociation energies obtained from these calculations, together with the experimental values and those resulting from SCF and FORS calculations are listed in Table 4.14. With the exception of the ground state of N_2 and the $B^2\Sigma^-$ excited state of CH, the theoretical results improve consistently in proceeding from the SCF to the FORS and the FORS IACC model. An analysis of the origin of the failures in N_2 and CH should prove constructive for a better understanding of the correlation error and appropriate improvements of the model.

The spectroscopic excitation energies obtained from these calculations for the CH and the NH molecules are listed in Table 4.15. With the exception of $B^2\Sigma^-$ state of CH, the agreement with the experiment is very good.

Table 4.12. Specifics of various states of some diatomic molecules

Molecule	State and Symmetry	No. of SAAPs[a]	No. of CFs	Equilibrium distance (bohr)	Symmetry of Dissociated species
		Homonuclear molecules			
H_2	$X^1\Sigma_g^+$	3	4	1.4	$^2S + ^2S$
N_2	$X^1\Sigma_g^+$	328	584	2.068	$^4S + ^4S$
O_2	$X^3\Sigma_g^-$	96	118	2.2817	$^3P + ^3P$
F_2	$X^1\Sigma_g^+$	16	22	2.68	$^2P + ^2P$
		Hydrides			
BH	$X^1\Sigma^+$	19	25	2.3289	$^2P + ^2S$
CH	$X^2\Pi$	18	22	2.1163	$^3P + ^2S$
	$a^4\Sigma^-$	10	11	2.0470	$^3P + ^2S$
	$A^2\Delta$	16	22	2.0823	$^1D + ^2S$
	$B^2\Sigma^-$	17	22	2.2080	$^3P + ^2S$
	$C^2\Sigma^+$	22	24	2.1057	$^1D + ^2S$
NH	$X^3\Sigma^-$	12	14	2.0	$^4S + ^2S$
	$a^1\Delta$	12	21	2.0	$^2D + ^2S$
	$b^1\Sigma^+$	19	25	2.0	$^2P + ^2S$
OH	$X^2\Pi$	10	12	1.8324	$^3P + ^2S$
FH	$X^1\Sigma^+$	8	10	1.7325	$^2P + ^2S$

[a] SAAPs in terms of Projected Localized FORS MOs (= Molecule adapted valence AOs).

Table 4.13. Energies obtained from FORS IACC model

Molecule	State and Symmetry	R = Equilibrium distance Energies (in hartree) SCF	FORS	IACC	ΔE^a (mh)
		Homonuclear molecules:			
H_2	$X^1\Sigma_g^+$	-1.1336	-1.1521	-1.1679	0.25
N_2	$X^1\Sigma_g^+$	-108.9853	-109.1345	-109.6660	6.33
O_2	$X^3\Sigma_g^-$	-149.6575	-149.7627	-150.4133	1.26
F_2	$X^1\Sigma_g^+$	-198.7640	-198.8443	-199.6673	0.95
		Hydrides:			
BH	$X^1\Sigma^+$	-25.1309	-25.1858	-25.3081	0.46
CH	$X^2\Pi$	-38.2786	-38.3135	-38.4921	0.76
	$a^4\Sigma^-$	-38.2892	-38.3073	-38.4580	1.68
	$A^2\Delta$	-38.1794	-38.1962	-38.3871	0.59
	$B^2\Sigma^-$	-38.1574	-38.2030	-38.3904	1.58
	$C^2\Sigma^+$	-38.1272	-38.1615	-38.3488	1.06
NH	$X^3\Sigma^-$	-54.9756	-55.0025	-55.2501	1.16
	$a^1\Delta$	-54.9087	-54.9298	-55.1939	0.92
	$b^1\Sigma^+$	-54.8442	-54.8977	-55.1559	1.36
OH	$X^2\Pi$	-75.4188	-75.4432	-75.7901	0.95
FH	$X^1\Sigma^+$	-100.0666	-100.0909	-100.5490	1.38

[a] ΔE = E(FOPC) - E(IACC). FOPC = First order perturbation correction, see Equation (4.16).

Separated atoms Energies (in hartree)		
SCF	FORS	IACC
-0.9996	-0.9996	-0.9996
-108.8008	-108.8008	-109.2304
-149.6168	-149.6168	-150.2286
-198.8156	-198.8156	-199.6246
-25.0287	-25.0599	-25.1589
-38.1881	-38.2055	-38.3580
-38.1881	-38.2055	-38.3580
-38.1308	-38.1476	-38.3121
-38.1881	-38.2055	-38.3580
-38.1308	-38.1476	-38.3121
-54.9002	-54.9002	-55.1150
-54.7953	-54.7953	-55.0281
-54.7271	-54.7620	-54.9838
-75.3082	-75.3082	-75.6141
-98.9076	-98.9076	-99.3121

Table 4.14. Dissociation energies obtained from FORS IACC model

Molecule	State and Symmetry	exp[b]	De (eV) SCF	FORS	IACC	Error[a] (eV) SCF	FORS	IACC
			Homonuclear molecules					
H_2	$X^1\Sigma_g^+$	4.75	3.64	4.15	4.58	1.11	0.6	0.17
N_2	$X^1\Sigma_g^+$	9.91	5.02	9.08	11.86	4.89	0.83	-1.95
O_2	$X^3\Sigma_g^+$	5.21	1.11	3.97	5.03	4.1	1.24	0.18
F_2	$X^1\Sigma_g^+$	1.66	-1.40	0.78	1.16	3.06	0.88	0.50
			Hydrides					
BH	$X^1\Sigma^+$	3.57	2.78	3.43	4.06	0.79	0.14	-0.49
CH	$X^2\Pi$	3.63	2.46	2.94	3.65	1.17	0.69	-0.02
	$a^4\Sigma^-$	2.91	2.75	2.77	2.72	0.16	0.14	0.19
	$A^2\Delta$	2.03	1.32	1.78	2.04	0.71	0.25	-0.01
	$B^2\Sigma^-$	0.41	-0.84	-0.07	0.88	1.25	0.48	-0.47
	$C^2\Sigma^+$	0.96	-0.10	0.38	1.00	1.06	0.58	-0.04
NH	$X^3\Sigma^-$	3.85	2.06	2.78	3.68	1.79	1.07	0.17
	$a^1\Delta$	4.67	3.08	3.66	4.51	1.59	1.01	0.16
	$b^1\Sigma^+$	4.80	3.18	3.69	4.68	1.62	1.11	0.12
OH	$X^2\Pi$	4.62	3.01	3.67	4.79	1.61	0.95	-0.17
FH	$X^1\Sigma^+$	6.12	4.33	4.99	6.45	1.79	1.12	-0.33

[a] Error = De(IACC) - De(exp).

[b] Molecular data were obtained from Huber and Herzberg[6] except for D_o^o from Piper[86] and atomic data from Moore[87].

Table 4.15. Excitation energies of diatomic molecules from SCF, FORS and FORS IACC calculations

Transition (eV)	SCF	FORS	FORS IACC	exp
CH $X^2\Pi \rightarrow a^4\Sigma^-$	-0.29	0.18	0.98	0.72
$\rightarrow A^2\Delta$	2.70	3.20	2.90	2.86
$\rightarrow B^2\Sigma^-$	3.30	3.02	2.81	3.16
$\rightarrow C^2\Sigma^+$	4.12	4.15	3.95	3.93
NH $X^3\Sigma^- \rightarrow a^1\Delta$	1.83	1.97	1.52	1.57
$\rightarrow b^1\Sigma^+$	3.58	2.84	2.49	2.63

V. AUGMENTATION OF THE FORS MODEL BY SELECTED EXCITATIONS FROM THE FULL REACTION SPACE

A. Introduction

1. Approaches to electron correlation

Consistently accurate predictions of chemical and physico-chemical properties cannot be had within the self-consistent-field approximation. To achieve this goal, electronic wavefunctions must be improved by taking into account interelectronic correlations. However, since the main objects of chemical interest are relative changes on energy surfaces, the aim of quantum chemical calculations is only the recovery of those parts of the correlation energy which change along reaction paths, rather than the total correlation energy. In other words, the changes of energy surfaces with variations of molecular geometry have to be determined with greater accuracy than the absolute values of the energy.

The most effective adaptation of wavefunctions to describe electron correlations consists of including odd powers of all interelectronic distances explicitly. But the mathematical difficulties of this approach have so far proven insurmountable for systems consisting of more than two electrons. The alternative is to expand the wavefunction in terms of antisymmetrized products of orbitals. Such methods can be classified as follows:

(i) Straight configuration interaction ("CI"). Here the orbitals are usually taken from a preliminary SCF calculation. Two options exist:

(a) All configurations are included which can be constructed from the basis set.

(b) Only a subset of configurations is selected for the configuration interaction calculation.

(ii) Configuration interaction coupled with orbital optimization, i.e. configuration mixing as well as orbital shapes are determined by energy minimization (MCSCF). Again two options exist:

(a) All configurations from a chosen set of configuration generating orbitals (CGOs) are included. The complete active space self-consistent-field (CASSCF)[26-29,88] is an example of this approach. In this case, orbital optimization can improve the wavefunction only if the number of CGOs is <u>smaller than the total</u> number of basis functions used to express the orbitals.

(b) Only a subset of configurations is selected for the MCSCF calculation, for example in the so-called pair theories.

(iii) Non-variational methods, in particular many-body perturbation theories, replacing the solution of the CI eigenvalue problem.

The number of configurations that can be handled is largest for the methods of type (iii) and smallest for the method of type (ii), with those of type (i) lying in between. On the other hand, the orbital optimization implicit in the methods of type (ii) permits a reduction in the number of configurations without serious damage to the quality of the results. In recent years, a combined approach has been found attractive. First an MCSCF calculation is carried out for a "reference function" of type (iib) consisting of a limited number of configurations. Then a CI calculation is performed by adding to the reference function a large number of configurations selected according to some principle.

2. Augmentation of the FORS model

The FORS method discussed in Chapters II and III is of type (iia). Its configuration generating orbitals are chosen on the basis of physico-chemical intuition: their number is equal to the number of valence orbitals on the participating atoms. For this reason, the model is expected to recover the non-dynamical correlation of the valence electrons. Its application to diatomic molecules[19] usually leads to a 70% to 90% recovery of the correlation contribution to dissociation, depending upon the system. Since the model is of type (iia), its limitations arise entirely from restricting the number of configurations generating orbitals and the inclusion of

"augmenting configurations" involving additional "external orbitals" is required in order to recover a greater part of the correlation energy in a non-empirical manner.

When the active space is expanded by including external orbitals, it is again necessary to choose between alternatives similar to those described by the aforementioned type (i), (ii), (iii). As regards to the selection of configurations, it is practical to classify the additional configurations, according to the number of external orbitals they contain, as "single excitations", "double excitations", etc., with respect to the Full Reaction Space. No assumptions are required regarding the external orbitals, if the additional augmenting configurations contain all configurations up to a specific excitation type (e.g. all single excitations, or all single and double excitations) which can be generated from the entire atomic orbital basis. On the other hand, essentially the same accuracy can be attained with a considerably smaller number of external configuration generating orbitals when they, too, are MCSCF optimized.

The approach taken in the present investigation is as follows. The full FORS wavefunction is chosen as zeroth approximation. To these a limited number of external configuration generating orbitals are added, which are then MCSCF optimized. As augmenting configurations we choose all configurations up to a certain excitation type that can be

generated in a manner to be described from these configuration generating orbitals. Since the FORS orbitals are dominant, their optimization is affected only negligibly by the augmenting configurations all of which have small weights. Therefore, the FORS orbitals are optimized only within the FORS calculation. They are kept "frozen" (i.e. their shapes are left unchanged) during the calculation with the augmented wavefunction, when the external orbitals are MCSCF optimized. However the mixing coefficients of the various configurations in the Full Reaction Space are permitted to readjust during the augmented calculation.

The questions to be explored concern the details of the configuration selection. In particular, which FORS configurations are chosen to generate excited configurations, which FORS orbitals are being replaced by external orbitals and which excitation levels are included.

If the FORS wavefunction Ψ_0 is improved by the admixture of excitation terms Ψ_ν, then the weight of these admixtures is, to the first order, given by

$$\langle\Psi_0|H|\Psi_\nu\rangle/\{\langle\Psi_0|H|\Psi_0\rangle-\langle\Psi_\nu|H|\Psi_\nu\rangle\} \quad . \qquad (5.1)$$

If single excitations are generated from the FORS wavefunction taken as a unit, then the interaction elements $\langle\Psi_0|H|\Psi_\nu\rangle$ vanish, according to the generalized Brillouin theorem, and no

single excitation improvement is possible. Such improvements do obtain, however, if single excitations are made out of individual contributing FORS configurations. In such cases, it is apparent that the denominator increases with the excitation level and greater improvements are therefore expected from additional single excitations.

It is important to note that in selecting those FORS configurations out of which excitations are made, one must consider not only SAAPs which contribute greatly to the FORS wavefunctions, but also those which contribute little or, because of symmetry reasons, possibly not at all.

3. Choices of molecules

The hydrogen fluoride and fluorine molecules are chosen as examples for two reasons. On the one hand, the contribution of correlation to their binding energies is particularly large and has proven to be difficult to recover. On the other hand, they have nevertheless a transparent electronic structure. The dissociation involves the cleavage of only one bond and the roles of the different orbitals, whether they are lone pairs or bonding, are easily identifiable. The FORS orbitals can essentially be divided into three groups[13b] according to their behavior during the dissociation process, as indicated by the following.

Orbital	Deformation	Occupancy
Inner shell	Essentially undeformed	Essentially unchanged
Lone pair	Essentially deformed	Essentially unchanged
Bonding	Severely deformed	Essentially changed

Since it seems questionable whether correlation in inner shell orbitals is important for molecule formation, calculations were performed with correlating orbitals to the inner shell for the FH molecule[89]. It was found that the energy lowering at the equilibrium distance and that for the separated atoms differed by less than 0.5 millihartree. Since we are interested in the dissociation energies rather than in the absolute energies, correlating orbitals for inner shells are omitted in the sequel.

B. The Hydrogen Fluoride Molecule

1. FORS wavefunction

The ground state of FH is a $^1\Sigma^+$ state, the equilibrium distance is R_e = 1.7325 bohr. All calculations were performed using the following quantitative basis: an unscaled (14s,7p,2d / 5s,3p,2d) basis, with polarization exponents of ζ_d=0.36 and 1.26 for F atom and an unscaled (6s,2p / 3s,2d) basis with ζ_p=0.4 and 1.6 for H atom. The SCF and FORS calculations yield the following results:

	$E(R_e)$ (hartree)	$E(R_\infty)$ (hartree)	ΔE (eV)
SCF	-100.0666	-99.9088	4.30
FORS	-100.0908	-99.9088	4.95

Since the experimental dissociation energy is 6.12 eV, only 36% of the correlation energy are recovered by the FORS wavefunction in this case.

The Full Reaction Space for the $^1\Sigma^+$ symmetry of FH is spanned by eight SAAPs in terms of which the FORS wavefunction is expressed. The first column of Table 5.1 lists these SAAPs. The second column lists the corresponding coefficients of the FORS wavefunction at the equilibrium distance. In this table, k denotes the fluorine inner shell orbital, s, x and y designate the fluorine lone pair orbitals and σ and σ^* are the bonding and antibonding orbitals respectively. All these orbitals are molecule-adapted by the MCSCF optimization. The spin function is

$$\Theta_0 = [(\alpha\beta-\beta\alpha)/\sqrt{2}]^5$$

and the antisymmetrizer is

$$\mathbf{A} = [\Sigma_P (-1)^P P] \; / \; \sqrt{[N!2^q]}$$

Table 5.1. FORS wavefunction for FH

SAAP	Coefficient
$\Phi_1 = A\ \{k^2 s^2 x^2 y^2 \sigma^2 \Theta_0\}$	0.994740
$\Phi_2 = A\ \{k^2 s^2 x^2 y^2 \sigma\sigma^* \Theta_0\}$	-0.010256
$\Phi_3 = A\ \{k^2 s^2 x^2 y^2 \sigma^{*2} \Theta_0\}$	-0.086545
$\Phi_4 = A\ \{k^2 x^2 y^2 \sigma^2 s\sigma^* \Theta_0\}$	-0.000927
$\Phi_5 = A\ \{k^2 x^2 y^2 \sigma^{*2} s\sigma \Theta_0\}$	0.045354
$\Phi_6 = A\ \{k^2 s^2 x^2 \sigma^2 \sigma^{*2} \Theta_0\}$	-0.011266
$\Phi_7 = A\ \{k^2 s^2 y^2 \sigma^2 \sigma^{*2} \Theta_0\}$	-0.011266
$\Phi_8 = A\ \{k^2 x^2 y^2 \sigma^2 \sigma^{*2} \Theta_0\}$	-0.024215

where q is the number of doubly occupied orbitals.

It should be noted that a unitary transformation is arbitrary among the orbitals in a Full Reaction Space. Any such transformation, while leaving the wavefunction invariant, will change the coefficients associated with various SAAPs. The coefficients in Table 5.1 result when the FORS MOs are determined as natural orbitals of the wavefunction. It is remarkable that the natural orbitals k, s, x, and y have the aforementioned localized character on fluorine. The extremely localized shapes of the natural orbitals s, x, and y are illustrated by the contour plot of Figure 5.1.

2. Augmented wavefunctions. First selection method

a. Calculation at the equilibrium distance Since the natural orbitals s, x and y have the character of lone pairs on fluorine, it is to be expected that their correlation changes only little when the molecule is formed. The two electrons in the orbitals σ and σ^*, on the other hand, are unpaired before bond formation and paired after bond formation and, therefore, experience a considerable change in correlation energy. In "zeroth order" this pairing process is described by the three configurations Φ_1, Φ_2 and Φ_3 of Table 5.1. It is seen that configurations Φ_1 and Φ_3 are indeed dominant. (The small coefficient of Φ_2 is due to the fact that the MOs are natural orbitals.) Accordingly, it is

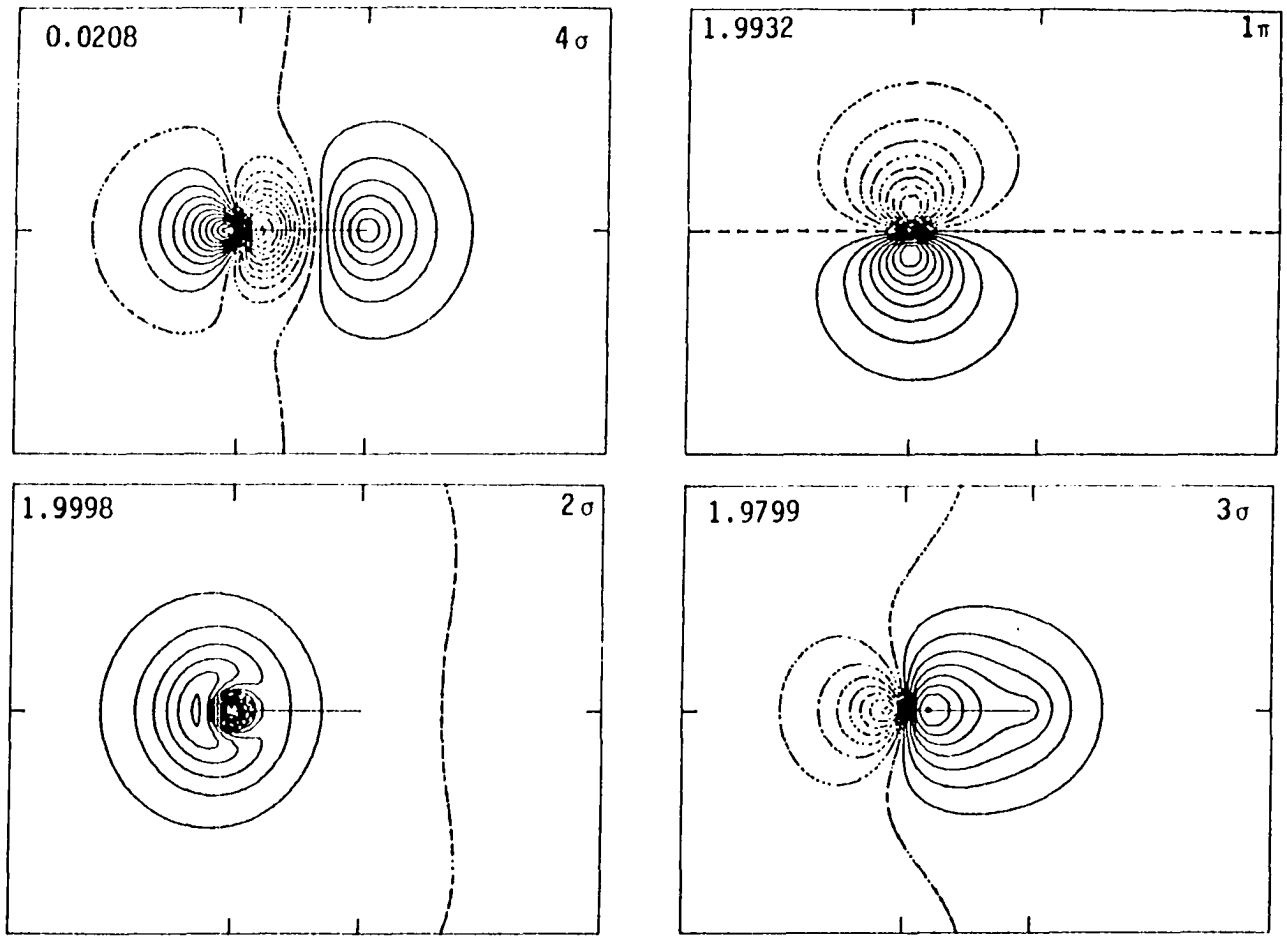

Figure 5.1. Natural molecular orbitals of the FORS wavefunction of FH at R = 1.7325 bohr. Numbers indicate occupancies

reasonable to consider excitations out of the SAAPs Φ_1, Φ_2, Φ_3 and, moreover, to allow more elaborate additional correlation in the bond orbitals σ, σ^* than in the lone pair orbitals.

The following types of excitations are therefore considered: single excitations out of s, x, y and single plus double excitations out of σ and σ^*. As regard to external orbitals, we consider one, two and three external orbitals of the various symmetry types. As mentioned before, these external orbitals are optimized by the MCSCF procedure in terms of the quantitative basis, while the FORS MOs are kept unchanged.

The results of these calculations for the equilibrium distance are reported in Table 5.2. The first column of this table lists the various excitation choices which were investigated. For example, type 3: $s \rightarrow 2\sigma'$ indicates that excitations were made only out of orbital s (as mentioned before, only single excitations are considered for s) and that two external orbitals σ' were made available. Thus all single excitations out of s into any one of the two external orbitals were constructed for the SAAPs Φ_1, Φ_2 and Φ_3 and added to the FORS wavefunction as augmenting configurations. On the other hand, type 10: $\sigma \rightarrow 1\sigma', 1\pi'$ indicates excitations were made out of σ and σ^* (as mentioned before, single and double excitations are considered for σ, σ^*) into one external σ' orbital and into one pair of external orbitals π_x' and π_y'.

Table 5.2. Augmented FORS calculations with selected excitations for dissociation energy of FH. Selection I

	Type of Excitations	No. of additional SAAPs	E at R_e [a] (hartree)	E at R_∞ [a] (hartree)	ΔE (eV)	$\Delta E-\Delta E_0$ (eV)
1	FORS	0	-100.0908	-99.9088	4.954	0
2	s→1σ′	4	-100.0994	-99.9179	4.939	-0.015
3	s→2σ′	8	-100.1017	-99.9179	5.002	0.048
4	π→1π′	8	-100.1265	-99.9095	5.904	0.950
5	π→2π′	16	-100.1274	-99.9095	5.927	0.973
6	σ→1σ′	3	-100.0943	-99.9088	5.048	0.094
7	σ→2σ′	7	-100.0943	-99.9088	5.048	0.094
8	σ→1π′	2	-100.0946	-99.9088	5.057	0.103
9	σ→2π′	6	-100.0952	-99.9088	5.072	0.118
10	σ→1σ′,1π′	5	-100.0981	-99.9088	5.152	0.198
11	σ→2σ′,2π′	13	-100.0994	-99.9088	5.187	0.233
12	s→2σ′;π→2π′; σ→2σ′,2π′	37	-100.1438	-99.9188	6.123	1.169
13	s→3σ′;π→2π′; σ→3σ′,2π′	46	-100.1439	-99.9188	6.124	1.170
14	s→2σ′;π→3π′; σ→2σ′,3π′	51	-100.1446	-99.9188	6.145	1.191
15	s→2σ′;π→2π′; σ→2σ′,2π′,1δ	39	-100.1439	-99.9188	6.124	1.170

[a] R_e = 1.7325 bohrs; R_∞ = 1000 bohrs.

Similarly, type 12 implies that all possible of the following excitations were considered: single excitations out of s, x, y and single plus double excitations out of σ, σ^* into the same external orbitals, namely two σ-type orbitals, two π_x-type orbitals and two π_y-type orbitals. The fifth column lists the predicted dissociation energy. The last column lists the improvement over the FORS result.

Comparison with the experimental dissociation energy of 6.12 eV shows that any one of the wavefunctions denoted as type 12 to 15 recovers the entire correlation contribution to the dissociation energy of FH. It is also seen that the correlation effects are almost additive. The s, π and σ improvements of the wavefunctions denoted as type 3, 5, 11 add up to a total of 1.256, which is comparable to the value listed for type 12. It seems that one correlating σ-type orbital is needed for s and another one for σ and that the same holds for the π-type orbitals correlating σ and π. Thus, a total of two σ' and two π' external orbitals are adequate. The correlations from additional σ', π' or δ orbitals are negligible when the external orbitals are optimized. This implies that the reported results are equivalent to what would be found if all possible excitations of the described types were included. In other words, no arbitrary selection has been introduced by limiting the number of external orbitals. The most remarkable result is that single excitations from the

lone pair type FORS π orbitals to external π orbitals provide by far the largest contribution to the correlation part of the dissociation energy beyond the FORS model.

It is possible to express the FORS configurations entirely in terms of the localized FORS orbitals. Contour plots of these localized orbitals are shown in Figure 5.2. It is seen that the orbitals s, x, and y are similar to those in Figure 5.1 and that the bonding/antibonding orbital pair is replaced by the molecule-adapted orbital $z=2p_z$ on fluorine and the molecule-adapted orbital h=1s on hydrogen. The corresponding eight SAAPs can be obtained simply by substituting the first column in Table 5.1 the orbitals z and h for σ and σ^*. (The expansion coefficients in the second column will be different of course.) The augmentation of the FORS wavefunction can then also be made in terms of these localized configurations. If one allows for single plus double excitations of the orbitals z and h, the results are very close to those discussed for the natural orbitals.

b. Calculation of dissociation curve Calculations with wavefunctions of types 12 of Table 5.2 were performed along the entire dissociation path. For comparison, calculations were also performed with the corresponding SCF and FORS wavefunctions. Total energies are tabulated in Table 5.3. These values were interpolated using the program

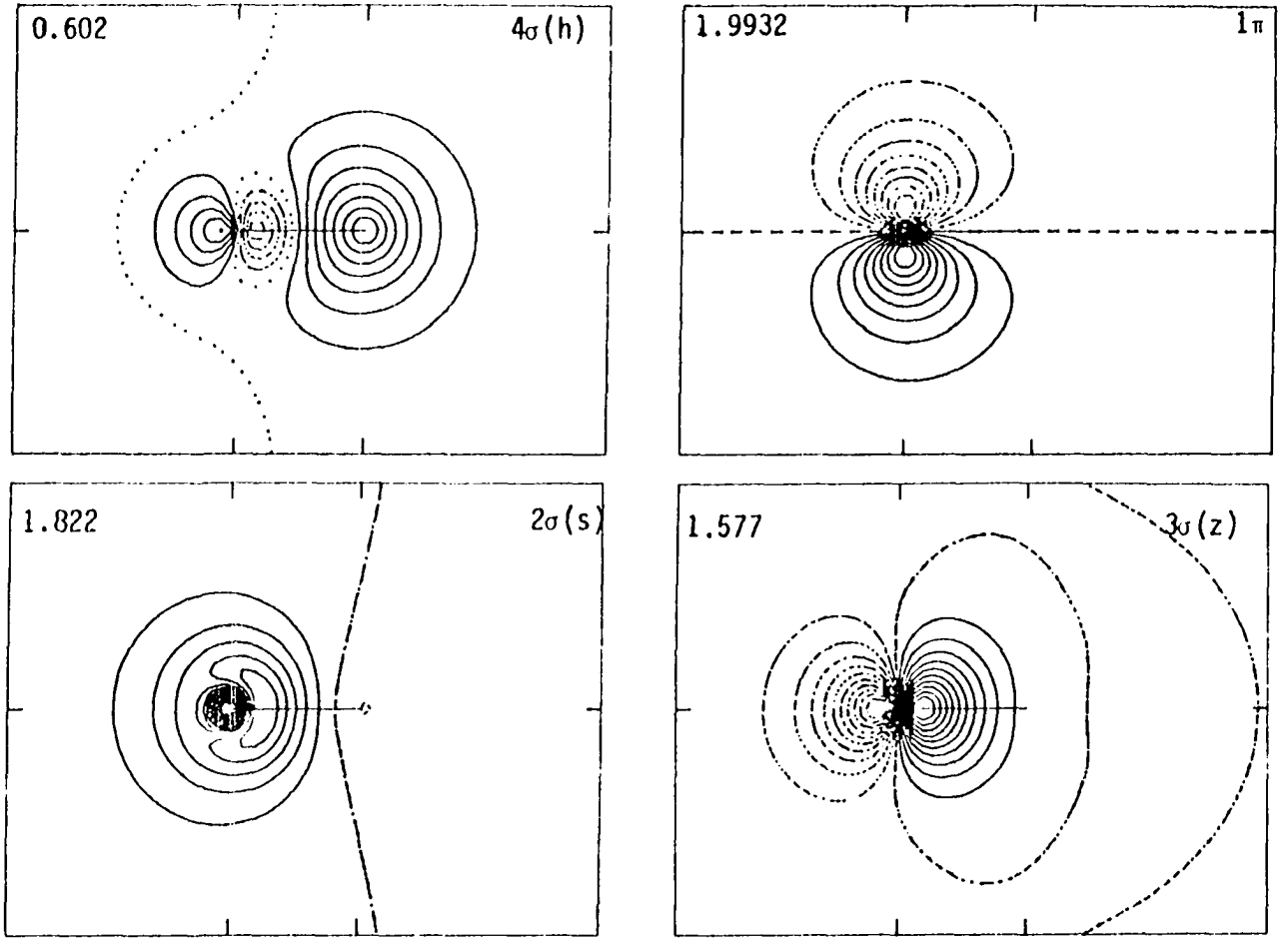

Figure 5.2. Projected localized molecular orbitals for the FORS wavefunction of FH at R = 1.7325 bohr. Numbers indicate occupancies

Table 5.3. Calculated molecular energies of FH as functions of the internuclear distance

R(bohr)	Total Energies (hartree)		
	SCF	FORS	Augmented FORS
1.1	-99.7456	-99.7578	-99.8033
1.3	-99.9656	-99.9811	-100.0294
1.4	-100.0184	-100.0356	-100.0851
1.5	-100.0485	-100.0676	-100.1179
1.55	-100.0574	-100.0775	-100.1285
1.6	-100.0631	-100.0843	-100.1358
1.65	-100.0662	-100.0885	-100.1404
1.7	-100.0671	-100.0905	-100.1435
1.72	-100.0669	-100.0908	-100.1439
1.7325	-100.0666	-100.0908	-100.1441
1.75	-100.0661	-100.0907	-100.1438
1.77	-100.0653	-100.0904	-100.1436
1.8	-100.0637	-100.0896	-100.1428
1.9	-100.0555	-100.0839	-100.1373
2.0	-100.0440	-100.0752	-100.1283
2.2	-100.0155	-100.0529	-100.1053
2.4	-99.9841	-100.0288	-100.0785
2.6	-99.9527	-100.0056	-100.0523
2.9	-99.9083	-99.9758	-100.0161
3.2	-99.8687	-99.9529	-99.9858
3.5	-99.8341	-99.9367	-99.9632
4.5	-99.7495	-99.9138	-99.9272
5.5	-99.6986	-99.9096	-99.9200
7.0		-99.9088	-99.9190
1000	-99.9088	-99.9088	-99.9188

DIAPOT[90]. The resulting potential curves are shown in Figure 5.3 The FORS curve, as well as the augmented FORS curve, unlike the SCF curve, treat the dissociation reaction

$$FH \longrightarrow F + H$$

qualitatively correctly. The program DIAPOT also yields the spectroscopic constants, given in Table 5.4, via a Dunham analysis[90]. Previous theoretical results[91-94] are also included for comparison. Only ab initio work which goes beyond the Hartree-Fock method, and which is later than 1972, is included. A bibliography of the older work may be found in references 91 and 95.

It is seen that the FORS calculations predict the spectroscopic constants reasonably well. This implies that the FORS model describes the potential curve quite well near the equilibrium distance. However, it fails to recover all the changes in the correlation energies as the atoms move apart. The additional excited configurations seem to achieve just that.

3. Augmented wavefunctions. Second selection method

In this approach, the procedure for selecting singly excited configurations is developed by analogy with the situation in the fluorine atom. In the latter, one can

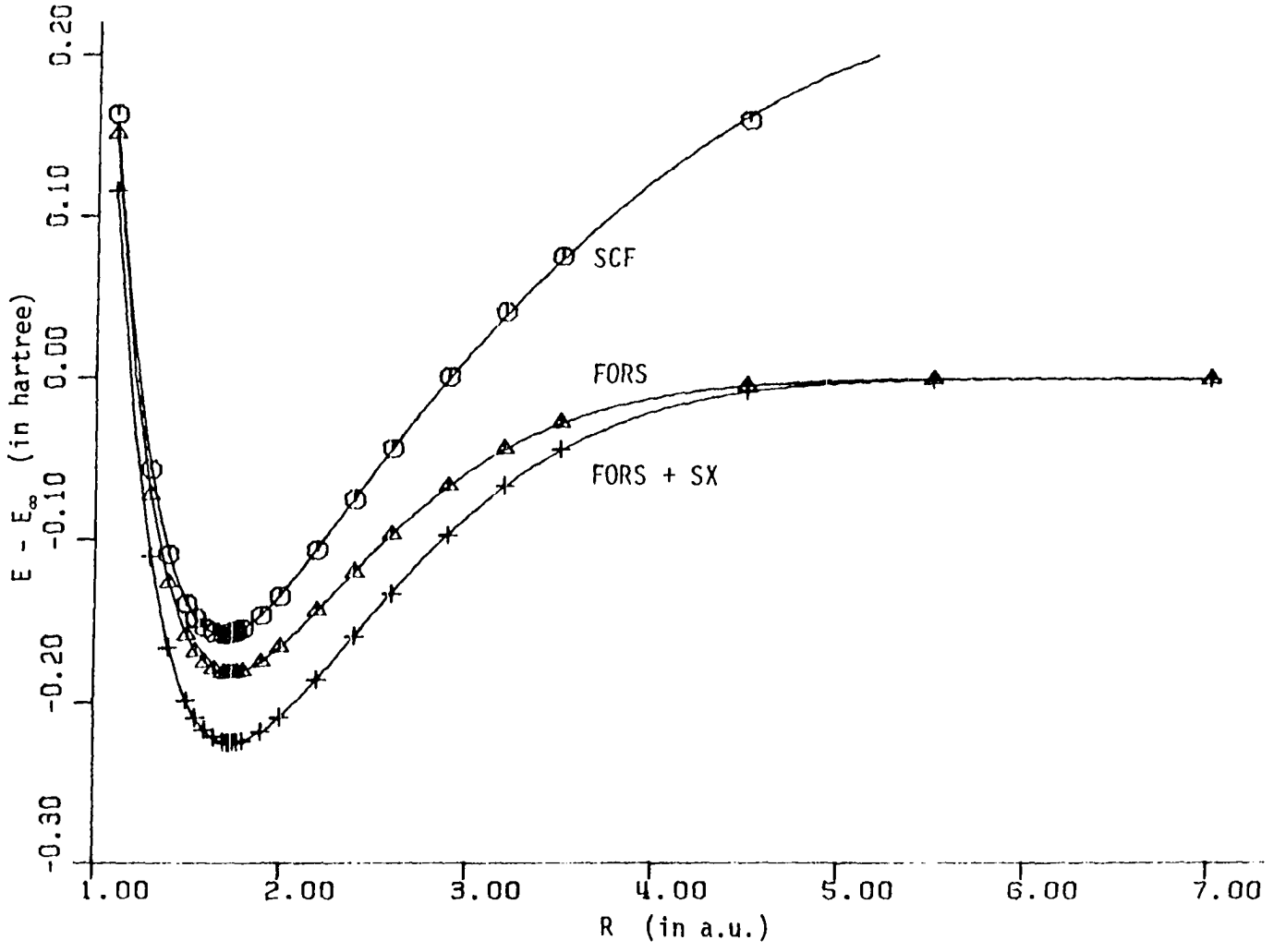

Figure 5.3. Potential curves for ground state of FH

Table 5.4. Spectroscopic constants of FH

Method	Reference	R_e (bohr)	D_e (eV)	B_e	ω_e (in 1/cm)	$\omega_e x_e$	α_e
SCF		1.698	4.307	21.80	4432	76.42	0.802
FORS		1.733	4.954	20.94	4136	99.86	0.832
Augm. FORS		1.733	6.130	20.93	4216	86.07	0.757
PNO-CI	91	1.723	5.69	21.15	4252	85.9	0.762
CEPA	91	1.733	5.83	20.95	4169	90.4	0.787
FO-CI	92	1.739	5.88	20.80	4210		
IEPA	93	1.756			4084		
OVC	94		6.18				
Exp.	6	1.733	6.12	20.96	4138	89.88	0.798

distribute the seven valence electrons in four different ways among the four valence orbitals 2s, $2p_x$, $2p_y$ and $2p_z$, as is shown in Table 5.5 in the rows denoted as I, II, III, IV, which correspond to SAAPs with symmetries $^2P(0)$, $^2P(x)$, $^2P(y)$, ^2S respectively. If one wishes to construct additional configurations to improve the wavefunction whose principal component is the $^2P(0)$ SAAP, then one can obtain such additional SAAPs by making single substitutions in <u>any one</u> of the "base configurations" I to IV, if only one chooses external orbitals of appropriate symmetries. In Table 5.5, appropriate symmetries for these external orbitals are shown in lines Ix, IIx, IIIx and IVx below those orbitals which they are replacing. These singly excited configurations are indeed the most important additions to the base configuration $^2P(0)$.

We shall now deduce analogous singly excited configurations for the FH molecule. Instead of the one $2p_z$ orbital, we have now the two bond orbitals σ and σ^*. As base configurations for excitations, we shall consider all those FORS configurations which have at least six electrons in the orbitals 2s, $2p_x$, $2p_y$ and the rest distributed among σ and σ^*. They are listed in Table 5.6 and denoted as Ia, Ib, Ic, IIa, IIb, IIIa, IIIb, IVa, IVb. In the last column, they are identified with the SAAPs in Table 5.1 if possible. It may be noted that they include Φ_5 which, after Φ_3, is the next most important contributor in the FORS wavefunction. As in the

Table 5.5. Orbital occupations for base configurations and single excitations for F atom

	Valence AO	s	x	y	z	SAAP Symmetry
I	occ. no.	2	2	2	1	$^2P(0)$
Ix	corr. orb.	s',d_o	x'	y'	z'	$^2P(0)$
II	occ. no.	2	2	1	2	$^2P(x)$
IIx	corr. orb.	d_{yz}	-	z'	y'	$^2P(0)$
III	occ. no.	2	1	2	2	$^2P(y)$
IIIx	corr. orb.	d_{xz}	z'	-	x'	$^2P(0)$
IV	occ. no.	1	2	2	2	^2S
IVx	corr. orb.	z'	d_{xz}	d_{yz}	s',d_o	$^2P(0)$

Table 5.6. Orbital occupations of base configurations and single excitations for $^1\Sigma^+$ state of FH

	FORS MO	s	x	y	σ	σ^*	FORS SAAP
Ia	occ. no.	2	2	2	2	0	Φ_1
Ib	occ. no.	2	2	2	1	1	Φ_2
Ic	occ. no.	2	2	2	0	2	Φ_3
Ix	corr. orb.	σ′	x′	y′	σ″	σ″	
IIa	occ. no.	2	2	1	2	1	--
IIb	occ. no.	2	2	1	1	2	--
IIx	corr. orb.	y″	δ_{xy}	σ″, $\delta_{x^2-y^2}$	y′	y′	
IIIa	occ. no.	2	1	2	2	1	--
IIIb	occ. no.	2	1	2	1	2	--
IIIx	corr. orb.	x″	σ″, $\delta_{x^2-y^2}$	δ_{xy}	x′	x′	
IVa	occ. no.	1	2	2	2	1	Φ_4
IVb	occ. no.	1	2	2	1	2	Φ_5
IVx	corr. orb.	σ″	x″	y″	σ′	σ′	

case of the fluorine atom, we have some base configurations that do not have the right symmetry $^1\Sigma^+$, namely types IIa, IIb, IIIa and IIIb. Again, appropriate symmetries are indicated in the rows Ix, IIx, IIIx and IVx for external orbitals, so that the correct overall symmetry ($^1\Sigma^+$) results when they are substituted for the orbitals directly above them, to form single excitations from the corresponding base configurations. The three correlating σ orbitals correspond to the s′, d_0 and z′ orbitals in the atom, the two degenerate π orbitals to the x′, y′ and d_{xz}, d_{yz} respectively, and the δ orbital to the remaining d orbitals in the atom.

Calculations were performed in which some or all of these single excited SAAPs are added to all FORS configurations and the results are listed in Table 5.7. It is apparent that the results of this approach are comparable to those obtained by the first selection procedure, if only single excitations are taken into account. This is so because the contribution from case 11 in Table 5.2 can be practically identified with that of all doubly excited configurations: on the one hand, only the bond orbitals σ, σ^* are subject to double replacements and, on the other hand, the contribution of the single substitutions is very much smaller than that of the double substitutions in case 11. Subtracting the value 0.233 of case 11 from the value 1.169 of case 12, one obtains 0.936, which differs only by 0.13 eV from the final value of Table 5.7.

Table 5.7. Augmented FORS calculations with selected excitations for dissociation energy of FH. Selection II

Excitations from	No. of additional SAAPs	E at R_e [a] (hartree)	E at R_∞ [a] (hartree)	ΔE (eV)	$\Delta E-\Delta E_0$ (eV)
FORS	0	-100.0908	-99.9088	4.954	0
Is	12	-100.1017	-99.9179	5.001	0.047
Iπ	16	-100.1274	-99.9095	5.927	0.973
Iσ	6	-100.0909	-99.9099	4.955	0.001
II + IIIs	16	-100.0957	-99.9208	4.760	-0.194
II + IIIπ	20	-100.0957	-99.9091	4.987	0.033
II + IIIσ	(=Iπ)				
IVs	6	-100.0913	-99.9097	4.941	-0.013
IVπ	(=II+IIIs)				
IVσ	(=Is)				
all of above	76	-100.1424	-99.9309	5.755	0.801

[a] R_e = 1.7325 bohrs; R_∞ = 1000 bohrs.

C. The Fluorine Molecule

1. FORS wavefunction

The ground state of F_2 is a $^1\Sigma_g^+$ state with an equilibrium distance of R_e = 2.68 bohr. All calculations were performed with an unscaled (14s,7p,2d / 4s,3p,2d) basis of even-tempered primitives with polarization exponents of ζ_d = 0.36 and 1.26. The calculations were simplified by adapting the atomic orbitals to g and u symmetry. The SCF and FORS calculations yield the following results:

	$E(R_e)$ (hartree)	$E(R_\infty)$ (hartree)	ΔE (eV)
SCF	-198.7641	-198.8156	-1.40
FORS	-198.8443	-198.8156	0.78

The experimental binding energy is 1.66 eV. Although the FORS calculation is still 0.9 eV short of the experimental value, it does in fact recover 71% of the correlation contribution to the binding energy.

If the natural molecular orbitals, which are symmetry-adapted, are used to construct configurations, then the Full Reaction Space for the $^1\Sigma_g^+$ symmetry is spanned by the ten SAAPs listed in the first column of Table 5.8. The second column contains the expansion coefficients of the FORS wavefunction for the ground state at the equilibrium distance.

Table 5.8. FORS wavefunction for F_2

SAAP	Coefficient
$\Phi_1 = A\{k_g^2 k_u^2 2\sigma_g^2 2\sigma_u^2 x_u^2 x_g^2 y_u^2 y_g^2 3\sigma_g^2 \Theta_0\}$	0.964860
$\Phi_2 = A\{k_g^2 k_u^2 2\sigma_g^2 2\sigma_u^2 x_u^2 x_g^2 y_u^2 y_g^2 3\sigma_u^2 \Theta_0\}$	-0.251894
$\Phi_3 = A\{k_g^2 k_u^2 2\sigma_g^2 x_u^2 x_g^2 y_u^2 y_g^2 3\sigma_g^2 2\sigma_u 3\sigma_u \Theta_0\}$	-0.019690
$\Phi_4 = A\{k_g^2 k_u^2 2\sigma_u^2 x_u^2 x_g^2 y_u^2 y_g^2 3\sigma_u^2 2\sigma_g 3\sigma_g \Theta_0\}$	0.048444
$\Phi_5 = A\{k_g^2 k_u^2 2\sigma_g^2 2\sigma_u^2 x_u^2 x_g^2 y_u^2 3\sigma_g^2 3\sigma_u^2 \Theta_0\}$	-0.028997
$\Phi_6 = A\{k_g^2 k_u^2 2\sigma_g^2 2\sigma_u^2 x_u^2 y_u^2 y_g^2 3\sigma_g^2 3\sigma_u^2 \Theta_0\}$	-0.007673
$\Phi_7 = A\{k_g^2 k_u^2 2\sigma_g^2 2\sigma_u^2 x_u^2 x_g^2 y_g^2 3\sigma_g^2 3\sigma_u^2 \Theta_0\}$	-0.028997
$\Phi_8 = A\{k_g^2 k_u^2 2\sigma_g^2 2\sigma_u^2 x_g^2 y_u^2 y_g^2 3\sigma_g^2 3\sigma_u^2 \Theta_0\}$	-0.007673
$\Phi_9 = A\{k_g^2 k_u^2 2\sigma_g^2 x_u^2 x_g^2 y_u^2 y_g^2 3\sigma_g^2 3\sigma_u^2 \Theta_0\}$	-0.025670
$\Phi_{10} = A\{k_g^2 k_u^2 2\sigma_u^2 x_u^2 x_g^2 y_u^2 y_g^2 3\sigma_g^2 3\sigma_u^2 \Theta_0\}$	-0.020033

Although the configuration generating orbitals used in Table 5.8 extend over both atoms, it is still possible to distinguish between inner shell, lone pair and bonding orbitals. The MOs k_g, k_u are the g and u linear combinations of the inner shell orbitals and the MOs $2\sigma_g$, $2\sigma_u$, x_g, x_u, y_g, y_u are the g and u linear combinations of the lone pair 2s, $2p_x$, $2p_y$ orbitals on the two atoms. This is apparent from the expansion coefficients in Table 5.8, and is confirmed by an examination of the orbitals[14]. The orbitals $3\sigma_g$ and $3\sigma_u$ correspond to the bonding and antibonding orbitals σ and σ^* of FH. It is therefore apparent that the configurations of Table 5.8 could also be expressed in terms of the left and right lone pair orbitals

$$s_L = (s_g + s_u)/\sqrt{2} \qquad s_R = (s_g - s_u)/\sqrt{2}$$
$$x_L = (x_g + x_u)/\sqrt{2} \qquad x_R = (x_g - x_u)/\sqrt{2}$$
$$y_L = (y_g + y_u)/\sqrt{2} \qquad y_R = (y_g - y_u)/\sqrt{2}$$

Because of the loss of the g/u symmetry, sixteen SAAPs, generated from these orbitals are needed to span the Full Reaction Space.

2. Augmented wavefunctions. First selection method

This approach is analogous to the one outlined in Section V.B.2a for FH. The difference is that, in F_2, we have twice

as many lone pair orbitals as in FH. As in FH, we consider only single excitations out of the six lone pair MOs $2\sigma_g$, $2\sigma_u$, x_g, x_u, y_g, y_u, but include single and double excitations out of the bonding MOs σ_g and σ_u. In contrast to FH, the basic pairing process during bond formation in F_2 is described by two SAAPs only, namely Φ_1 and Φ_2 which correspond to Φ_1 and Φ_3 in FH. The SAAP corresponding to Φ_2 of FH has u symmetry; it may be noticed that, even in FH, it has a small coefficient. Thus, by analogy to F_2, we consider here only excitations of the aforementioned kinds from the configurations Φ_1 and Φ_2. Since there are more lone pair orbitals to be correlated, it can be expected that more external orbitals will be required before saturation occurs.

As in the case of FH, calculations were performed using certain subgroups of configurations as well as all configurations. The results at the equilibrium distance are listed in Table 5.9. They are identified by a notation similar to that used in Table 5.2. The conclusions which emerge from these results on F_2 are in close agreement with those found for FH. Again, the contributions from various types of excitations are nearly additive.

In particular one observes, as in FH, that <u>single excitations from lone pair type FORS π orbitals to external π orbitals provide by far the largest contributions to the correlation part of the dissociation energy, beyond the FORS</u>

Table 5.9. Augmented FORS calculations with selected excitations for dissociation energy of F_2. Selection I

Case	Excitations	No. of additional SAAPs	E at R_e[a] (hartree)	E at R_∞[a] (hartree)	ΔE (eV)	ΔE-ΔE$_0$ (eV)
1	FORS	0	-198.8443	-198.8178	0.720	0
2	s→1σ_g',1σ_u'	8	-198.8589	-198.8359	0.625	-0.095
3	s→2σ_g',1σ_u'	12	-198.8646	-198.8359	0.782	0.061
4	s→2σ_g',2σ_u'	16	-198.8667	-198.8359	0.838	0.117
5	π→1π_u',1π_g'	16	-198.8859	-198.8193	1.814	1.093
6	π→2π_u',1π_g'	24	-198.8864	-198.8193	1.825	1.104
7	π→2π_u',2π_g'	32	-198.8868	-198.8194	1.834	1.114
8	σ→1σ_g',1σ_u'	4	-198.8453	-198.8179	0.746	0.025
9	σ→2σ_g',1σ_u'	7	-198.8464	-198.8179	0.777	0.057
10	σ→2σ_g',2σ_u'	10	-198.8453	-198.8179	0.747	0.027
11	σ→1π_u',1π_g'	4	-198.8444	-198.8178	0.721	0.001
12	σ→2π_u',1π_g'	8	-198.8460	-198.8178	0.766	0.046
13	σ→2π_u',2π_g'	12	-198.8460	-198.8178	0.767	0.047
14	σ→1σ_g',1σ_u', 1π_u',1π_g'	8	-198.8469	-198.8179	0.791	0.070
15	σ→2σ_g',1σ_u', 2π_u',1π_g'	15	-198.8482	-198.8179	0.8251	0.105

[a] R_e = 1.7325 bohr; R_∞ = 1000 bohr.

Table 5.9. continued

Case	Excitations	No. of additional SAAPs	E at R_e[a] (hartree)	E at R_∞[a] (hartree)	ΔE (eV)	$\Delta E-\Delta E_0$[b] (eV)
16	$\sigma\rightarrow 2\sigma_g', 2\sigma_u', 2\pi_u', 2\pi_g'$	22	-198.8485	-198.8179	0.833	0.113
17	$s\rightarrow 2\sigma_g', 1\sigma_u'$; $\pi\rightarrow 2\pi_u', 1\pi_g'$; $\sigma\rightarrow 2\sigma_g', 1\sigma_u', 2\pi_u', 1\pi_g'$	51	-198.9082	-198.8375	1.923	1.203
18	$s\rightarrow 2\sigma_g', 2\sigma_u'$; $\pi\rightarrow 2\pi_u', \pi\rightarrow 2\pi_g'$; $\sigma\rightarrow 2\sigma_g', 2\sigma_u', 2\pi_u', 2\pi_g'$	70	-198.9103	-198.8377	1.977	1.257

model. The most likely explanation of this remarkable fact seems to be that the π orbitals in the neutral FORS configurations (FH, FF) would like to have somewhat different shape than those in the ionic FORS configurations (F^-H^+, F^-F^+), and that the addition of singly excited configurations approximates this modification to first order.

Unfortunately, in F_2 the inclusion of all additional configurations leads to a dissociation energy which overshoots the experimental value. The included configurations are therefore more effective for the molecule F_2 than for the F atom.

3. Augmented wavefunctions. Second selection method

a. Calculation at the equilibrium distance This approach corresponds to the second selection procedure described for FH. In analogy to Section V.B.3, we consider here as base configurations for single excitations all those SAAPs in which the orbitals $2\sigma_g$, $2\sigma_u$, x_g, x_u, y_g, y_u, σ_g and σ_u are at least occupied by fifteen electrons. There are fifteen SAAPs of this kind, namely Φ_1, Φ_2, Φ_4, Φ_5 of Table 5.8 and the SAAPs Φ_{11} to Φ_{21} listed in Table 5.10 which do not have $^1\Sigma_g^+$ symmetry. Table 5.11 for F_2 corresponds to Table 5.6 for FH. It lists the fifteen base configurations and relates their types to those of Tables 5.5 and 5.6. Below each base configuration are given the appropriate symmetries for external orbitals which will yield singly excited SAAPs of

Table 5.10. Some FORS configurations which have vanishing coefficients in the ground state of F_2

SAAP
$\Phi_{11} = \mathbf{A}\{k_g^2 k_u^2 2\sigma_g^2 2\sigma_u^2 x_u^2 x_g^2 y_u^2 y_g^2 3\sigma_g 3\sigma_u \Theta_0\}$
$\Phi_{12} = \mathbf{A}\{k_g^2 k_u^2 2\sigma_g^2 2\sigma_u^2 x_u^2 x_g^2 y_u^2 3\sigma_g^2 y_g 3\sigma_u \Theta_0\}$
$\Phi_{13} = \mathbf{A}\{k_g^2 k_u^2 2\sigma_g^2 2\sigma_u^2 x_u^2 x_g^2 y_u^2 3\sigma_u^2 y_g 3\sigma_g \Theta_0\}$
$\Phi_{14} = \mathbf{A}\{k_g^2 k_u^2 2\sigma_g^2 2\sigma_u^2 x_u^2 y_u^2 y_g^2 3\sigma_g^2 x_g 3\sigma_u \Theta_0\}$
$\Phi_{15} = \mathbf{A}\{k_g^2 k_u^2 2\sigma_g^2 2\sigma_u^2 x_u^2 y_u^2 y_g^2 3\sigma_u^2 x_g 3\sigma_g \Theta_0\}$
$\Phi_{16} = \mathbf{A}\{k_g^2 k_u^2 2\sigma_g^2 2\sigma_u^2 x_u^2 x_g^2 y_g^2 3\sigma_g^2 y_u 3\sigma_u \Theta_0\}$
$\Phi_{17} = \mathbf{A}\{k_g^2 k_u^2 2\sigma_g^2 2\sigma_u^2 x_u^2 x_g^2 y_g^2 3\sigma_u^2 y_u 3\sigma_g \Theta_0\}$
$\Phi_{18} = \mathbf{A}\{k_g^2 k_u^2 2\sigma_g^2 2\sigma_u^2 x_g^2 y_u^2 y_g^2 3\sigma_g^2 x_u 3\sigma_u \Theta_0\}$
$\Phi_{19} = \mathbf{A}\{k_g^2 k_u^2 2\sigma_g^2 2\sigma_u^2 x_g^2 y_u^2 y_g^2 3\sigma_u^2 x_u 3\sigma_g \Theta_0\}$
$\Phi_{20} = \mathbf{A}\{k_g^2 k_u^2 2\sigma_g^2 x_u^2 x_g^2 y_u^2 y_g^2 3\sigma_u^2 2\sigma_u 3\sigma_g \Theta_0\}$
$\Phi_{21} = \mathbf{A}\{k_g^2 k_u^2 2\sigma_u^2 x_u^2 x_g^2 y_u^2 y_g^2 3\sigma_g^2 2\sigma_g 3\sigma_u \Theta_0\}$

Table 5.11. Orbital occupations for base configurations and single excitations for $^1\Sigma_g^+$ of F_2 molecule

Type	SAAP	Occ. No. / Type of Corr. Orb. $2\sigma_g$	$2\sigma_u$	$1\pi_{ux}$	$1\pi_{uy}$	$1\pi_{gx}$	$1\pi_{gy}$	$3\sigma_g$	$3\sigma_u$
I	1	2	2	2	2	2	2	2	0
		a	b	c	d	e	f	a	
	2	2	2	2	2	2	2	0	2
		a	b	c	d	e	f		b
	11	2	2	2	2	2	2	1	1
		b	a	e	f	c	d		
IIg	12	2	2	2	2	2	1	2	1
		d	f	g	a,h	i	b,j	d	f
	13	2	2	2	2	2	1	1	2
		f	d	i	b,j	g	a,h	f	d
IIIg	14	2	2	2	2	1	2	2	1
		c	e	a,h	g	b,j		c	e
	15	2	2	2	2	1	2	1	2
		e	c	b,j	i	a,h		e	c
IIu	16	2	2	2	1	2	2	2	1
		f	d	i	b,j			f	d
	17	2	2	2	1	2	2	1	2
		d	f	g	a,h			d	f

Table 5.11. continued

Type	SAAP	Occ. No. / Type of Corr. Orb. $2\sigma_g$	$2\sigma_u$	$1\pi_{ux}$	$1\pi_{uy}$	$1\pi_{gx}$	$1\pi_{gy}$	$3\sigma_g$	$3\sigma_u$
IIIu	18	2	2	1	2	2	2	2	1
		e	c	b,j				e	c
	19	2	2	1	2	2	2	1	2
		c	e	a,h				c	e
IV	4	2	1	2	2	2	2	2	1
		a	b	c	d	e	f	a	b
	5	1	2	2	2	2	2	1	2
		a	b	c	d	e	f	a	b
	20	2	1	2	2	2	2	1	2
			a	e	f	c	d	b	a
	21	1	2	2	2	2	2	2	1
		b		e	f	c	d	b	a

Note: The blank spaces in the table indicate that excitation from that orbital will result in configurations already generated from other SAAPs in the same group. External orbitals are abbreviated as follows:

$a = \sigma_g'$; $b = \sigma_u'$;

$c = \pi_{xu}'$; $d = \pi_{yu}'$; $e = \pi_{xg}'$; $f = \pi_{yg}'$;

$g = \delta_g(xy)$; $h = \delta_g(x^2-y^2)$; $i = \delta_u(xy)$; $j = \delta_u(x^2-y^2)$

$^1\Sigma_g^+$ symmetry by single replacement of the corresponding base orbitals.

Again calculations are performed in which some or all of these singly excited SAAPs are added to all FORS configurations. The results are listed in Table 5.12. As in the previous cases, the effect of the different types of contributions are seen to be approximately additive. As was the case in FH, the overall result (1.13 eV) obtained by this approach, which considers single excitations only, agrees with the effect of all single excitations in the first approach (case 18 minus case 16 of Table 5.9: 1.257-0.113=1.144 eV).

b. Calculation of dissociation curve Calculations of type 8 of Table 5.12 are performed along the entire dissociation curve. The results of these calculations as well as those of SCF and FORS calculations are listed in Table 5.13. With the help of the DIAPOT program[91] these energies are interpolated and spectroscopic constants extracted via a Dunham analysis[91]. The dissociation curves are plotted in Figure 5.4. The spectroscopic constants are listed in Table 5.14 together with previous theoretical results[96-97].

The SCF wavefunction fails to predict binding and the minimum geometry obtained by fitting the curve is 0.15 bohr too short. The minimum on the FORS potential curve is 0.10 bohr too long and the dissociation energy calculated is too

Table 5.12. Augmented FORS calculations with selected excitations for dissociation energy of F_2. Selection II

	Type of excitations	No. of additional SAAPs	E at R_e[a] (hartree)	E at R_∞[a] (hartree)	ΔE (eV)	ΔE-ΔE_o (eV)
1	FORS	0	-198.8443	-198.8178	0.720	0
2	Is	16	-198.8667	-198.8377	0.790	0.070
3	Iπ	32	-198.8869	-198.8194	1.837	1.117
4	Iσ	4	-198.8443	-198.8179	0.720	0
5	IIs	64	-198.8674	-198.8417	0.700	-0.020
6	IIπ	64	-198.8455	-198.8184	0.737	0.017
	IIσ(=Iπ)					
7	IIIs	16	-198.8459	-198.8194	0.721	0.001
	IIIπ(=IIs)					
	IIIσ(=Is)					
8	all of above	196	-198.9294	-198.8614	1.850	1.130

[a] R_e = 1.7325 bohr; R_∞ = 1000 bohr.

Table 5.13. Calculated energies for F_2

R(bohr)	Total Energies (hartree) SCF	FORS	Augmented FORS
1.4	-197.1045	-197.1152	-197.1684
1.7	-198.2264	-198.2457	-198.3121
2.0	-198.6266	-198.6580	-198.7384
2.2	-198.7273	-198.7699	-198.8560
2.4	-198.7649	-198.8214	-198.9092
2.5	-198.7697	-198.8341	-198.9217
2.6	-198.7683	-198.8414	-198.9276
2.65	-198.7659	-198.8435	-198.9291
2.68	-198.7640	-198.8443	-198.9294
2.7	-198.7626	-198.8448	-198.9295
2.72	-198.7610	-198.8451	-198.9290
2.75	-198.7584	-198.8454	-198.9286
2.8	-198.7536	-198.8455	-198.9275
2.85	-198.7483	-198.8452	-198.9258
2.9	-198.7425	-198.8446	-198.9242
3.1	-198.7166	-198.8401	-198.9134
3.3	-198.6889	-198.8346	-198.9014
4.0	-198.6010	-198.8217	-198.8719
5.0	-198.5199	-198.8178	-198.8624
7.0	-198.4517	-198.8177	-198.8610
10.0	-198.4215	-198.8178	-198.8617
1000	-198.8156	-198.8178	-198.8614

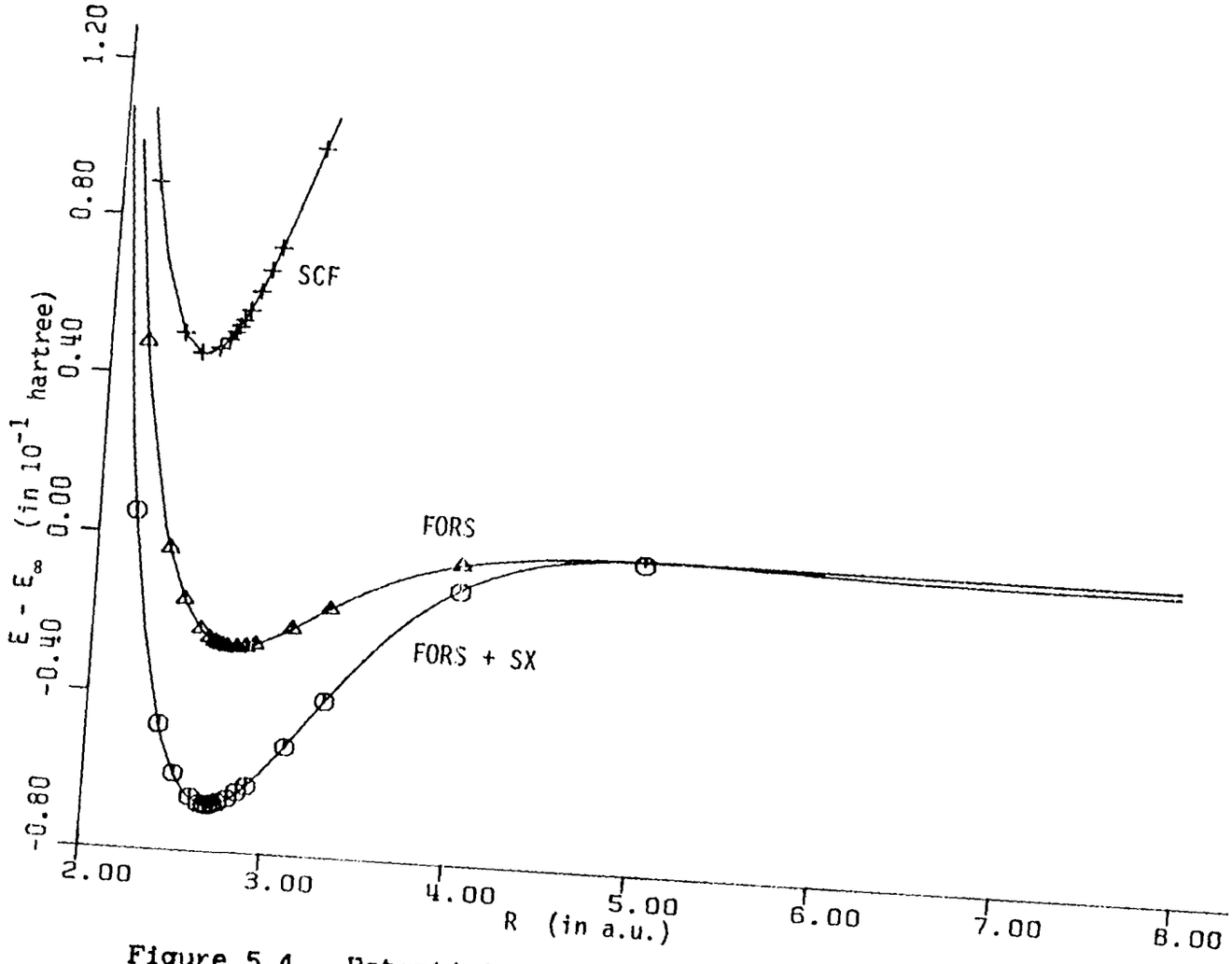

Figure 5.4. Potential energy curves for ground state of F_2

Table 5.14. Spectroscopic constants of F_2

Method	Reference	R_e (bohr)	D_e (eV)	B_e	ω_e (in 1/cm)	$\omega_e x_e$	α_e
SCF		2.528		0.9917	1248.8	6.69	0.0083
FORS		2.789	0.753	0.8149	702.0	15.80	0.0182
Augm. FORS		2.694	1.854	0.8734	943.2	10.87	0.0116
OVC	96	2.67	1.67	0.88	942		0.0160
IEPA	97	2.781			795	16	
CEPA	97	2.666			945	14	
PNO-CI	97	2.606			1150	10	
Exp.	6	2.68	1.658	0.8902	916.6	11.24	0.0138

small by 0.9 eV. Augmentation of the FORS wavefunction greatly improves the results: the predicted equilibrium distance is within 0.01 bohr of the experimental value and the dissociation energy is within 0.2 eV of the experimental result. The good prediction of the spectroscopic constants indicates that the wavefunction describes the energy curve adequately near the equilibrium. The overestimation of the dissociation energy for the augmented FORS curve implies that the wavefunction recovers more correlation near the equilibrium distance than for the dissociated atoms. Fine tuning of the selection scheme is required to overcome this shortcoming.

D. Conclusion

The ab initio augmentation of the FORS model discussed in this section substantially improves its performance in predicting dissociation energies. It can therefore be concluded that single excitations of lone pair type orbitals and single plus double excitations of bonding orbitals generate those configurations which, together with the Full Reaction Space, closely describe that part of the electron correlation which changes upon dissociation. It can also be concluded that MCSCF optimization of a few external orbitals is an adequate substitute for the inclusion of all possible configurations of the corresponding type. As a consequence

the number of augmenting configurations containing external orbitals is kept quite low. It is somewhat disappointing that in F_2 there is still left an error of about 0.1 to 0.2 eV, i.e. up to 5 kcal/mole, in the binding energies.

VI. LITERATURE CITED

1. L. C. Allen and A. M. Karo, Rev. Mod. Phys. 32, 275 (1960).

2. H. F. Schaefer III, Methods of Electronic structure Theory (Plenum Press, New York, 1977).

3. P. Carsky and M. Urban, Ab Initio Calculations, Methods and Applications in Chemistry, edited by G. Berthier, M. J. S. Dewar, H. Fischer, K. Furui, H. Hartmann, H. H. Jaffe, J. Jorther, W. Kutzelnigg, K. Ruedenberg, E. Scrocco and W. Zeil (Springer-Verlag, Berlin, 1980).

4. S. Fraga, J. Karwowski and K. M. S. Saxena, Handbook of Atomic Data (Elsevier, Amsterdam, 1976).

5. A. Veillard and E. Clementi, J. Chem. Phys. 49, 2415 (1968).

6. K. P. Huber and G. Herzberg, Constants of Diatomic Molecules (Van Nostrand Reinhold, New York, 1979).

7. R. C. Raffenetti, J. Chem. Phys. 59, 5936 (1973).

8. R. C. Raffenetti, Int. J. Quantum Chem. Symp. 9, 289 (1974).

9. R. D. Bardo and K. Ruedenberg, J. Chem. Phys. 60, 918 (1974).

10. D. F. Feller and K. Ruedenberg, Theor. Chim. Acta (Berl.) 52, 231 (1979).

11. M. W. Schmidt and K. Ruedenberg, J. Chem. Phys. 71, 3962 (1979).

12. The ALIS program system (Ames Laboratory, Iowa State University) was developed by the Quantum Chemistry Group at ISU and released in May, 1979. The ALIS system also contains a version of the BIGGMOLI integral program.

13. a) K. Ruedenberg and K. R. Sundberg, in Quantum Science, edited by J. L. Calais, O. Goscinski, J. Linderberg and Y. Ohrn (Plenum Press, New York, 1976), p. 505; b) L. M. Cheung, K. R. Sundberg and K. Ruedenberg, Int. J. Quantum Chem. 16, 1103 (1979).

14. a) K. Ruedenberg, M. W. Schmidt, M. M. Gilbert and S. T. Elbert, Chem. Phys. 71, 41 (1982); b) K. Ruedenberg, M. W. Schmidt and M. M. Gilbert, Chem. Phys. 71, 51 (1982); c) K. Ruedenberg, M. W. Schmidt, M. M. Gilbert and S. T. Elbert, Chem. Phys. 71, 65 (1982).

15. M. G. Dombek, Ph.D. Dissertation, Iowa State University (1977).

16. D. F. Feller, Ph.D. Dissertation, Iowa State University (1979).

17. R. P. Johnson and M. W. Schmidt, J. Am. Chem. Soc. 103, 3244 (1981).

18. D. F. Feller, M. W. Schmidt and K. Ruedenberg, J. Am. Chem. Soc. 104, 960 (1982).

19. M. W. Schmidt, Ph.D. Dissertation, Iowa State University (1982).

20. B. Lam and R. P. Johnson, J. Am. Chem. Soc. 105, 7479 (1983).

21. A. C. Wahl and G. Das, in Methods of Electronic Structure Theory, edited by H. F. Schaefer III (Plenum Press, New York, 1977), and references therein.

22. G. C. Lie and E. Clementi, J. Chem. Phys. 60, 1275 and 1288 (1974).

23. D. M. Silver, E. L. Mehler and K. Ruedenberg, J. Chem. Phys. 52, 1174, 1181 and 1206 (1970).

24. T. H. Dunning, D. C. Cartwright, W. J. Hunt, P. J. Hay and F. W. Bobrowicz, J. Chem. Phys. 64, 4755 (1976).

25. K. Kirby-Docken and B. Liu, J. Chem. Phys. 66, 4309 (1977)

26. P. E. H. Siegbahn, A. Heiberg, B. O. Roos and B. Levy, Physica Scripta 21, 323 (1980).

27. B. O. Roos, P. R. Taylor and P. E. M. Siegbahn, Chem. Phys. 48, 157 (1980).

28. B. O. Roos, Int. J. Quantum Chem. 14, 175 (1980).

29. P. E. M. Siegbahn, J. Almlof, A. Heiberg and B. O. Roos, J. Chem. Phys. 74 (1981).

30. K. Ruedenberg, L. M. Cheung and S. T. Elbert, Int. J. Quantum Chem. 16, 1069 (1979).

31. K. Ruedenberg, Phys. Rev. Lett. 27, 1105 (1971).

32. W. I. Salmon and K. Ruedenberg, J. Chem. Phys. 57, 2776 (1972).

33. W. I. Salmon, K. Ruedenberg and L. M. Cheung, J. Chem. Phys. 57, 2787 (1972).

34. A. C. Hurley, Introduction to the Electron Theory of Small Molecules (Academic Press, London, 1976), pp 186-189.

35. H. E. Zimmerman, J. Am. Chem. Soc. 88, 1566 (1966).

36. W. Th. A. M. van der Lugt and L. J. Oosterhoff, J. Am. Chem. Soc. 91, 6042 (1969).

37. J. Michl, Mol. Photochem. 4, 243 (1972).

38. L. Salem, J. Am. Chem. Soc. 96, 3486 (1974)

39. J. Michl, Top Curr. Chem. 46, 1 (1974).

40. H. E. Zimmerman, Acc. Chem. Res. 10, 312 (1982).

41. L. Salem, Acc. Chem. Res. 12, 87 (1979).

42. R. J. Buenker, V. Bonacic-Koutecky and L. Pogliani, J. Chem. Phys. 73, 1836 (1980).

43. a) G. Orlandi, P. Palmieri and G. Pogga, J. Chem. Soc. Faraday Trans. 2 77, 71 (1981); b) J. Tennyson and J. N. Murrell, Nouv. J. Chim. 5, 361 (1981); c) M. Persico, J. Am. Chem. Soc. 102, 7839 (1980); d) I. Baraldi, M. C. Bruni, F. Momicchioli and G. Ponterini, Chem. Phys. 52, 415 (1980); e) G. Orlandi and G. Marconi, Nuovo Cimento Soc. Ital. Fis. B. 63B, 332 (1981); f) J. P. Malrieu, Theoret. Chim. Acta 59, 251 (1981); g) I. Nebot-Gil and J. P. Malrieu, J. Am. Chem. Soc. 104, 3320 (1982); h) V. Bonacic-Koutecky

and M. Persico, D. Dohnert and A. Sevin, J. Am. Chem. Soc. 104, 6900 (1982).

44. a) T. Tezuka, O. Kikuchi, K. N. Houk, M. N. Paddon-Row, C. M. Santiago, N. G. Rondon, J. C. Williams Jr. and R. Wells-Gandour, J. Am. Chem. Soc. 103, 1367 (1981); b) V. Bonacic-Koutecky, J. Am. Chem. Soc. 100, 396 (1978); c) W. G. Dauben and J. S. Ritscher, J. Am. Chem. Soc. 92, 2925 (1970); d) W. G. Dauben, M. S. Kellog, J. I. Seeman, N. D. Wietmeyer and P. H. Wenschuh, Pure Appl. Chem. 33, 197 (1973); e) O. Kikuchi, H. Kubota and K. Suzuki, Bull. Chem. Soc. Jpn. 54, 1126 (1981); f) G. Trinquier, N. Paillous, A. Lattes and J. P. Malrieu, Nouv. J. Chim. 1, 403 (1977); g) C. M. Meerman van Bentham, H. J. C. Jacobs and J. J. C. Mulder, Nouv. J. Chim. 2, 123 (1978); h) B. H. Baretz, A. K. Singh and R. S. H. Liu, Nouv. J. Chim. 5, 297 (1981); i) S. S. Hixson, R. O. Day, L. A. Franke and V. J. Ramachandra Rao, J. Am. Chem. Soc. 102, 412 (1980); j) P. J. Kropp and F. P. Tise, J. Am. Chem. Soc. 103, 7293 (1981).

45. W. T. Borden, J. Chem. Phys. 45, 2512 (1966).

46. a) C. S. Drucker, V. G. Toscano and R. G. Weiss, J. Am. Chem. Soc. 95, 6482 (1973); b) O. Rodriguez and H. Morrison, Chem. Commun. 13, 679 (1971).

47. T. J. Stierman and R. P. Johnson, J. Am. Chem. Soc. 105, 2492 (1983).

48. C. E. Dykstra and H. F. Schaefer III, in The Chemistry of Ketenes, Allenes and Related Compounds, Part I, edited by S. Patai (John Wiley and Sons, New York, 1980), pp 1-44.

49. a) R. J. Buenker, J. Chem. Phys. 48, 1368 (1968); b) L. J. Schaad, L. A. Burnelle and K. P. Dressler, Theor. Chim. Acta 15, 91 (1969); c) L. J. Schaad, Tetrahedron 26, 4115 (1970); d) L. Radom and J. A. Pople, J. Am. Chem. Soc. 92, 4786 (1970); e) C. E. Dykstra, J. Am. Chem. Soc. 99, 2060 (1977); f) V. Staemmler, Theor. Chim. Acta 45, 89 (1977); g) R. Seeger, R. Krishnan, J. A. Pople and P. V. R. Schleyer, J. Am. Chem. Soc. 99, 7103 (1977); h) K. Krohg-Jespersen, J. Comput. Chem. 3, 571 (1982); i) R. C. Bingham, M. J. Dewar and D. H. Lo, J. Comput. Chem. 97, 1294 (1975).

50. W. R. Roth, G. Ruf and P. W. Ford, Chem. Ber. 107, 48 (1974).

51. B. R. Brooks and H. F. Schaefer, J. Chem. Phys 70, 5092 (1979).

52. a) J. A. Pincock and R. J. Boyd, Can. J. Chem. 55, 2482 (1977); b) A. Sevin and L. Arnaud-Danon, J. Org. Chem. 46, 2346 (1981); c) J. H. Davis, W. A. Goddard III and R. G. Bergman, J. Am. Chem. Soc. 99, 2427 (1977).

53. a) D. J. Pasto, M. Haley and D. Chipman, J. Am. Chem. Soc. 100, 5272 (1978); b) P. W. Dillon and G. R. Underwood, J. Am. Chem. Soc. 99, 2435 (1977).

54. a) P. W. Dillon and G. R. Underwood J. Am. Chem. Soc. 96, 779 (1974); b) A. Greenberg and J. F. Liebman, Strained Organic Molecules (Academic Press, New York, 1979).

55. M. W. Schmidt, R. O. Angus Jr. and R. P. Johnson, J. Am. Chem. Soc. 104, 6838 (1982).

56. M. Balci and W. M. Jones, J. Am. Chem. Soc. 102, 7607 (1980).

57. W. Moffitt, Proc. Roy. Soc. A 210, 224 (1951).

58. W. Moffitt, Proc. Roy. Soc. A 210, 245 (1951).

59. W. Moffitt, Rept. Prog. Phys. 17, 173 (1954).

60. A. C. Hurley, Proc. Phys. Soc. A 68, 149 (1955).

61. A. C. Hurley, Proc. Phys. Soc. A 69, 49 (1956).

62. A. C. Hurley, Proc. Phys. Soc. A 69, 301 (1956).

63. A. C. Hurley, Proc. Phys. Soc. A 69, 767 (1956).

64. A. C. Hurley, Proc. Roy. Soc. A 248, 119 (1958).

65. A. C. Hurley, Proc. Roy. Soc. A 249, 402 (1958).

66. A. C. Hurley, J. Chem. Phys. 28, 532 (1958).

67. A. C. Hurley, Rev. Mod. Phys. 35, 448 (1963).

68. R. G. Parr, The Quantum Theory of Molecular Electronic Structure (W. A. Benjamin, New York, 1963), pp 101-108.

69. G. G Balint-Kurti and M. Karplus, in Orbital Theories of Molecules and Solids, edited by N. H. Marsh (Clarendon Press, Oxford, 1974), Chapter 6.

70. Error = HF energy - Exact energy; Exact energies from a) C. L. Pekeris, Phys. Rev. 112, 1649 (1958); HF energies for H^-, He and Li^+ from b) C. Froese-Fischer, The Hartree-Fock Method for AToms, A Numerical Approach (John Wiley and Sons, New York, 1977); HF energy for Ne^{8+} from c) E. Clementi and C. Roetti, Atomic Data and Nuclear Data Tables 14, 177 (1974).

71. K. J. Miller and K. Ruedenberg, J. Chem. Phys. 48, 3414 (1968).

72. E. V. Ludena and M. Gregori, J. Chem. Phys. 71, 2235 (1979).

73. G. Verhaegen and C. M. Moser, J. Phys. B 3, 478 (1970).

74. T. Arai, Rev. Mod. Phys. 32, 370 (1960).

75. R. S. Mulliken, J. Chem. Phys. 23, 1833 (1955).

76. G. G. Balint-Kurti and M. Karplus, J. Chem. Phys. 50, 478 (1969).

77. D. Grevy and G. Verhaegen, Int. J. Quantum Chem. 12, 115 (1977).

78. J. Lieven, J. Breulet and G. Verhaegen, Theoret. Chim. Acta (Berlin) 60, 339 (1981).

79. J. P. Desclaux, C. M. Moser and G. Verhaegen, J. Phys. B 4, 296 (1971).

80. E. Clementi, IBM J. Res. Dev. 9, 1 (1965).

81. H. Hotop and W. C. Lineberger, J. Phys. Chem. Ref. Data 4, 539 (1975).

82. H. F. Schaeffer III, R. A. Klemm and F. E. Harris, J. Chem. Phys. 51, 4643 (1969).

83. B. Lam, M. W. Schmidt, K. Ruedenberg, Atomic State Functions for the Valence Configurations snpm in terms of Spin Adapted Products of Real Atomic Orbitals, Iowa State University, 1984, to be published.

84. The SKUNK program system was developed by members of the Quantum Chemistry Group at Iowa State University. It contains various utility programs.

85. B. Lam, M. W. Schmidt, K. Ruedenberg, Intra-Atomic Correlation Correction in the FORS model, Iowa State University, 1984, to be published.

86. L. G. Piper, J. Chem. Phys. 70, 3417 (1979).

87. C. E. Moore, National Bureau of Standards Monograph, 467 (1949).

88. P. E. M. Siegbahn, J. Chem. Phys. 70, 5391 (1979).

89. B. Lam, Iowa State University, 1982, unpublished.

90. P. Valtazanos, DIAPOT program, Iowa State University, 1980, unpublished.

91. W. Meyer and P. Rosmus, J. Chem. Phys. 63, 2356 (1975).

92. V. Bondybey, P. K. Pearson and H. F. Schaefer III, J. Chem. Phys. 57, 1123 (1972).

93. H. Lischka, Theor. Chim. Acta (Berl.) 31, 39 (1973).

94. W. J. Stevens, J. Chem. Phys. 58, 1264 (1973).

95. P. E. Cade, An Annotated Bibliography of Quantum Mechanical Calculations on the First Row Diatomics Hydrides, Technical Report (Laboratory of Molecular Structure and Spectra, University of Chicago, 1966).

96. G. Das and A. C. Wahl, J. Chem. Phys. 56, 3532 (1972).

97. R. Ahlrichs, H. Lischka, B. Zurawski and W. Kutzelnigg, J. Chem. Phys. 63, 4685 (1975).

VII. ACKNOWLEDGEMENTS

First of all, I would like to thank my thesis advisor, Professor Klaus Ruedenberg, for his guidance over the years. I consider it my privilege to have had the opportunity to work with him. My deepest gratitude to Dr. Stephen Elbert who generously shared his expertise in computer programming. Special thanks to Dr. Michael Schmidt who, with near infinite patience, taught me most of what I know about quantum chemistry. I am also grateful to Professor Richard Johnson for the collaboration on the calculations of allene.

Thanks to many friends and colleagues, they know who they are, who have helped to make my stay in Ames, in most part, enjoyable. In particular, I would like to thank Dr. James Evans who patiently listened and empathized. But most of all, I am forever indebted to my dearest friend, Dr. Chi-Keung Chan, for his tolerance and love. Last but by no means the least, I would like to dedicate this dissertation to my parents, my sister, my brothers and their families. Without their continuous support and endless encouragement, this work would have not been possible.